University of Milano-Bicocca
School of Medicine and School of Science

PhD program in Translational and Molecular Medicine
DIMET

ROLE OF TREATMENTS AND GENETIC ALTERATIONS ON ATHEROSCLEROSIS AND CHOLESTEROL METABOLISM: STUDIES IN ANIMAL MODELS

Doctor Dellera Federica
Matr. No: 787799

Coordinator: Professor Andrea Biondi
Tutor: Doctor Roberto Giovannoni
Co-tutor: Professor Giulia Chiesa

XXIX CYCLE
ACADEMIC YEAR 2015/2016

Table of contents

Chapter 1

General introduction

CHOLESTEROL AND LIPOPROTEIN METABOLISM

Cholesterol is an important component of cell membranes (1), as well as the precursor molecule for the synthesis of steroid hormones, vitamin D and bile salts. It is derived from the diet or synthesized within the body. The typical human diet contains 200–500 mg of cholesterol. Cholesterol also enters the intestine in bile (800–1200 mg day^{-1}). The principal sites of cholesterol synthesis are the liver and the Central Nervous System (CNS). Cholesterol can be lost from the body mainly as the fractions of bile salts and intestinal cholesterol which are not absorbed. Both dietary cholesterol and that synthesized *de novo* are transported through the circulation in lipoprotein particles.

Cholesterol blood levels in humans are typically in the range 100–300 mg dl^{-1}. The principal plasma lipoproteins are the chylomicrons, Very Low Density Lipoproteins (VLDLs), Low Density Lipoproteins (LDLs) and High Density Lipoproteins (HDLs) (2).

Chylomicrons are synthesized in the intestinal mucosal cells directly from dietary fats, namely triglycerides, cholesterol and phospholipids, and apoprotein (apo) B48, which is synthesized in these cells. Their density is low because their

size is large (100 nm) and they contain large amounts of lipid (especially triglycerides). Their large size precludes penetration of the capillary membrane, so they are secreted by intestinal mucosa into the lymphatics and then enter the circulation by way of the thoracic duct. Once in the blood, chylomicrons acquire apo E and apo C-II and are progressively reduced in size by the action of lipoprotein lipase, which is bound to the capillary endothelium and catalyzes the removal of free fatty acids from the chylomicron triglyceride pool. The continued action of lipoprotein lipase leaves the chylomicron nearly depleted of triglyceride. The depleted chylomicron remnant particle exits this pathway by its uptake into the hepatocyte through a receptor-mediated process, with the chylomicron apo E serving as the ligand for the hepatic LDL receptor (LDLR). In the hepatocyte the chylomicron remnant releases its contents (ie, the remaining triglycerides, cholesteryl esters, phospholipids, and apoproteins). The hepatocyte reassembles these chylomicron remnant–derived products, along with endogenous triglycerides and cholesteryl esters, into VLDLs and secretes them into the circulation for the next phase of

delivery of lipids to the periphery. Like chylomicrons, VLDLs are also triglyceride-rich and contain apo C-II and apo E. However, unlike chylomicrons, they contain fewer triglycerides, are smaller, and now carry apo B-100 instead of apo B-48. Lipoprotein lipase reduces VLDL triglyceride content further, leaving the particles progressively smaller, more dense, and more cholesterol-enriched as it moves down this cascade to intermediate density lipoprotein (IDL). Hydrolysis of IDL triglycerides to free fatty acids is mediated by another lipase, hepatic lipase, and LDL soon appears as the terminal particle in this pathway. Actually, about one third of the VLDL is cleared by the hepatic LDLR, whereas two thirds pass down this cascade, terminating as LDL. The transition of VLDL to IDL is accompanied by the transfer of apo C-II (to HDL) and is also removed (again to HDL) during the transition of IDL to LDL apo E. Hence, LDL contains only apo B-100, like the upstream precursor particles (IDL and VLDL) (3).

The forward movement of lipids to the peripheral cells is the key pathway for delivery of free fatty acids. It is also the only pathway for delivering cholesterol.

The metabolic balance of cholesterol is achieved by reverse cholesterol transport (RCT), a multi-step process mediated by HDLs which consists in the transfer of excess cholesterol arriving at the tissues back to the liver. HDLs are synthesized in the cells of intestinal mucosa and liver and secreted as a disk-shaped nascent HDL particles containing only a small amount of phospholipid and apo A-I (preβ–HDLs). Preβ–HDL gains unesterified (free) cholesterol from peripheral cells by an aqueous diffusion pathway from the cell membrane to the particle. The efflux of cholesterol is facilitated by the binding of the nascent HDL particle to cell-surface receptors (e.g. scavenger receptor B1 [SRB1]). Free cholesterol, being amphipathic, is absorbed onto the surface of the HDL from a "donor" cell membrane. Lecithin-cholesterol acyltransferase (LCAT), activated by apo A-I, catalyzes cholesterol esterification, causing the lipophilic cholesteryl ester molecule to enter the core of the HDL particle, thereby freeing up space on the surface of the particle for further cholesterol adsorption. HDL gradually matures to its spherical shape (α-HDL). Along with cholesterol absorption, HDL accumulates apo C-II and apo E from the VLDL and IDL.

Removal of lipids from the mature α-HDL particle occurs by two pathways, a direct pathway and an indirect pathway. The direct pathway mainly involves a selective lipid uptake pathway mediated by SR-B1 (4). The indirect pathway is characterized by the transfer of cholesteryl esters from α-HDL to apo B–containing lipoproteins (VLDL, IDL, and LDL) mediated by cholesteryl ester transfer protein (CETP) (6). Since cholesterol removal by HDL is accomplished by shuttling to these particles, their uptake by the liver is essential for the disposal of HDL cholesterol. In the liver, the hepatocytes expressing LDLR on their cell surface recognize apo B as well as apo E. Thus, hepatic LDLR mediates the uptake of chylomicron remnant, VLDL, IDL, and LDL.

Figure 1 (**Fig. 1**) (7) summarizes the scheme for synthesis, interaction and degradation of lipoproteins.

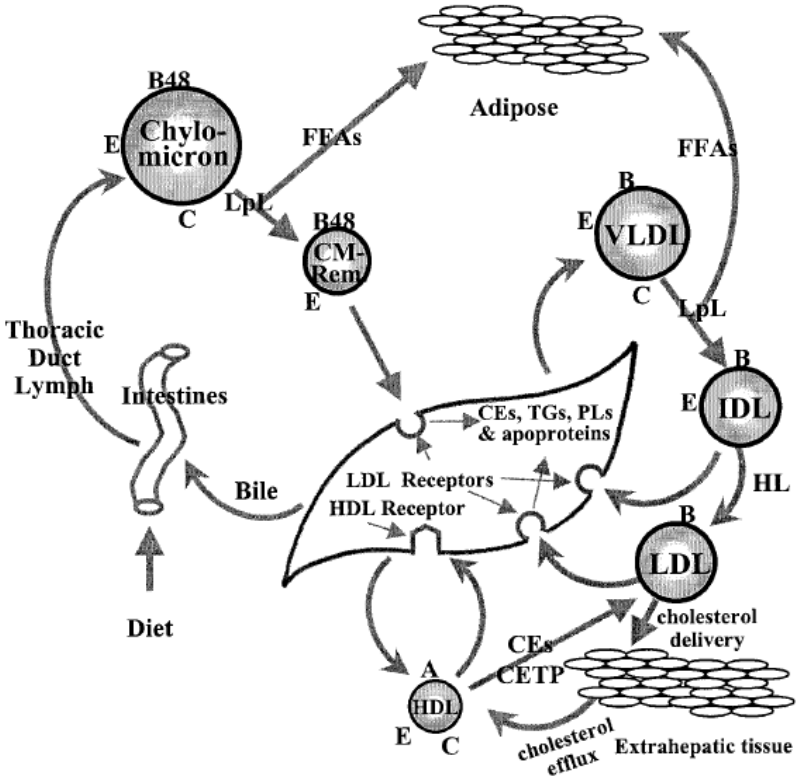

Fig. 1 Lipoprotein synthesis and metabolism

Abbreviations: LpL, Lipoprotein lipase; HL, hepatic lipase; CE, cholesteryl ester; A, B48, C, and E, apolipoproteins; B, apo B-100; TG, triglyceride; PL, phospholipid; FFA, free fatty acid; CM Rem, chylomicron remnant (Gilbert-Barnes E, Barnes L, 2000).

LDLR

As previously discussed, the LDLR is the primary pathway for removal of cholesterol from the circulation and its activity is accurately regulated by intracellular cholesterol levels. The discovery of the LDLR had its roots in the study of the mechanisms responsible for familial hypercholesterolemia (FH), an autosomal dominant metabolic disorder in which patients are characterized by plasma cholesterol levels ranging from 300 mg dL^{-1} to as high as 1500 mg dL^{-1} (8). Patients with FH are at increased risk of cardiovascular disease and those with the highest cholesterol levels often have advanced atherosclerosis before 10 years of age. FH was first recognized as a genetic disorder over 70 years ago when it was observed that extreme hypercholesterolemia that was accompanied by xanthomas (cholesterol deposits in tendons and skin) and angina was an inherited disorder. In the early 1970s Goldstein and Brown demonstrated that fibroblasts isolated from patients with homozygous FH had defective feedback inhibition of the enzyme 3-hydroxy-3-methylglutaryl CoA reductase (HMGCR), the rate-limiting enzyme for cholesterol synthesis. In 1974 they were able to

demonstrate the existence of a LDLR by showing that fibroblasts from patients with homozygous FH were unable to bind LDL at the cell surface. The following year they showed that the LDLR regulated HMGCR activity by controlling the cellular uptake of exogenous cholesterol rather than through signaling via a second messenger as they originally hypothesized. The LDLR internalized LDL from plasma leading to release of cholesterol into the cell which appeared to be responsible for the feedback inhibition of HMGCR that they had observed in their earlier studies.

The LDLR protein was isolated and sequenced in 1982 and the gene cloned in 1985 (9, 10). In the population, reduced LDLR activity frequently contributes to hypercholesterolemia which over time leads to the development of atherosclerosis.

The transcription of LDLR is primarily under the control of the transcription factor Sterol regulatory element-binding protein 2 (SREBP-2) (11). SREBP-2 is an endoplasmic reticulum transmembrane protein that exists in a complex with the sterol-sensing proteins SREBP cleavage–activating protein and insulin-induced gene 1. The SREBP/SREBP

cleavage–activating protein complex moves to the Golgi apparatus when the intracellular cholesterol concentration decreases. Proteases in the Golgi cleave SREBP-2 to release the active SREBP-2 transcription factor, which translocates to the nucleus and stimulates transcription of LDLR (12). Like many other plasma membrane receptors, LDLR is transported to the plasma membrane via the endoplasmic reticulum–Golgi pathway. LDL-bound LDLR is endocytosed through a clathrin-dependent pathway and, after releasing its cargo in the late endosome, the LDLR is either recycled back to the plasma membrane or degraded in the lysosome (13).

In addition to SREBP pathway, LDLR is also regulated by post-translational mechanisms that determine its stability. One of those involves the activity of Proprotein convertase subtilisin/kexin type 9 (PCSK9) (see next paragraph), which binds directly to the extracellular domain of the LDLR and alters its stability and trafficking by interfering with its recycling after endocytosis, thereby promoting its lysosomal degradation (14 - 16).

Moreover, the nuclear receptors Liver X receptor (LXR) LXRα and LXRβ work with SREBPs to maintain cholesterol

homeostasis. When cellular cholesterol levels rise, oxysterols are formed and serve as ligands for LXRs (17). Activation of LXR by oxysterols induces the expression of genes encoding proteins essential for cholesterol efflux from cells, including ATP-binding cassette transporter A1 (ABCA1) and ATP-binding cassette transporter G1 (ABCG1), phospholipid transfer protein, ADP-ribosylation factor-like 7, and apo E (18, 19). The expression of these factors promotes the transfer of excess intracellular cholesterol to extracellular acceptors, such as apo A-I, apo E, and HDL, thereby facilitating reverse cholesterol transport from peripheral tissues (20 - 22).

PCSK9

Seidah et al. (23) first characterized PCSK9, which is expressed in hepatocytes, kidney, mesenchymal cells, intestinal ileum and colon epithelia as well as in embryonic brain telencephalon neurons. Shortly thereafter, it was reported that single-point gain-of-function mutations (ser127-to-arg and F216L) in the PCSK9 gene are associated with autosomal dominant hypercholesterolemia (24). Experimental studies established the central role of PCSK9 in regulation of cholesterol homeostasis by enhancing the endosomal and lysosomal degradation of cell surface receptors that regulate lipid metabolism in a non-enzymatic fashion (25).

PCSK9 is synthesized as a 73-kDa zymogen of 692 amino acids and contains a signal peptide, a prodomain (residues 31 to 152) and a catalytic domain (residues 153 to 451) followed by a C-terminal domain (residues 452 to 692) (26). PCSK9 undergoes intramolecular autocatalytic processing in the endoplasmic reticulum to form a 14-kDa prodomain and a 63-kDa mature PCSK9 (27). After cleavage, the prodomain remains closely attached to the catalytic domain of PCSK9 blocking the substrate-binding site (23, 28

- 30). Autocatalytic cleavage is required for trafficking PCSK9 from the endoplasmic reticulum (ER) to the secretory pathway (31). In the extracellular pathway, PCSK9 is secreted from the trans-Golgi network and internalized together with the LDLR in clathrin-coated endosomes, promoting degradation of LDLR (31). In the intracellular pathway, PCSK9 is directly sorted to lysosomes together with LDLR, leading to its degradation (**Fig. 2**) (25, 32). Secretion of the prodomain together with a catalytically inactive PCSK9 was shown to promote regular degradation of LDLR, suggesting that secreted PCSK9 acts as a chaperone rather than as a catalytic enzyme (33, 34).

As described in the previous paragraph, the major part of circulating LDL-cholesterol (LDL-C) is removed from the plasma by hepatic uptake. This process is mediated via LDLR that internalizes bound LDL particles by endocytosis (35). After intracellular dissociation, the LDLR recycles to the cell surface for reuse. Low intracellular cholesterol levels activate the sterol regulatory element binding protein-2 (SREBP-2), leading to increased LDLR gene expression, which enhances LDL-C clearance from the circulation (36). Of note, SREBP-2 also induces expression

of PCSK9, leading to LDLR degradation, thus limiting hepatic cholesterol uptake and increasing circulating LDL-C (36). This highly coordinated expression pattern contributes to a self-regulatory system preventing excessive cholesterol uptake in order to preserve cholesterol homeostasis.

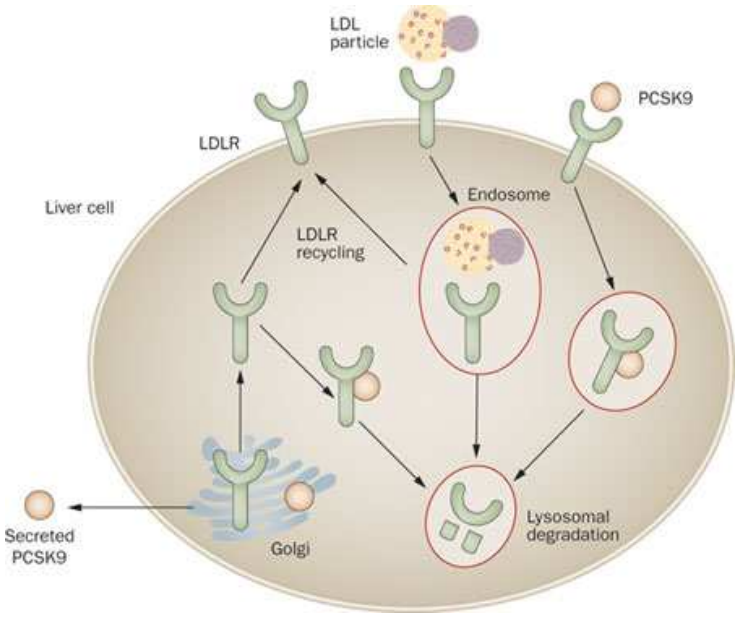

Fig. 2 The PCSK9 protein acts through endogenous and exogenous mechanisms.

Exogenously, circulating PCSK9 protein binds to the LDLR. Once internalized into the liver cell, the PCSK9 protein directs the LDLR to the lysosome for degradation. Intrinsically, PCSK9, which is secreted from the Golgi apparatus, binds the LDLR before it reaches the cell

surface, leading it to lysosomal degradation (Brautbar A, Ballantyne CM, 2011).

PATHOGENESIS OF ATHEROSCLEROSIS

Abnormalities in lipid metabolism play a critical role in the development of atherosclerosis.

Atherosclerosis is a chronic disease characterized by the narrowing of arteries caused by a buildup of plaque and it is the major cause of death and morbidity in the United States and the industrial world, being the underlying cause of heart attack, stroke, and peripheral vascular disease (37). In particular, the discovery by Virchow more than 100 years ago that atheroma contained a yellow fatty substance, later identified as cholesterol, suggested a role for lipids in the pathogenesis of atherosclerosis (38).

Atherosclerosis is a complex disease, involving many cell types and circulating mediators and resulting in an inflammatory state. The key stages of atherosclerosis development have been briefly described in the following paragraphs.

Initiation and Fatty Streak Phase of Atherosclerotic Lesions

Endothelial cells of arteries respond to mechanical and molecular stimuli to regulate tone (39), hemostasis (40),

and inflammation (41) throughout the circulation. Endothelial cell dysfunction is an initial step in atherosclerotic lesion formation and is more likely to occur at arterial curves and branches that are subjected to low shear stress and disturbed blood flow (42, 43). These mechanical stimuli activate signaling pathways leading to a dysfunctional endothelium, that is barrier compromised, prothrombotic, and proinflammatory (44). In regions resistant to atherosclerosis, the transcription factors Kruppel-like factors (KLF) 2 and 4 are activated in a process which enhances expression of endothelial nitric oxide synthase (eNOS) (45 – 47). The increased nitric oxide (NO) production promotes endothelial cell migration and survival thereby maintaining an effective barrier (48). In addition, the expression of superoxide dismutase (SOD) is increased to reduce cellular oxidative stress (46). In atherosclerosis susceptible regions, reduced expression of eNOS and SOD leads to compromised endothelial barrier integrity (**Fig. 3**) (49), leading to increased accumulation and retention of subendothelial atherogenic apo B-containing lipoproteins (LDL) and remnants of VLDL and chylomicrons (50, 51). KLF2, KLF4, and NO production

inhibit activation of the nuclear factor kappa B (NF-κB) pathway. Increased NF-κB activation in atherosclerosis susceptible areas leads to endothelial cell activation (**Fig. 3**) (49), as evidenced by increased expression of monocyte adherence proteins (Vascular Cell Adhesion Molecule 1, VCAM-1; Intercellular Adhesion Molecule 1, ICAM-1; P-selectin) and proinflammatory receptors (toll-like receptor 2, TLR2) and cytokines (Monocyte Chemoattractant Protein 1, MCP-1; Interleukin 8, IL-8) (47, 52, 53). In addition, endothelial cell activation leads to increased production of reactive oxygen species (54) that can cause oxidative modification of apo B-containing lipoproteins. Besides mechanical stimuli, endothelial cell activation is increased by various molecular stimuli, including oxidized LDL, cytokines, advanced glycosylation end products, and pathogen-associated molecules (55 - 58). In contrast, an atheroprotective function of HDL is to prevent endothelial activation and enhance NO production to maintain barrier integrity (59).

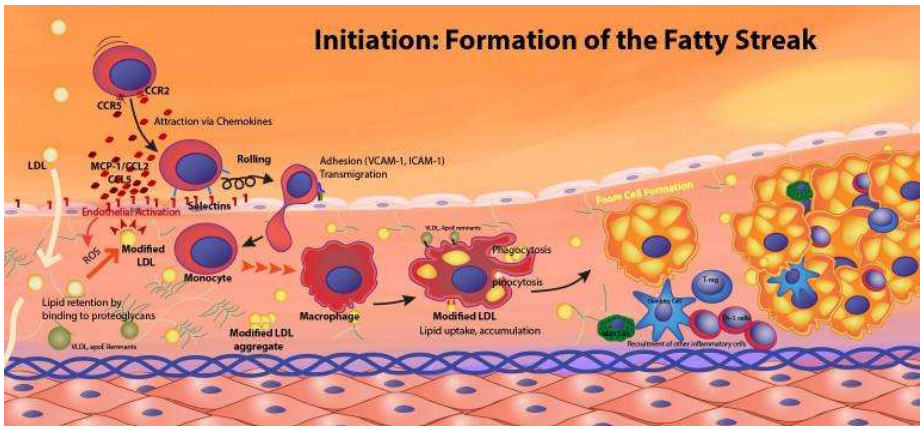

Fig. 3 Initiation of atherosclerotic lesion

Schematic view of the cascade of events leading to the accumulation and retention of subendothelial LDL and remnants of VLDL and chylomicrons, with formation of the fatty streak.
(Linton MR F et al for De Groot LJ, Chrousos G, Dungan K, et al 2000 - 2015).

Activation of endothelial cells causes a monocyte recruitment cascade involving rolling, adhesion, activation and transendothelial migration (**Fig. 3**) (49). Selectins, especially P-selectin, mediate the initial rolling interaction of monocytes with the endothelium. Monocyte adherence is then promoted by endothelial cell immunoglobulin-G proteins including VCAM-1 and ICAM-1 (60). Potent chemoattractant factors such as MCP-1 and IL-8 then induce migration of monocytes into the subendothelial space (61-63). Intimal macrophages also result from proliferation of monocyte/macrophages, especially in more advanced lesions (64). Although macrophages are the main infiltrating cells, other cells contribute to development of lesions including dendritic cells,mast cells and T cells (**Fig. 3**) (49). T cells regulate the proinflammatory phenotype of macrophages. Antigen-specific activated T helper 1 (Th-1) cells produce interferon (IFN) that converts macrophages to a proinflammatory M1 phenotype. Regulatory T (T-reg) cells produce anti-inflammatory cytokines (e.g. Transforming Growth Factor β, TGF-β) and inhibit activation of Th-1 cells leading more anti-inflammatory M2

macrophages. During the initial fatty streak phase of atherosclerosis (**Fig. 3**) (49), the monocyte-derived macrophages internalize the retained apo B-containing lipoproteins, which are degraded in lysosomes, where excess free cholesterol is trafficked to the ER to be esterified by acyl CoA:cholesterol acyltransferase (ACAT), and the resulting CE is packaged into cytoplasmic lipid droplets, which are characteristic of foam cells (65, 66). Modification of apo B lipoproteins via oxidation and glycation enhances their uptake through a number of receptors not down-regulated by cholesterol including CD36, scavenger receptor A, and lectin-like receptor family (67, 68). Enzyme-mediated aggregation of apo B lipoproteins enhances uptake via phagocytosis (69, 70). In addition, native remnant lipoproteins can induce foam cell formation via a number of apo E receptors (LRP1 and VLDLR).

The triggering of macrophage inflammatory pathways is also a critical event in lesion development. Inflammatory M1 phenotype macrophages exhibit increased oxidative stress, impaired cholesterol efflux and enhanced cytokine/chemokine secretion, leading to more

LDL/remnant oxidation, endothelial cell activation, monocyte recruitment, and foam cell formation (71-76) . Macrophage foam cell formation and cholesterol dependent inflammatory receptor signaling can be reduced by the removal of cholesterol by atheroprotective HDL and apo A-I via a number of mechanisms including ABCA1, ABCG1, Scavenger receptor class B member 1 (SR-BI), and aqueous diffusion (77-80). Lipid-poor apo A-I stimulates efflux via ABCA1, whereas lipidated apo A-I or mature HDL are the main drivers of efflux via ABCA1, ABCG1, SR-BI, and aqueous diffusion (77, 81-83).

Progression to Advanced Atherosclerotic Lesions

Fatty streaks do not result in clinical complications and can even undergo regression. However, once smooth muscle cells infiltrate and the lesions become more advanced, regression is less likely to occur (84, 85). Small populations of vascular smooth muscle cells (VSMCs) already present in the intima proliferate in response to growth factors produced by inflammatory macrophages (86). In addition, macrophage-derived chemoattractants cause tunica media

smooth muscle cells to migrate into the intima and proliferate (**Fig. 4**) (49). Critical smooth muscle cell chemoattractants and growth factors include Platelet-derived growth factor (PDGF) isoforms (87), matrix metalloproteinases (88), fibroblast growth factors (FGF) (89), and heparin-binding epidermal growth factor (HB-EGF) (90) **(Fig. 4)** (49). The accumulating VSMCs produce a complex extracellular matrix composed of collagen, proteoglycans, and elastin to form a fibrous cap over a core comprised of foam cells. As lesions advance, substantial extracellular lipid accumulates in the core, in part due to large CE-rich particles arising from dead macrophage foam cells (91, 92).

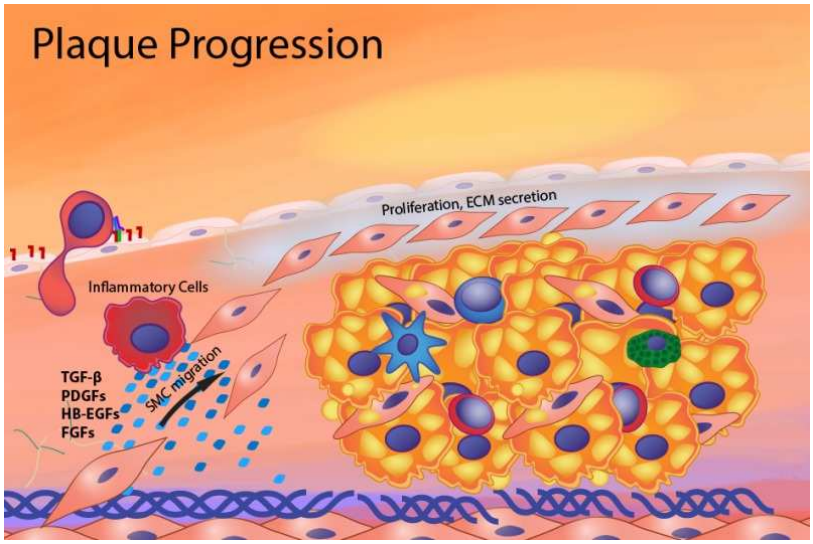

Fig. 4 Progression to advanced atherosclerotic lesions

This stage is mediated by VSMC proliferation and accumulation, to form a fibrous cap over a core of foam cells through the production of extracellular matrix. (Linton MR F et al for De Groot LJ, Chrousos G, Dungan K, et al 2000 - 2015).

Vulnerable Plaque Formation and Rupture

The advanced atherosclerotic lesion is essentially a nonresolving inflammatory condition leading to formation of the vulnerable plaque, increasing the risk of plaque rupture. The vulnerable plaque is characterized by two fundamental morphological changes: 1) Formation of a necrotic core and 2) Thinning of the fibrous cap. Sections of the atheroma with a deteriorated fibrous cap are subject to rupture **(Fig. 5)** (49, 93, 94). Plaque rupture leads to acute exposure of procoagulant and prothrombotic factors from the necrotic core of the lesion to platelets and procoagulant factors in the lumen, thereby causing thrombus formation **(Fig. 5)** (49, 93, 94). Thrombus formation accounts for the majority of clinical events with acute occlusive thrombosis causing myocardial infarction, unstable angina, sudden cardiac death, and stroke (93, 94).

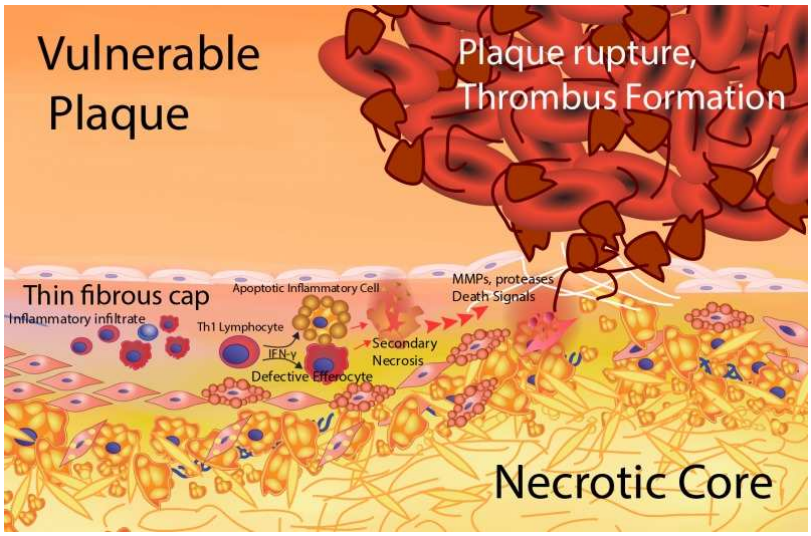

Fig. 5 Vulnerable plaque formation

In advanced lesions, plaque is characterized by the formation of a necrotic core and a thin fibrous cap. Deteriorated fibrous caps are subject to rupture, with the increased risk of thrombus formation (Linton MR F et al for De Groot LJ, Chrousos G, Dungan K, et al 2000 - 2015).

ARTERIAL INJURY RESPONSE: NEOINTIMAL HYPERPLASIA

Once the atherosclerotic plaque develops in a way which interferes with blood flow, the only current treatments available to alleviate vascular occlusion are limited to surgical procedures such as transluminal coronary angioplasty, percutaneous delivery of balloon-expanded stents, directional coronary atherectomy and coronary bypass surgery. Unfortunately, a common undesirable outcome of these interventions is represented by restenosis secondary to neointimal hyperplasia, which remains a major problem after this kind of procedures (95). Neointimal formation can be suppressed by the topical administration of antiproliferative drugs. In percutaneous coronary intervention the concept of "local drug delivery" has been used for almost a decade with great success. In recent years, drug-eluting stents and drug coated balloons (96) have also been increasingly used in the treatment of peripheral arterial disease, even though further validations in large randomized trials are needed.

The development of neointimal hyperplasia is a complex process initiated by injury and exposure of the VSMC to circulating blood elements. The process is further

characterized by platelet aggregation, leukocyte chemotaxis, VSMC proliferation and migration, extracellular matrix (ECM) changes, and, finally, endothelial cell proliferation.

The carotid artery balloon injury model in rats is an important method to study the molecular and cellular mechanisms involved in neointimal formation and vascular remodeling (97). This approach consists of isolating a segment of carotid artery vasculature in an anesthetized laboratory rat, creating an arteriotomy incision in the external carotid branch through which the balloon catheter is inserted, advancement of the catheter through the common carotid artery, repeated inflation and withdrawal of the catheter to induce endothelial cell loss and mural distension, and removal of the catheter with closure of the arteriotomy and resumption of blood flow through the common carotid artery and internal carotid artery branch. The initiating event in neointimal hyperplasia is endothelial denudation, which exposes the underlying VSMC to circulating blood elements activating a cascade of events culminating in neointimal formation (98). After endothelial loss, platelets aggregate and adhere to the site of injury.

After platelet aggregation and adherence, leukocyte chemotaxis occurs. Leukocytes are responsible for the secretion of many cytokines and growth factors that influence the subsequent events in neointimal hyperplasia (99). One example is macrophages that produce PDGF and interleukin-1 (IL-1), which both promote VSMC proliferation and are released in the arterial wall during the repair process (100, 101). In conjunction with leukocyte chemotaxis, VSMC proliferation and migration are the fundamental characteristics of neointimal hyperplasia. This proliferation is, in part, initially mediated by the release of basic fibroblast growth factor (bFGF), which is a potent mitogen for VSMC in vivo (102). Proliferation begins as early as 24 hours after injury and continues for several weeks (103). Under the influence of PDGF, VSMC begin migrating to the intima between 1 to 3 days after injury (104). Other growth factors such as TGF-β and angiotensin II might also promote intimal thickening.

The ECM generally acts as a barrier to VSMC migration from the media to the intima; however, after injury the ECM is modified to allow for the movement of cells. Migration and matrix reconfiguration are associated with

an increase in the expression and activity of matrix-degrading enzymes (105, 106). Among these proteolytic enzymes, two families seem to be important in this regard, the matrix metalloproteases (MMP), and the enzymes of the plasmin system.

Finally, to restore the barrier of the endothelium disrupted by injury, endothelial proliferation must occur. Concurrent with VSMC proliferation and migration, endothelial regeneration begins through stimulation by bFGF. This regeneration begins from the ends of the denuded area and approaches the center within several weeks, restoring endothelial continuity.

MOUSE MODELS FOR THE STUDY OF ATHEROSCLEROSIS

Research on genetically-modified mouse models is crucial to provide insights into the role of genes and environmental factors in atherosclerotic process.

Wild-type mice are quite resistant to atherosclerosis as a result of high levels of antiatherosclerotic HDL and low levels of proatherogenic LDL and VLDL. Therefore, the current mouse models for atherosclerosis are based on perturbations of lipoprotein metabolism through dietary or genetic manipulations. One of the most commonly used mouse models is represented by apo E–deficient mice (apo $E^{-/-}$ mice), in which targeted deletion of the *apoE* gene leads to severe hypercholesterolemia and spontaneous atherosclerosis, and LDLR–deficient mice ($LDLR^{-/-}$ mice or LDLR KO mice), in which atherosclerosis develops especially when animals are fed a lipid-rich diet.

Apo $E^{-/-}$ mice

Apo E is synthesized in the liver and in macrophages and exerts important antiatherogenic functions. As a constituent of plasma lipoproteins it serves as a ligand for

the cell-surface lipoprotein receptors such as LDLR and LDLR-related proteins (LRPs) (107), thereby promoting the uptake of atherogenic particles from the circulation. Consequently, homozygous deletion of the *apoE* gene in mice results in a pronounced increase in the plasma levels of LDL and VLDL attributable to the failure of LDLR- and LRP- mediated clearance of these lipoproteins. Therefore, the phenotype of apo $E^{-/-}$ mice is characterized by the spontaneous development of atherosclerotic lesions, even on a standard chow diet which is low in its fat content (< 40 g kg^{-1}) and does not contain cholesterol. Lesions of apo $E^{-/-}$ mice resemble their human counterparts and develop over time from initial fatty streaks to complex lesions. The development of lesions can be strongly accelerated by a high-fat, high-cholesterol (HFC) diet (108). Because of the rapid development of atherosclerosis, the apo $E^{-/-}$ model has been used widely, despite considerable limitations. An important limitation linked to the complete absence of apo E protein is that the model is dominated by high levels of plasma cholesterol. For instance, on a chow diet plasma cholesterol concentrations are about 8 mmol L^{-1}, compared with 2 mmol L^{-1} for the wild-type C57Bl/6 mouse, and can

become >70 mmol L^{-1} on a HFC diet (109). Another limit is that most plasma cholesterol is confined to VLDL and not to LDL particles as in humans.

$LDLR^{-/-}$ mice

In humans, mutations in the gene for the LDLR cause familial hypercholesterolemia. Mice which lack the gene for LDLR show a moderately elevated plasma cholesterol level when maintained on a standard chow diet (about 5 mmol L^{-1} versus 2 mmol L^{-1} in wild-type animals), and they develop atherosclerosis only slowly. On HFC diet feeding, $LDLR^{-/-}$ mice show strongly elevated plasma cholesterol (> 25 mmol L^{-1}) and rapid development of atherosclerosis (107). The plasma lipoprotein profile of $LDLR^{-/-}$ mice resembles that of humans, with the cholesterol being confined mainly to the LDL fraction. Interestingly, $LDLR^{-/-}$ mice coupled with an apo B-editing deficiency ($LDLR^{-/-}$/ apo $BEC^{-/-}$ mice) (110) or combined with human apo B100 transgenic mice ($LDLR^{-/-}$/apo $B^{+/+}$) (111) show a large increase in plasma LDL cholesterol and develop

atherosclerosis on a low-fat diet. The morphology of the lesions in LDLR$^{-/-}$ mice is similar to that of apo E$^{-/-}$ mice, with the plaques developing in a time-dependent manner. In the light of these evidences, the LDLR $^{-/-}$ mouse represents a more moderate model than the apo E$^{-/-}$ mouse, mainly because of the milder degree of hyperlipidemia (112, 113).

PCSK9 ANIMAL MODELS

PCSK9 $^{-/-}$ mice

PCSK9 knockout results in viable and fertile mice exhibiting severe hypocholesterolemia (114, 115),with an ≈40% and ≈80% drop in total cholesterol and LDL-C, respectively (PCSK9$^{-/-}$ or PCSK9 KO mice) (116). In comparison, liver-specific PCSK9$^{-/-}$ mice exhibit ≈27% less circulating cholesterol, suggesting that liver PCSK9 contributes to ≈70% of the cholesterol phenotype (116). Interestingly, the liver-specific loss of PCSK9 expression (115) resulted in its complete absence from circulation, demonstrating that hepatocytes are the primary source of plasma PCSK9 (117). In mice fed a high-fat, high-cholesterol diet, gene inactivation of PCSK9 significantly reduced aortic cholesteryl esters, which were markedly increased by overexpression of PCSK9, resulting in accelerated development of atherosclerotic plaque (118). Effects which are comparable were observed in apo E-deficient mice expressing null, normal, or high levels of PCSK9 (118). Interestingly, circulating LDL-C levels differed only slightly among these animals, and it is unclear whether the slightly

higher LDL-C level found in transgenic mice is the only cause of the marked increase in plaque burden observed in these animals (118). In $LDLR^{-/-}$ mice expressing null, normal, or high levels of PCSK9, the circulating cholesterol levels and aortic accumulation of cholesteryl esters were similar to those of wild-type mice, indicating that the harmful effect of PCSK9 on atherogenesis is mediated mainly by degradation of LDLR (118).

L-HOMOARGININE: A NOVEL PROTECTIVE AGENT AGAINST CARDIOVASCULAR DISEASE

L-homoarginine synthesis

L-Homoarginine is a nonproteinogenic amino acid structurally related to L-arginine. Circulating L-homoarginine concentrations have been linked to single-nucleotide polymorphisms (SNPs) in several population-based studies. Genome-wide association studies (GWAS) from the Gutenberg Health Study first identified an association between L-homoarginine plasma concentrations and SNPs related to the L-arginine:glycine amidinotransferase (AGAT) gene on chromosome 15 (119). The leading SNP rs1288775 encodes for the exchange of A ->T, resulting in the missense mutation Gln110His within the second exon of the AGAT gene. Carriers of two AA alleles showed higher plasma concentrations, that is [2.24 (1.75, 2.95) µmol L^{-1}] [mean (interquartile range)], whereas L-homoarginine was lower in AT carriers [2.08 (1.55, 2.54) µmol L^{-1}] and lowest in TT carriers [1.80 (1.40, 2.28) µmol L^{-1}], representing a gene dose-dependent decrease by 16 and

24%, respectively. The minor allele frequency was 6% for AA carriers. GWAS from patients of the Ludwigshafen RIsk and Cardiovascular Health (LURIC) study and from participants of the Young Finns Study confirmed the strong association between circulating L-homoarginine and SNPs related to the AGAT gene (120). AGAT was demonstrated to be the rate-limiting enzyme of creatine synthesis. In kidney, AGAT catalyzes the transfer of L-arginine's guanidino group to glycine producing guanidinoacetate and ornithine **(Fig. 6)** (121). In the liver, methylation of guanidinoacetate is catalyzed by guanidinoacetate N-methyltransferase (GAMT), resulting in creatine formation (122). Creatine represents a rapidly available energy buffer especially in heart and brain. AGAT knockout mice are lacking creatine and guanidinoacetate. AGAT deficient mice display a lean phenotype with muscular dystrophy, which is completely reversible on creatine supplementation (123, 124). Further metabolic analysis revealed that humans and mice with AGAT deficiency are inefficient at synthesizing L-homoarginine from L-arginine and L-lysine (119, 125).

AGAT is able to transfer the guanidine group from L-arginine not only to glycine but also to L-lysine, thereby

producing not only guanidinoacetate but also L-homoarginine, respectively **(Fig. 6)** (121).

It is noteworthy that L-homoarginine was identified as a component of different species of Lathyrus (grass pea) as well (126).

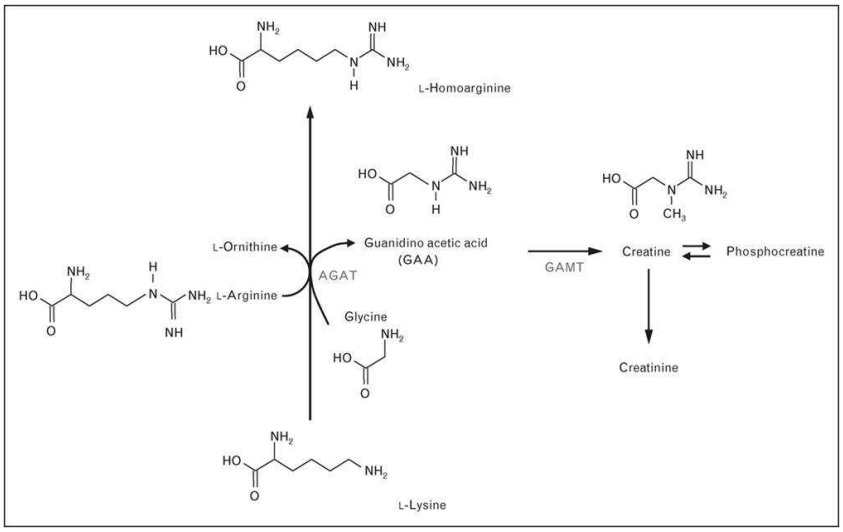

Fig. 6 Synthesis of L-homoarginine

L-homoargine mainly derives from the action of AGAT enzyme, which is able to transfer the guanidine group from L-arginine to L-lysine, thereby producing L-homoarginine (Atzler D, Schwedhelm E, Choe CU, 2015).

L-homoarginine physiology

Recent studies have indicated that homoarginine is involved in vascular function and disease. In particular, because of its structural similarity with L-arginine, L-homoarginine is able to interfere with L-arginine pathways. Probably the most important function of L-arginine is to serve as substrate for NO synthesis. Several studies showed that L-homoarginine can represent an alternative substrate for NOS (127, 128), even though weaker than L-arginine. Consistently, studies conducted in mice (129) revealed lower maximal NO levels, but more sustained NO formation after L-homoarginine supplementation compared with arginine. Circulating nitrate concentrations, an indirect measure for NOS activity, were increased even 8h after L-homoarginine treatment, whereas nitrate levels in arginine supplemented mice returned to baseline after 4h (129).

In particular, Radomski et al. studied the physiological role of L-homoarginine in human platelets. In this context, L-homoarginine was found to inhibit aggregation of human platelets stimulated with collagen similarly to L-arginine (130). However, the physiological relevance of these

findings needs further validation because L-homoarginine was effective only in supraphysiological concentrations.

In addition to these findings, several groups have shown that homoarginine is able to inhibit the enzyme arginase, suggesting increased L-arginine levels and subsequently increased NO formation (127, 131). Compared to L-arginine, L-homoarginine plasma concentrations *in vivo* are relatively low and high concentrations were required *in vitro* for arginase inhibition. Therefore, further investigations are needed to clarify L-homoarginine's physiological significance as an endogenous metabolite of the NO pathway.

Role of L-homoarginine in cardiovascular disease (CVD)

In healthy humans, circulating concentrations of L-homoarginine are about 2 to 3 µmol L^{-1} with age-related and sex-related differences. Reference ranges for serum L-homoarginine obtained from healthy participants of the population-based Study of Health in Pomerania were 1.41–5.00 and 1.20–5.53 µmol L^{-1} (2.5th; 97.5th percentile), for men and women, respectively (133). In 2010, Marz et al. (133) published data from the LURIC and 4D (Die Deutsche

Diabetes Dialyse) studies, showing a strong association between low L-homoarginine serum levels and increased cardiovascular and all-cause mortality. Cross-sectional analyses of these studies linked L-homoarginine to markers of endothelial function (i.e., intercellular adhesion molecule-1 and vascular cell adhesion molecule-1), suggesting that L-homoarginine might improve endothelial function. The association of L-homoarginine with overall mortality and cardiovascular death in a population of older age has been recently confirmed by the results from the Hoorn study (134).

Low L-homoarginine was shown to predict fatal strokes in the LURIC study and was associated with sudden cardiac death or death due to heart failure in the 4D study (135, 136). To elucidate the clinical phenotypes involved, circulating L-homoarginine was associated with angiographic ejection fraction and laboratory parameters of heart failure, specifically N-terminal pro B-type natriuretic peptide, suggesting a positive correlation between L-homoarginine and myocardial function. Taken together, angiographic, laboratory, and clinical parameters of heart failure are associated with L-homoarginine levels,

but the underlying pathophysiological mechanism remains unclear. Some authors suggest that low L-homoarginine levels might indicate reduced intracellular energy stores, which is a hallmark of heart failure (137). Clinical studies have confirmed cellular and molecular causal associations of L-homoarginine with creatine (135, 123). As described, phosphorylated creatine serves as a spatial and temporal energy buffer and key components of the creatine:phosphocreatine system are downregulated in the failing heart (137). In line with this observation, a moderate elevation of intracellular creatine protects mice from acute myocardial infarction (138). Murine studies and cell culture experiments have shown that levels of both creatine and homoarginine are dependent on AGAT and, therefore, positively correlate with each other (119, 123). Association studies in humans have confirmed this finding (119, 120). Therefore, it was hypothesized that circulating L-homoarginine might indicate the status of intracellular energy stores in heart failure. However, recent results suggest that the association of creatine and heart failure is not as trivial as presumed. In this context, Phillips et al. (139) reported that chronically increased myocardial

creatine leads to the development of progressive hypertrophy and heart failure, suggesting rather a bell-shaped association of creatine. Lygate et al. (140) furthermore reported that creatine-deficient mice revealed an unaltered response to chronic myocardial infarction, suggesting that creatine might be a dispensable metabolite for left ventricular remodeling and development of chronic heart failure following myocardial infarction. Thus, the relevance of creatine and L-homoarginine within cardiac energetics in heart failure remains unclear. Other studies have suggested an increased risk of cerebrovascular disease in patients with chronic kidney disease (141). A large meta-analysis revealed that the overall risk ratio for patients with reduced estimated glomerular filtration rate of less than 60 ml/min/1.73 m^2 was 1.43 (confidence interval 1.31–1.57, P<0.001) (142). Cross-sectional analyses of the Leeds Stroke cohort, LURIC study, and 4D study revealed positive correlations of circulating L-homoarginine with parameters of kidney function, that is creatinine levels and estimated glomerular filtration rate (119, 133, 135). Given that AGAT is mainly expressed in the kidney, renal dysfunction and damage might be associated with reduced

AGAT expression and, therefore, reduced L-homoarginine production. The involvement of L-homoarginine in renal NO metabolism might also be an explanation for the association of L-homoarginine with renal function. NOS, which is expressed in the kidney, regulates renal hemodynamics and is regulated in response to injury [30]. Therefore, interplay between L-homoarginine, renal hemodynamics, kidney damage, and finally mortality is highly relevant (143).

In the Hoorn cohort of older participants as well as in patients undergoing coronary angiography (LURIC), circulating L-homoarginine positively correlated with systolic and diastolic blood pressure (134, 144). An increase of L-homoarginine levels by about 0.5 μmol L^{-1} was associated with an increase of systolic blood pressure by 3.9 mmHg. Given that an increase of systolic blood pressure by 20 or 10 mmHg diastolic is associated with doubling of cardiovascular mortality (145), it is very unlikely that blood pressure changes are involved in mediating the beneficial effects of L-homoarginine in vascular disease. In addition to smoking and hypertension, associations between L-homoarginine and metabolic parameters have

been described. Positive correlations were found with body mass index (BMI) and triglyceride levels, but not with low-density lipoprotein or high-density lipoprotein cholesterol levels. In the LURIC study, no correlation was found between L-homoarginine and parameters of glucose metabolism (i.e., hemoglobin A1c and diabetes), whereas results from the Hoorn study (144) indicated a positive correlation between L-homoarginine with hemoglobin A1c. Because of the conflicting data between the studies, it remains unclear whether L-homoarginine has a causal effect on blood pressure and metabolic parameters or whether these effects are mediated by creatine metabolism.

DIETARY FISH COMPONENTS: EFFECT ON CARDIOVASCULAR DISEASE

Lowering LDL-C is a central goal in the prevention of cardiovascular disease. Although genetic factors and aging are important in determining the overall risk, many are the evidences indicating the crucial role of molecules derived from food, the so-called nutraceuticals, which appeared to play a role in the prevention and treatment of CVD (146).

Marine environment, in particular the ocean, is enhancing its importance as a source for novel compounds, which may serve in improving health of the worldwide population.

Observational studies reported in the 1970s showed that the Greenland Inuit populations had a low incidence of coronary artery disease that was related to their traditional lifestyle and in particular their distinctive dietary habits, characterized by the consumption of cold-water marine fish and artic mammals, rich in W-3 (or n-3) polyunsaturated fatty acids (PUFAs), particularly eicosapentaenoic acid (EPA, 20:5 n-3) and docosahexaenoic acid (DHA, 22:6 n-3) (147-149). Subsequently, prospective epidemiological studies reported that high fish consumption was associated with a lower mortality from coronary artery disease (150, 151) and several data highlighted that n-3 PUFAs are able to affect lipid profile (152-154), arrhythmia (155), platelet activity (156, 157), endothelial function (158, 159), inflammation (160), and blood pressure (161), as displayed in figure 7 **(Fig. 7)** (162) .

This said, it is possible that the potential benefits of fish consumption could, in addition to n-3 PUFAs, be attributed

to other nutrients, such as minerals, vitamins and proteins (163) **(Fig. 7)** (162), as emerged by recent clinical trials.

In particular, published data have demonstrated the importance of fish protein hydrolysates containing bioactive peptides for the prevention/management of cardiovascular disease, being able to affect the lipid profile and blood pressure (164) **(Fig. 7)** (162).

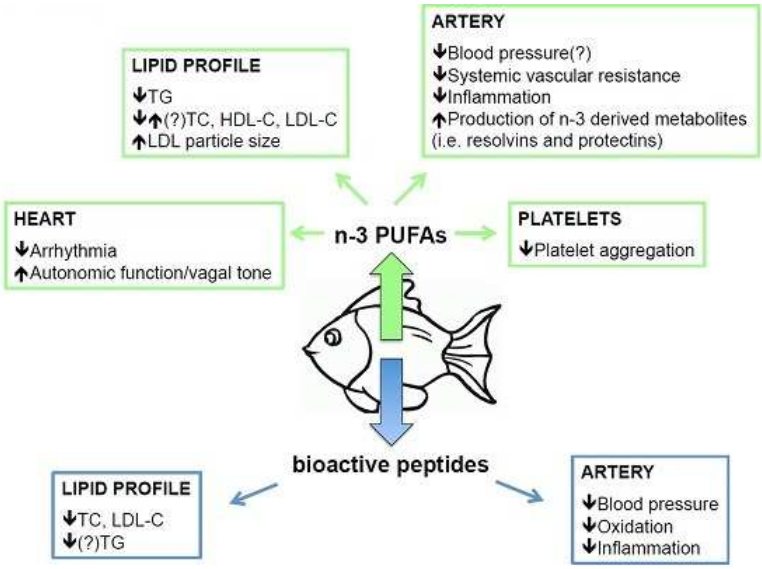

Fig. 7 Importance of fish-derived n-3 PUFAs and bioactive peptides for cardiovascular health.

These molecules are able to exert multiple beneficial effects on lipid profile, blood pressure, inflammation and platelet aggregation. (Chiesa G et al, 2016).

Fish Proteins and Dyslipidemias

In studies conducted in animals, it was observed that proteins from different fish species are able to exert hypocholesterolemic activity when compared with casein as protein source (165). The mechanisms responsible for this hypocholesterolemic effect have not been fully elucidated. The amino acid composition of dietary proteins probably influences plasma cholesterol levels. On this respect, dietary proteins with a low ratio of methionine-glycine and lysine-arginine, such as fish proteins, seem to favor a hypocholesterolemic effect (166, 167), in contrast with bovine casein, which tends to increase cholesterol levels and is characterized by a high ratio of methionine-glycine and lysine-arginine (168). The mechanisms responsible for the hypocholesterolemic effect of fish proteins include increased hepatic LDLR expression (169, 170). Moreover, administration of fish protein hydrolysates to rats was shown to lead to an increased hepatic cholesterol 7α-hydroxylase expression and higher cholesterol and bile acids fecal content compared with casein-fed animals (171). In this study, a hypotriglyceridemic effect by fish protein hydrolysate was

observed as well. In addition, consumption of a cod-fish protein supplement by overweight adults had no effect on triglycerides or HDL-C levels, but significantly decreased serum LDL-C levels from baseline (172).

Given these evidences, further studies are required on larger cohorts and for longer time spans in order to confirm the hypocholesterolemic effect of fish protein intake.

Fish Proteins and hypertension

Peptides from different food sources have been demonstrated to exert antihypertensive activity both in experimental models and in human volunteers (173). The discovery of antihypertensive peptides from marine organisms started in the early 1990s, when “Katsuobushi”, a Japanese seasoning prepared from bonito, a fish from tuna family, was examined for its potential to inhibit the activity of angiotensin-converting enzyme (ACE). Fujita et al. (174) developed a thermolysin hydrolysate from “Katsuobushi”. This hydrolysate was administered to normotensive human subjects and to patients with mild or moderate hypertension in a small-scale clinical trial. The

hydrolysate contained the previously described ACE inhibitory peptide LKPNM (175).

A significant decrease of both systolic and diastolic blood pressure was reported (176). Potent ACE inhibitory peptides derived from salmon were also found to possess strong antihypertensive effect in spontaneously hypertensive rats (SHR) (177).

Fish-derived bioactive peptides have enormous potential and have been utilized in the production of pharmaceutical products with an active functional role and effect on health; for example, blood pressure lowering capsules have been manufactured that contain Katsuobushi Oligopeptide LKPNM which is converted into its active form (LKP) by digestive enzymes (Vasotensin 120TTM by Metagenics, Aliso Viejo, CA, USA; PeptACETM Peptides 90 by Natural Factors, Monroe, WA, USA) (178).

MICRORNAS: ROLE IN LIPOPROTEIN METABOLISM AND ATHEROSCLEROSIS

A class of short non-coding RNAs, termed microRNAs (miRNAs), has recently emerged. MiRNAs act as critical regulators of a wide variety of physiologic functions, from development and metabolic regulation to aging and disease progression (179).

MiRNA transcripts are encoded both in intergenic regions and within introns of genes and can be transcribed either through their own promoters or in concert with their host genes. In the canonical miRNA biogenesis pathway, a primary miRNA transcript (pri-miRNA) is transcribed by the Polymerase II enzyme, after which it undergoes processing by the Drosha/DGCG8 complex to generate a precursor miRNA transcript (pre-miRNA). Following export to the cytoplasm, a pre-miRNA undergoes further cleavage by DICER to generate a mature miRNA duplex of 20-23 nucleotides in length. Argonaute proteins then help to mediate the separation of the miRNA strands and incorporation into the RNA-induced silencing complex (RISC). Within the RISC, miRNAs bind partially complementary target sites, primarily within messenger

RNA (mRNA) 3' untranslated regions (3'UTRs), resulting in translational repression and/or mRNA destabilization (180, 181) **(Fig. 8)** (182). Since the seed region required for miRNA target recognition is small, individual miRNAs have the capacity to regulate over 100 mRNA targets (183, 184) and some miRNAs have been demonstrated to target numerous genes within interrelated pathways to facilitate complex physiologic changes. miRNAs could also play an important role in the communication process among organs, since it has been shown that they are transported through the blood stream in exosomes (185), apoptotic bodies (186), HDL particles (187) and in complexes with Argonaute 2 (Ago2) (188). These circulating miRNAs are able to regulate the expression of target mRNAs after the uptake by recipient cells (189, 190). In addition, the stability of miRNAs within the blood and the relative ease with which their expression can be measured, suggest that circulating miRNAs may be utilized as biomarkers of disease development and progression. Indeed, circulating pools of numerous miRNAs have been found to be dysregulated in a wide variety of different disease states including cardiovascular diseases, such as hypertension, coronary

artery disease, myocardial infarction, and heart attack (191).

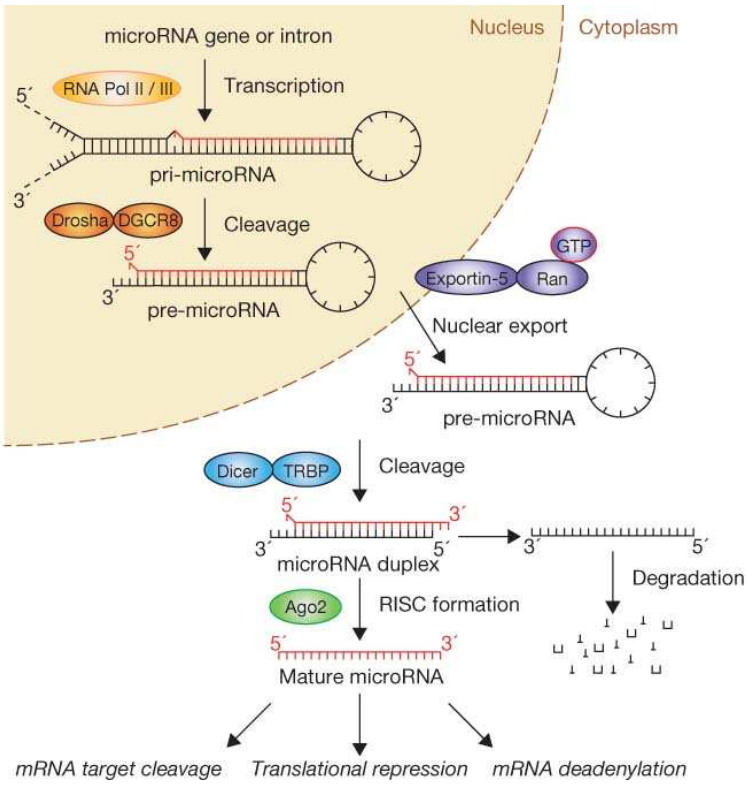

Fig. 8. MiRNA biogenesis

MiRNA genes are transcribed to form a capped and polyadenylated transcript primary miRNA (pri-miRNA). It is cleaved by the RNase III Drosha and DGCR8 up to a hairpin-like precursor miRNA (pre-miRNA). The pre-miRNA is exported from the nucleus into the cytoplasm, where it is further cleaved by the RNase III Dicer up to an imperfect duplex of miRNA (guide strand) and miRNA* (passenger strand). One

of the strands (often guiding strand) incorporates into RISC complex. miRNA-loaded RISC recognizes its target mRNA leading to translational inhibition and/or degradation of the mRNA. Abbreviations: RNA Pol, RNA polymerase; Ago2, Argonaute 2. (Winter J, 2009).

MiRNA regulation of HDL metabolism

HDL particles are the key system able to remove excess cholesterol from peripheral cells through RCT (see General Introduction).

Recent studies indicated miRNAs as important regulators of RCT, including HDL biogenesis, cellular cholesterol efflux, and biliary secretion, as summarized in figure 9 **(Fig.9)** (192). In particular, miR-33 acts on ABCA1 at the level of the liver and the macrophages which are in the atherosclerotic plaque, thus interfering with HDL biogenesis and cholesterol efflux. Another important target of miR-33 is represented by cytochrome P450 7A1 (CYP7A1), involved in bile acid synthesis and secretion. Consistent with these findings, recent reports in different animal models have shown that the therapeutic inhibition of miR-33 increases circulating HDL levels and determines regression of atherosclerotic lesions (193, 194).

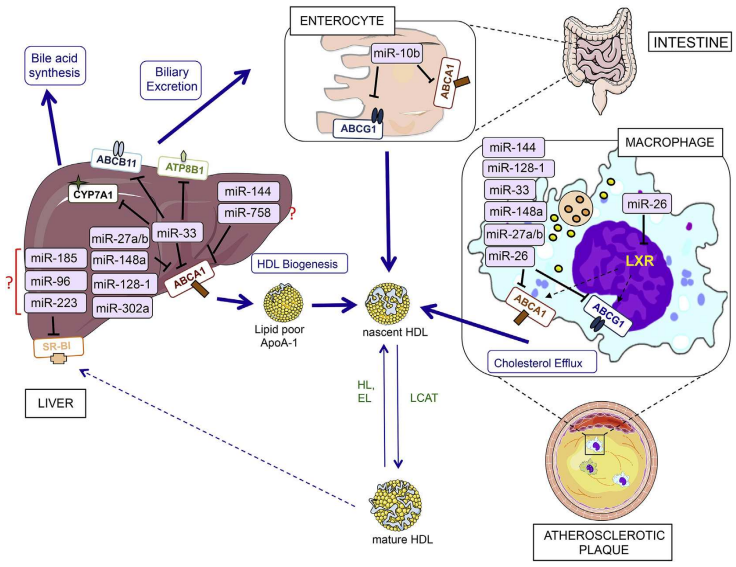

Fig. 9 Action of miRNAs on genes involved in HDL metabolism

(Rotllan N et al, 2016)

MiRNA regulation of LDL metabolism

High levels of LDL-C are the primary risk factor for the development of atherosclerotic plaques. For this reason, miRNAs regulating LDL-C metabolism may act on promising therapeutic targets for patients at risk of CVD **(Fig. 10)** (192). An example is represented by miR-30c. Increased levels of miR-30c have been shown to reduce plasma lipids. These effects are due in part to its targeting action on microsomal transfer protein (MTP), which is involved in VLDL secretion. In support of these evidences, overexpression of miR-30c was shown to reduce plaque formation in apo E-deficient mice, while inhibition of miR-30c led to more severe hyperlipidemia and atherosclerotic plaque formation (195).

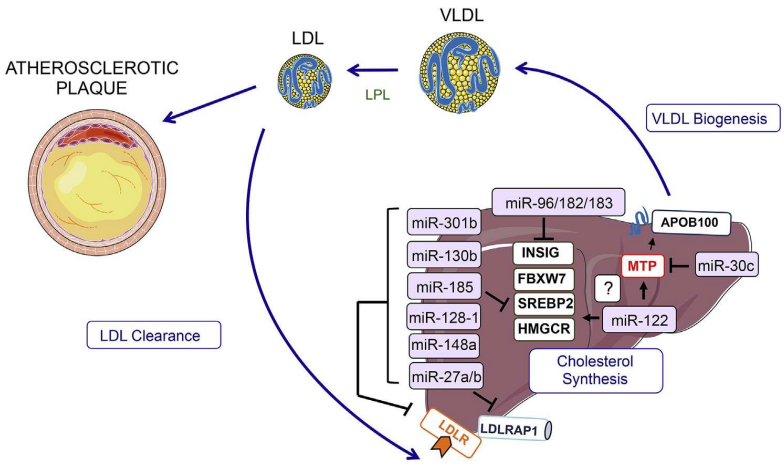

Fig. 10 Action of miRNAs on genes involved in LDL metabolism

(Rotllan N et al, 2016)

Therapeutic implications of miRNAs in atherosclerosis and CVD

As described in the previous paragraphs, several miRNAs are important regulators of genes involved in cholesterol metabolism and in atherosclerosis.

Therefore, approaches to modulate either positively or negatively the expression of miRNAs for therapeutic purposes appeared to be promising. For those miRNAs that are downregulated under disease states, forced miRNA re-expression strategy is used to recover miRNA expression, whereas for those miRNAs upregulated, anti-miRNA strategy is employed to suppress their expression. An example of anti-miRNA strategy is the inhibition of miR-148a, which has been demonstrated to alter plasma LDL-C levels by increasing LDLR activity. This mechanism is similar to that of statins and other approaches demonstrated to be effective in human patients. (196, 197). Furthermore, inhibition of miR-148a, or other miRNAs that target ABCA1, would be expected to both promote HDL biogenesis in the liver and enhance cholesterol efflux in arterial macrophages, which may be of greater clinical relevance than simply altering circulating HDL levels.

SCOPE OF THE THESIS

Chapter 2: L-homoarginine administration reduces neointimal hyperplasia in balloon-injured rat carotids.

L-homoarginine has recently emerged as a novel cardiovascular risk factor, since data from clinical studies have indicated that low homoarginine concentrations independently predict mortality from cardiovascular disease.

The possible role of L-homoarginine on smooth muscle cell proliferation and migration that can occur after arterial balloon angioplasty has never been explored. To this aim, we investigated the effect of L-homoarginine administration in a rat model of carotid balloon injury.

Chapter 3: A salmon protein hydrolysate exerts lipid-independent anti-atherosclerotic activity in Apo E-deficient mice.

Fish consumption is considered health beneficial as it decreases cardiovascular disease risk through effects on plasma lipids and inflammation. We investigated the effect of a salmon protein hydrolysate on atherosclerosis

development in apo E-deficient mice fed a high-fat diet with 5% salmon protein hydrolysate for 12 weeks.

Chapter 4: MiRNA expression profiles of tissues involved in cholesterol metabolism from athero-prone and athero-resistant mouse models.

MiRNAs constitute a class of small non-coding RNAs which act as potent post-transcriptional regulators of gene expression. In recent years, several miRNAs have been directly linked to the regulation of key genes involved in cholesterol metabolism and atherosclerosis development. We proposed to identify miRNA expression profiles of tissues involved in cholesterol metabolism in both physiological and pathological conditions of dyslipidemias and atherosclerosis development in order to identify members of transcriptional regulatory circuits potentially involved in cholesterol metabolism and regulated by miRNAs. These findings are expected to contribute to the definition of a panel of biomarkers of atherosclerosis development.

References

1. Myant NB (1981). The Biology of Cholesterol and Related Steroids.William Heinemann Medical Books Ltd, London.
2. Durrington PN, Mackness B & Mackness MI (2001). Paraoxonase and atherosclerosis. Arterioscler Thromb Vasc Biol 21, 473–480.
3. Tulenko TN, Sumner AE (2002). The physiology of lipoproteins. J Nucl Cardiol 9(6):638-49.
4. Trigatti B, Rigotti A, Krieger M (2000). The role of high-density lipoprotein receptor SR-BI in cholesterol metabolism. Curr Opin Lipidol 11:123–32.
5. Fidge N. (1999). High density lipoprotein receptors, binding proteins, and ligands. J Lipid Res 40:187–201.
6. Tall A, Jiang X, Luo Y, Silver D (2000). 1999 George Lyman Duff Memorial Lecture: lipid transfer proteins, HDL metabolism and atherogenesis. Arterioscler Thromb Vasc Biol 20:1185–8.
7. Gilbert-Barnes E, Barnes L, editors (2000). Metabolic diseases: foundations of clinical management,

genetics and pathology. Volume I. Natick [MA]: Eaton Publishing p. 283-322.

8. Goldstein JL, Brown MS (2009).The LDL receptor. Arterioscler Thromb Vasc Biol 29(4):431–438.
9. Schneider WJ, Beisiegel U, Goldstein JL, Brown MS (1982). Purification of the low density lipoprotein receptor, an acidic glycoprotein of 164,000 molecular weight. J Biol Chem 257(5):2664–2673.
10. Sudhof TC, Goldstein JL, Brown MS, Russell DW (1985). The LDL receptorgene: a mosaic of exons shared with different proteins. Science 228(4701):815–822.
11. Goldstein JL, Brown MS (1990). Regulation of the mevalonate pathway. Nature 343:425–430.
12. Brown MS, Goldstein JL (1997). The SREBP pathway: regulation of cholesterol metabolism by proteolysis of a membrane-bound transcription factor. Cell 89:331–340.
13. Brown MS, Goldstein JL (1979). Receptor-mediated endocytosis: insights from the lipoprotein receptor system. Proc Natl Acad Sci USA 76:3330–3337.

14. Kwon HJ, Lagace TA, McNutt MC, Horton JD, Deisenhofer J (2008). Molecular basis for LDL receptor recognition by PCSK9. Proc Natl Acad Sci USA 105:1820–1825.
15. Zhang DW, Garuti R, Tang WJ, Cohen JC, Hobbs HH (2008). Structural requirements for PCSK9-mediated degradation of the low-density lipoprotein receptor. Proc Natl Acad Sci USA 105:13045–13050.
16. Zhang DW, Lagace TA, Garuti R, Zhao Z, McDonald M, Horton JD, Cohen JC, Hobbs HH (2007). Binding of proprotein convertase subtilisin/kexin type 9 to epidermal growth factor-like repeat A of low density lipoprotein receptor decreases receptor recycling and increases degradation. J Biol Chem 282:18602–18612.
17. Janowski BA, Grogan MJ, Jones SA, Wisely GB, Kliewer SA, Corey EJ, Mangelsdorf DJ (1999). Structural requirements of ligands for the oxysterol liver X receptors LXRalpha and LXRbeta. Proc Natl Acad Sci USA 96:266–271.
18. Repa JJ, Turley SD, Lobaccaro JA, Medina J, Li L, Lustig K, Shan B, Heyman RA, Dietschy JM,

Mangelsdorf DJ (2000). Regulation of absorption and ABC1-mediated efflux of cholesterol by RXR heterodimers. Science 289:1524–1529.

19. Venkateswaran A, Laffitte BA, Joseph SB, Mak PA, Wilpitz DC, Edwards PA, Tontonoz P (2000). Control of cellular cholesterol efflux by the nuclear oxysterol receptor LXR alpha. Proc Natl Acad Sci USA 97:12097–12102.

20. Bortnick AE, Rothblat GH, Stoudt G, Hoppe KL, Royer LJ, McNeish J, Francone OL (2000). The correlation of ATP-binding cassette 1 mRNA levels with cholesterol efflux from various cell lines. J Biol Chem 275:28634–28640.

21. Klucken J, Büchler C, Orsó E, Kaminski WE, Porsch-Ozcürümez M, Liebisch G, Kapinsky M, Diederich W, Drobnik W, Dean M, Allikmets R, Schmitz G (2000). ABCG1 (ABC8), the human homolog of the Drosophila white gene, is a regulator of macrophage cholesterol and phospholipid transport. Proc Natl Acad Sci USA 97:817–822.

22. Wang N, Silver DL, Costet P, Tall AR (2000). Specific binding of ApoA-I, enhanced cholesterol efflux, and

altered plasma membrane morphology in cells expressing ABC1. J Biol Chem 275:33053–33058.

23. Seidah NG, Benjannet S, Wickham L, et al (2003). The secretory proprotein convertase neural apoptosis-regulated convertase 1 (NARC-1): liver regeneration and neuronal differentiation. Proc Natl Acad Sci U S A 100:928–33.
24. Abifadel M, Varret M, Rabès JP, et al (2003). Mutations in PCSK9 cause autosomal dominant hypercholesterolemia. Nat Genet 34:154–6.
25. Seidah NG, Prat A (2012). The biology and therapeutic targeting of the proprotein convertases. Nat Rev Drug Discov 11:367–83.
26. Lambert G, Charlton F, Rye KA, Piper DE (2009). Molecular basis of PCSK9 function. Atherosclerosis 203:1–7.
27. Seidah NG, Prat A (2007). The proprotein convertases are potential targets in the treatment of dyslipidemia. J Mol Med (Berl) 85:685–96.
28. Hampton EN, Knuth MW, Li J, Harris JL, Lesley SA, Spraggon G (2007). The self-inhibited structure of full-length PCSK9 at 1.9 A reveals structural

homology with resistin within the C-terminal domain. Proc Natl Acad Sci U S A 104:14604–9.

29. Piper DE, Jackson S, Liu Q, et al (2007) The crystal structure of PCSK9: a regulator of plasma LDL-cholesterol. Structure 15:545–52.
30. Kwon HJ, Lagace TA, McNutt MC, Horton JD, Deisenhofer J (2008). Molecular basis for LDL receptor recognition by PCSK9. Proc Natl Acad Sci U S A 105:1820–5.
31. Lagace TA, Curtis DE, Garuti R, et al (2006). Secreted PCSK9 decreases the number of LDL receptors in hepatocytes and in livers of parabiotic mice. J Clin Invest 116:2995–3005.
32. Brautbar A, Ballantyne CM (2011). Pharmacological strategies for lowering LDL cholesterol: statins and beyond. Nat Rev Cardiol 8(5):253-65.
33. Li J, Tumanut C, Gavigan JA, et al (2007). Secreted PCSK9 promotes LDL receptor degradation independently of proteolytic activity. Biochem J 406:203–7.
34. McNutt MC, Lagace TA, Horton JD (2007). Catalytic activity is not required for secreted PCSK9 to reduce

low density lipoprotein receptors in HepG2 cells. J Biol Chem 282:20799–803.

35. Dietschy JM, Turley SD, Spady DK (1993). Role of liver in the maintenance of cholesterol and low density lipoprotein homeostasis in different animal species, including humans. J Lipid Res 34:1637–59.
36. Horton JD, Shah NA, Warrington JA, et al (2003). Combined analysis of oligonucleotide microarray data from transgenic and knockout mice identifies direct SREBP target genes. Proc Natl Acad Sci U S A 100: 12027-32.
37. Mozaffarian D, Benjamin EJ, Go AS, Arnett DK, Blaha MJ, Cushman M, de Ferranti S, Despres JP, Fullerton HJ, Howard VJ, Huffman MD, Judd SE, Kissela BM, Lackland DT, Lichtman JH, Lisabeth LD, Liu S, Mackey RH, Matchar DB, McGuire DK, Mohler ER, 3rd, Moy CS, Muntner P, Mussolino ME, Nasir K, Neumar RW, Nichol G, Palaniappan L, Pandey DK, Reeves MJ, Rodriguez CJ, Sorlie PD, Stein J, Towfighi A, Turan TN, Virani SS, Willey JZ, Woo D, Yeh RW, Turner MB (2015). Heart disease and stroke statistics--2015

update: a report from the American Heart Association. Circulation. 131:e29-322.

38. Mayerl C, Lukasser M, Sedivy R, Niederegger H, Seiler R, Wick G (2006). Atherosclerosis research from past to present--on the track of two pathologists with opposing views, Carl von Rokitansky and Rudolf Virchow. Virchows Arch 449:96-103.
39. Luscher TF, Dohi Y, Tanner FC, Boulanger C (1991). Endothelium-dependent control of vascular tone: effects of age, hypertension and lipids. Basic Res Cardiol. 86 Suppl 2:143-158.
40. Dahlback B (2000). Blood coagulation. Lancet 355:1627-1632.
41. Luscinskas FW, Gimbrone MA, Jr (1996). Endothelial-dependent mechanisms in chronic inflammatory leukocyte recruitment. Annu Rev Med 47:413-421.
42. Davies PF (1995). Flow-mediated endothelial mechanotransduction. Physiol Rev 75:519-560.
43. Gimbrone MA, Jr., Topper JN, Nagel T, Anderson KR, Garcia-Cardena G (2000). Endothelial dysfunction,

hemodynamic forces, and atherogenesis. Ann N Y Acad Sci 902:230-239; discussion 239-240.

44. Gimbrone MA, Jr., Garcia-Cardena G (2013). Vascular endothelium, hemodynamics, and the pathobiology of atherosclerosis. Cardiovasc Pathol 22:9-15.
45. Chiplunkar AR, Curtis BC, Eades GL, Kane MS, Fox SJ, Haar JL, Lloyd JA (2013). The Kruppel-like factor 2 and Kruppel-like factor 4 genes interact to maintain endothelial integrity in mouse embryonic vasculogenesis. BMC Dev Biol 13:40.
46. Topper JN, Cai J, Falb D, Gimbrone MA, Jr (1996). Identification of vascular endothelial genes differentially responsive to fluid mechanical stimuli: cyclooxygenase-2, manganese superoxide dismutase, and endothelial cell nitric oxide synthase are selectively up-regulated by steady laminar shear stress. Proceedings of the National Academy of Sciences of the United States of America 93:10417-10422.
47. SenBanerjee S, Lin Z, Atkins GB, Greif DM, Rao RM, Kumar A, Feinberg MW, Chen Z, Simon DI, Luscinskas

FW, Michel TM, Gimbrone MA, Jr., Garcia-Cardena G, Jain MK (2004). KLF2 Is a novel transcriptional regulator of endothelial proinflammatory activation. J Exp Med 199:1305-1315.

48. Lei J, Vodovotz Y, Tzeng E, Billiar TR (2013). Nitric oxide, a protective molecule in the cardiovascular system. Nitric Oxide 35:175-185.
49. Linton MF, Yancey PG, Davies SS, Jerome WGJ, Linton EF, Vickers KC. In: De Groot LJ, Chrousos G, Dungan K, Feingold KR, Grossman A, Hershman JM, Koch C, Korbonits M, McLachlan R, New M, Purnell J, Rebar R, Singer F,Vinik A, editors. Endotext [Internet]. South Dartmouth (MA): MDText.com,Inc.; 2000 - 2015.
50. Gerrity RG, Naito HK, Richardson M, Schwartz CJ (1979). Dietary induced atherogenesis in swine. Morphology of the intima in prelesion stages. Am J Pathol 95:775-792.
51. Schwenke DC, Carew TE (1989). Initiation of atherosclerotic lesions in cholesterol-fed rabbits. II. Selective retention of LDL vs. selective increases in

LDL permeability in susceptible sites of arteries. Arteriosclerosis. 9:908-918.

52. Yurdagul A, Jr., Chen J, Funk SD, Albert P, Kevil CG, Orr AW (2013). Altered nitric oxide production mediates matrix-specific PAK2 and NF-kappaB activation by flow. Mol Biol Cell 24:398-408.
53. Hamik A, Lin Z, Kumar A, Balcells M, Sinha S, Katz J, Feinberg MW, Gerzsten RE, Edelman ER, Jain MK (2007). Kruppel-like factor 4 regulates endothelial inflammation. J Biol Chem 282:13769-13779.
54. Ungvari Z, Wolin MS, Csiszar A (2006). Mechanosensitive production of reactive oxygen species in endothelial and smooth muscle cells: role in microvascular remodeling? Antioxid Redox Signal 8:1121-1129.
55. Cominacini L, Pasini AF, Garbin U, Davoli A, Tosetti ML, Campagnola M, Rigoni A, Pastorino AM, Lo Cascio V, Sawamura T (2000). Oxidized low density lipoprotein (ox-LDL) binding to ox-LDL receptor-1 in endothelial cells induces the activation of NF-kappaB through an increased production of intracellular

reactive oxygen species. J Biol Chem 275:12633-12638.

56. Collins T, Read MA, Neish AS, Whitley MZ, Thanos D, Maniatis T (1995). Transcriptional regulation of endothelial cell adhesion molecules: NF-kappa B and cytokine-inducible enhancers. FASEB J 9:899-909.
57. Park S, Yoon SJ, Tae HJ, Shim CY (2011). RAGE and cardiovascular disease. Front Biosci (Landmark Ed) 16:486-497.
58. Dauphinee SM, Karsan A (2006). Lipopolysaccharide signaling in endothelial cells. Lab Invest 86:9-22.
59. Kratzer A, Giral H, Landmesser U (2014). High-density lipoproteins as modulators of endothelial cell functions: alterations in patients with coronary artery disease. Cardiovasc Res 103:350-361.
60. Galkina E, Ley K (2007) Vascular adhesion molecules in atherosclerosis. Arterioscler Thromb Vasc Biol 27:2292-2301.
61. Gu L, Okada Y, Clinton SK, Gerard C, Sukhova GK, Libby P, Rollins BJ (1998). Absence of monocyte chemoattractant protein-1 reduces atherosclerosis in

low density lipoprotein receptor-deficient mice. Molecular Cell 2:275-281.

62. Gerszten RE, Garcia-Zepeda EA, Lim YC, Yoshida M, Ding HA, Gimbrone MA, Jr., Luster AD, Luscinskas FW, Rosenzweig A (1999). MCP-1 and IL-8 trigger firm adhesion of monocytes to vascular endothelium under flow conditions. Nature 398:718-723.
63. Boisvert WA, Santiago R, Curtiss LK, Terkeltaub RA (1998). A leukocyte homologue of the IL-8 receptor CXCR-2 mediates the accumulation of macrophages in atherosclerotic lesions of LDL receptor-deficient mice. Journal of Clinical Investigation 101:353-363.
64. Robbins CS, Hilgendorf I, Weber GF, Theurl I, Iwamoto Y, Figueiredo JL, Gorbatov R, Sukhova GK, Gerhardt LM, Smyth D, Zavitz CC, Shikatani EA, Parsons M, van Rooijen N, Lin HY, Husain M, Libby P, Nahrendorf M, Weissleder R, Swirski FK (2013). Local proliferation dominates lesional macrophage accumulation in atherosclerosis. Nat Med 19:1166-1172.
65. Brown M, Goldstein J, Krieger M, Ho Y, Anderson R (1979). Reversible accumulation of cholesteryl esters

in macrophages incubated with acetylated lipoproteins. J Cell Biol 82:597-613.

66. Brown MS, Goldstein JL (1983). Lipoprotein metabolism in the macrophage: implications for cholesterol deposition in atherosclerosis. Annu. Rev. Biochem 52:223-261.
67. Moore KJ, Freeman MW (2006). Scavenger receptors in atherosclerosis: beyond lipid uptake. Arterioscler Thromb Vasc Biol 26:1702-1711.
68. Younis N, Sharma R, Soran H, Charlton-Menys V, Elseweidy M, Durrington PN (2008). Glycation as an atherogenic modification of LDL. Curr Opin Lipidol 19:378-384.
69. Torzewski M, Lackner KJ (2006). Initiation and progression of atherosclerosis--enzymatic or oxidative modification of low-density lipoprotein? Clin Chem Lab Med 44:1389-1394.
70. Torzewski M, Suriyaphol P, Paprotka K, Spath L, Ochsenhirt V, Schmitt A, Han SR, Husmann M, Gerl VB, Bhakdi S, Lackner KJ (2004). Enzymatic modification of low-density lipoprotein in the arterial wall: a new role for plasmin and matrix

metalloproteinases in atherogenesis. Arterioscler Thromb Vasc Biol 24:2130-2136.

71. Colin S, Chinetti-Gbaguidi G, Staels B (2014). Macrophage phenotypes in atherosclerosis. Immunol Rev 262:153-166.
72. Adamson S, Leitinger N (2011). Phenotypic modulation of macrophages in response to plaque lipids. Curr Opin Lipidol 22:335-342.
73. Bolick DT, Skaflen MD, Johnson LE, Kwon SC, Howatt D, Daugherty A, Ravichandran KS, Hedrick CC (2009). G2A deficiency in mice promotes macrophage activation and atherosclerosis. Circ Res 104:318-327.
74. Wang XQ, Panousis CG, Alfaro ML, Evans GF, Zuckerman SH (2002). Interferon-gamma-mediated downregulation of cholesterol efflux and ABC1 expression is by the Stat1 pathway. Arterioscler Thromb Vasc Biol 22:e5-9.
75. Brand K, Mackman N, Curtiss LK (1993). Interferon-gamma inhibits macrophage apolipoprotein E production by posttranslational mechanisms. J Clin Invest 91:2031-2039.

76. Peled M, Fisher EA (2014). Dynamic Aspects of Macrophage Polarization during Atherosclerosis Progression and Regression. Front Immunol 5:579.
77. Ye D, Lammers B, Zhao Y, Meurs I, Van Berkel TJ, Van Eck M (2011). ATP-binding cassette transporters A1 and G1, HDL metabolism, cholesterol efflux, and inflammation: important targets for the treatment of atherosclerosis. Curr Drug Targets 12:647-660.
78. Yancey PG, Jerome WG, Yu H, Griffin EE, Cox BE, Babaev VR, Fazio S, Linton MF (2007). Severely altered cholesterol homeostasis in macrophages lacking apoE and SR-BI. J Lipid Res 48:1140-1149.
79. Fioravanti J, Medina-Echeverz J, Berraondo P (2011). Scavenger receptor class B, type I: a promising immunotherapy target. Immunotherapy 3:395-406.
80. Kellner-Weibel G, de la Llera-Moya M (2011). Update on HDL receptors and cellular cholesterol transport. Curr Atheroscler Rep 13:233-241.
81. Phillips MC (2014). Molecular mechanisms of cellular cholesterol efflux. J Biol Chem 289:24020-24029.
82. Yancey PG, Bortnick AE, Kellner-Weibel G, de la Llera-Moya M, Phillips MC, Rothblat GH (2003).

Importance of different pathways of cellular cholesterol efflux. Arterioscler Thromb Vasc Biol 23:712-719.

83. Oram JF, Wolfbauer G, Vaughan AM, Tang C, Albers JJ (2003). Phospholipid transfer protein interacts with and stabilizes ATP-binding cassette transporter A1 and enhances cholesterol efflux from cells. J Biol Chem 278:52379-52385.
84. Fisher EA, Feig JE, Hewing B, Hazen SL, Smith JD (2012). High-density lipoprotein function, dysfunction, and reverse cholesterol transport. Arterioscler Thromb Vasc Biol 32:2813-2820.
85. Puri R, Nissen SE, Ballantyne CM, Barter PJ, Chapman MJ, Erbel R, Libby P, Raichlen JS, St John J, Wolski K, Uno K, Kataoka Y, Nicholls SJ (2013). Factors underlying regression of coronary atheroma with potent statin therapy. Eur Heart J 34:1818-1825.
86. Schwartz SM (1999). The intima : A new soil. Circ Res 85:877-879.
87. Raines EW (2004). PDGF and cardiovascular disease. Cytokine Growth Factor Rev 15:237-254.

88. Johnson JL (2007). Matrix metalloproteinases: influence on smooth muscle cells and atherosclerotic plaque stability. Expert Rev Cardiovasc Ther 5:265-282.
89. Yang X, Liaw L, Prudovsky I, Brooks PC, Vary C, Oxburgh L, Friesel R (2015). Fibroblast growth factor signaling in the vasculature. Curr Atheroscler Rep 17:509.
90. Molloy CJ, Taylor DS, Pawlowski JE (1999). Novel cardiovascular actions of the activins. J Endocrinol 161:179-185.
91. Chao F, Blanchette-Mackie E, Chen Y, Dickens B, Berlin E, Amende L, Skarlatos S, Gamble W, Resau J, Mergner W, Kruth H (1990). Characterization of two unique cholesterol-rich lipid particles isolated from human atherosclerotic lesions. Am J Pathol 136:169-179.
92. Kruth H (1984). Localization of unesterified cholesterol in human atherosclerotic lesions. Demonstration of filipin-positive, oil-red-O-negative particles. Am J Pathol 114:201-208.

93. Virmani R, Burke AP, Kolodgie FD, Farb A (2002). Vulnerable plaque: the pathology of unstable coronary lesions. J Interv Cardiol 15:439-446.
94. Libby P (2013). Mechanisms of acute coronary syndromes and their implications for therapy. N Engl J Med 368:2004-2013.
95. Ahanchi SS, Tsihlis ND, Kibbe MR (2007). The role of nitric oxide in the pathophysiology of intimal hyperplasia. J Vasc Surg 45 Suppl A:A64-73.
96. Buechel R, Stirnimann A, Zimmer R, Keo H, Groechenig E (2012). Drug-eluting stents and drug-coated balloons in peripheral artery disease. Vasa 41(4):248-61.
97. Tulis DA (2007). Rat carotid artery balloon injury model. Methods Mol Med 139: 1.
98. Clowes AW, Reidy MA, Clowes MM (1983). Mechanisms of stenosis after arterial injury. Lab Invest 49:208-15.
99. Mitra AK, Del Core MG, Agrawal DK (2005). Cells, cytokines and cellular immunity in the pathogenesis of fibroproliferative vasculopathies. Can J Physiol Pharmacol 83:701-15.

100. Ross R, Raines EW, Bowenpope DF (1986). The biology of platelet-derived growth-factor. Cell 46:155-69.

101. Libby P, Warner SJ, Friedman GB (1988). Interleukin-1: a mitogen for human vascular smooth-muscle cells that induces the release of growth-inhibitory prostanoids. J Clin Invest 81:487-98.

102. Lindner V, Lappi DA, Baird A, Majack RA, Reidy MA (1991). Role of basic fibroblast growth factor in vascular lesion formation. Circ Res 68:106-13.

103. Clowes AW, Clowes MM, Reidy MA (1986). Kinetics of cellular proliferation after arterial injury. III. Endothelial and smooth muscle growth in chronically denuded vessels. Lab Invest 54:295-303.

104. Chen Z, Lee FY, Bhalla KN, Wu J (2006). Potent inhibition of plateletderived growth factor-induced responses in vascular smooth muscle cells by BMS-354825 (dasatinib). Mol Pharmacol 69:1527-33.

105. Bendeck MP, Zempo N, Clowes AW, Galardy RE, Reidy MA (1994). Smooth muscle cell migration and matrix metalloproteinase expression after arterial injury in the rat. Circ Res 75:539-45.

106. Hasenstab D, Forough R, Clowes AW (1997). Plasminogen activator inhibitor type 1 and tissue inhibitor of metalloproteinases-2 increase after arterial injury in rats. Circ Res 80:490-6.

107. Knowles JW, Maeda N (2000). Genetic modifiers of atherosclerosis in mice. Arterioscler Thromb Vasc Biol 20:2336 –2345.

108. Nakashima Y, Plump AS, Raines EW, Breslow JL, Ross R (1994). ApoE-deficient mice develop lesions of all phases of atherosclerosis throughout the arterial tree. Arterioscler Thromb. 14:133–140.

109. Scalia R, Gooszen ME, Jones SP, Hoffmeyer M, Rimmer DM III, Trocha SD, Huang PL, Smith MB, Lefer AM, Lefer DJ (2001). Simvastatin exerts both anti-inflammatory and cardioprotective effects in apolipoprotein E-deficient mice. *Circulation*. 103:2598 –2603.

110. Powell-Braxton L, Veniant M, Latvala RD, Hirano KI, Won WB, Ross J, Dybdal N, Zlot CH, Young SG, Davidson NO (1998). A mouse model of human familial hypercholesterolemia: markedly elevated low density lipoprotein cholesterol levels and severe

atherosclerosis on a low-fat chow diet. Nat Med 4:934 –938.

111. Sanan DA, Newland DL, Tao R, Marcovina S, Wang J, Mooser V, Hammer RE, Hobbs HH (1998). Low density lipoprotein receptor-negative mice expressing human apolipoprotein B-100 develop complex atherosclerotic lesions on a chow diet: no accentuation by apolipoprotein (a). Proc Natl Acad Sci U S A 95:4544–4549.

112. Srivastava RA, Jahagirdar R, Azhar S, Sharma S, Bisgaier CL (2006). Peroxisome proliferator-activated receptor-alpha selective ligand reduces adiposity, improves insulin sensitivity and inhibits atherosclerosis in LDL receptor-deficient mice. Mol Cell Biochem 285:35–50.

113. Kooistra T, Verschuren L, de Vries-van der Weij, Koenig W, Toet K, Princen HM, Kleemann R (2006). Fenofibrate reduces atherogenesis in ApoE*3Leiden mice: evidence for multiple antiatherogenic effects besides lowering plasma cholesterol. Arterioscler Thromb Vasc Biol 26:2322–2330.

114. Rashid S, Curtis DE, Garuti R, Anderson NN, Bashmakov Y, Ho YK, Hammer RE, Moon YA, Horton JD (2005). Decreased plasma cholesterol and hypersensitivity to statins in mice lacking Pcsk9. Proc Natl Acad Sci U S A 102:5374–5379. 26.

115. Zaid A, Roubtsova A, Essalmani R, Marcinkiewicz J, Chamberland A, Hamelin J, Tremblay M, Jacques H, Jin W, Davignon J, Seidah NG, Prat A (2008). Proprotein convertase subtilisin/kexin type 9 (PCSK9): hepatocyte-specific low-density lipoprotein receptor degradation and critical role in mouse liver regeneration. Hepatology 48:646–654.

116. Cohen J, Pertsemlidis A, Kotowski IK, Graham R, Garcia CK, Hobbs HH (2005). Low LDL cholesterol in individuals of African descent resulting from frequent nonsense mutations in PCSK9. Nat Genet 37:161–165.

117. Roubtsova A, Munkonda MN, Awan Z, Marcinkiewicz J, Chamberland A, Lazure C, Cianflone K, Seidah NG, Prat A (2011). Circulating proprotein convertase subtilisin/kexin 9 (PCSK9) regulates VLDLR protein

and triglyceride accumulation in visceral adipose tissue. Arterioscler Thromb Vasc Biol 31:785–791.

118. Denis M, Marcinkiewicz J, Zaid A, et al (2012). Gene inactivation of proprotein convertase subtilisin/kexin type 9 reduces atherosclerosis in mice. Circulation 125:894–901.

119. Choe CU, Atzler D, Wild PS, et al (2013) Homoarginine levels are regulated by L-arginine:glycine amidinotransferase and affect stroke outcome: results from human and murine studies. Circulation 128:1451–1461.

120. Kleber ME, Seppala I, Pilz S, et al (2013). Genome-wide association study identifies 3 genomic loci significantly associated with serum levels of homoarginine: the AtheroRemo Consortium. Circ Cardiovasc Genet 6:505–513.

121. Atzler D, Schwedhelm E, Choe CU (2015). L-homoarginine and cardiovascular disease. Curr Opin Clin Nutr Metab Care 18(1):83-8.

122. Brosnan JT, da Silva RP, Brosnan ME (2011). The metabolic burden of creatine synthesis. Amino Acids 40:1325–1331.

123. Choe CU, Nabuurs C, Stockebrand MC, et al (2013). L-arginine:glycine amidinotransferase deficiency protects from metabolic syndrome. Hum Mol Genet 22:110–123.

124. Nabuurs CI, Choe CU, Veltien A, et al (2013). Disturbed energy metabolism and muscular dystrophy caused by pure creatine deficiency are reversible by creatine intake. J Physiol 591:571–592.

125. Davids M, Ndika JD, Salomons GS, et al (2012). Promiscuous activity of arginine:-glycine amidinotransferase is responsible for the synthesis of the novel cardiovascular risk factor homoarginine. FEBS Lett 586:3653–3657.

126. Nunn PB, Bell EA, Watson AA, Nash RJ (2010). Toxicity of nonprotein amino acids to humans and domestic animals. Nat Prod Commun 5:485–504.

127. Hrabak A, Bajor T, Temesi A (1994). Comparison of substrate and inhibitor specificity of arginase and nitric oxide (NO) synthase for arginine analogues and related compounds in murine and rat macrophages. Biochem Biophys Res Commun 198:206–212.

128. Moali C, Boucher JL, Sari MA, et al (1998). Substrate specificity of NO synthases: detailed comparison of L-arginine, homo-L-arginine, their N omega-hydroxy derivatives, and N omega-hydroxynor-L-arginine. Biochemistry 37:10453–10460.
129. Pentyala J, Rao SL (1999). Sustained nitric oxide generation with L-homoarginine. Res Commun Biochem Cell Mol Biol 3:223–232.
130. Radomski MW, Palmer RM, Moncada S (1990). An L-arginine/nitric oxide pathway present in human platelets regulates aggregation. Proc Natl Acad Sci U S A 87:5193–5197.
131. Reczkowski RS, Ash DE (1994). Rat liver arginase: kinetic mechanism, alternate substrates, and inhibitors. Arch Biochem Biophys 312:31–37.
132. Atzler D, Schwedhelm E, Nauck M, et al (2014). Serum reference intervals of homoarginine, ADMA, and SDMA in the Study of Health in Pomerania. Clin Chem Lab Med 52(12):1835-42.
133. März W, Meinitzer A, Drechsler C, et al (2010). Homoarginine, cardiovascular risk, and mortality. Circulation 122:967–975.

134. Pilz S, Teerlink T, Scheffer PG, et al (2014). Homoarginine and mortality in an older population: the Hoorn study. Eur J Clin Invest 44:200–208.

135. Pilz S, Meinitzer A, Tomaschitz A, et al (2011). Low homoarginine concentration is a novel risk factor for heart disease. Heart 97:1222–1227.

136. Drechsler C, Meinitzer A, Pilz S, et al (2011). Homoarginine, heart failure, and sudden cardiac death in haemodialysis patients. Eur J Heart Fail 13:852–859.

137. Lygate CA, Schneider JE, Neubauer S (2013). Investigating cardiac energetics in heart failure. Exp Physiol 98:601–605.

138. Lygate CA, Bohl S, ten Hove M, et al (2012). Moderate elevation of intracellular creatine by targeting the creatine transporter protects mice from acute myocardial infarction. Cardiovasc Res 96:466–475.

139. Phillips D, Ten Hove M, Schneider JE, et al (2010). Mice over-expressing the myocardial creatine transporter develop progressive heart failure and

show decreased glycolytic capacity. J Mol Cell Cardiol 48:582–590.

140. Lygate CA, Aksentijevic D, Dawson D, et al (2013). Living without creatine: unchanged exercise capacity and response to chronic myocardial infarction in creatine-deficient mice. Circ Res 112:945–955.

141. Ninomiya T (2013). Risk of stroke in kidney disease. Contrib Nephrol 179:58 66.

142. Lee M, Saver JL, Chang KH, et al (2010). Low glomerular filtration rate and risk of stroke: meta-analysis. BMJ 341:c4249.

143. Ravani P, Maas R, Malberti F, et al (2013). Homoarginine and mortality in predialysis chronic kidney disease (CKD) patients. PLoS One 8:e72694.

144. Van der Zwan LP, Davids M, Scheffer PG, et al (2013). L-Homoarginine and L-arginine are antagonistically related to blood pressure in an elderly population: the Hoorn study. J Hypertens 31:1114–1123.

145. Kannel WB, Wolf PA (2008). Framingham Study insights on the hazards of elevated blood pressure. JAMA 300:2545–2547.

146. Brower V (1998). Nutraceuticals: Poised for a healthy slice of the healthcare market? Nat Biotechnol 16,728–731.

147. Bang HO, Dyerberg J, Nielsen AB (1971). Plasma lipid and lipoprotein pattern in Greenlandic West-coast Eskimos. Lancet 1, 1143–1145.

148. Bang HO, Dyerberg J, Hjoorne N (1976). The composition of food consumed by Greenland Eskimos. Acta Med Scand 200, 69–73.

149. Bang HO, Dyerberg J, Sinclair HM (1980). The composition of the Eskimo food in north western Greenland. Am J Clin Nutr 33, 2657–2661.

150. Albert CM, Hennekens CH, O'Donnell CJ, Ajani UA, Carey VJ, Willett WC, Ruskin JN, Manson JE (1998). Fish consumption and risk of sudden cardiac death. JAMA 279, 23–28.

151. Maehre HK, Jensen IJ, Elvevoll EO, Eilertsen KE (2015). Omega-3 Fatty Acids and Cardiovascular Diseases: Effects, Mechanisms and Dietary Relevance. Int J Mol Sci 16, 22636–22661.

152. Nestel PJ (1990). Effects of n-3 fatty acids on lipid metabolism. Annu Rev Nutr 10, 149–167.

153. Harris WS (1997). N-3 fatty acids and serum lipoproteins: Human studies. Am J Clin Nutr 65, 1645S–1654S.

154. Roche HM, Gibney MJ (2000). Effect of long-chain n-3 polyunsaturated fatty acids on fasting and postprandial triacylglycerol metabolism. Am J Clin Nutr 71, 232S–237S.

155. Kang JX, Leaf A (1996). Antiarrhythmic effects of polyunsaturated fatty acids. Recent studies. Circulation 94, 1774–1780.

156. Dyerberg J, Bang HO, Stoffersen E, Moncada S, Vane JR (1978). Eicosapentaenoic acid and prevention of thrombosis and atherosclerosis? Lancet 2, 117–119.

157. Leaf A, Weber PC (1988). Cardiovascular effects of n-3 fatty acids. N Engl J Med 318, 549–557.

158. Pischon T, Hankinson SE, Hotamisligil GS, Rifai N, Willett WC, Rimm EB (2003). Habitual dietary intake of n-3 and n-6 fatty acids in relation to inflammatory markers among US men and women. Circulation 108, 155–160.

159. Morgan DR, Dixon LJ, Hanratty CG, El-Sherbeeny N, Hamilton PB, McGrath LT, Leahey WJ, Johnston GD,

McVeigh GE (2006). Effects of dietary omega-3 fatty acid supplementation on endothelium-dependent vasodilation in patients with chronic heart failure. Am J Cardiol 97 547–551.

160. Tagawa H, Shimokawa H, Tagawa T, Kuroiwa-Matsumoto M, Hirooka Y, Takeshita A (1999). Long-term treatment with eicosapentaenoic acid augments both nitric oxide-mediated and non-nitric oxide-mediated endothelium-dependent forearm vasodilatation in patients with coronary artery disease. J Cardiovasc Pharmacol 33, 633–640.

161. Morris MC, Sacks F, Rosner B (1993). Does fish oil lower blood pressure? A meta-analysis of controlled trials. Circulation 88, 523–533.

162. Chiesa G, Busnelli M, Manzini S, Parolini C (2016). Nutraceuticals and bioactive components from fish for dyslipidemia and cardiovascular risk reduction. Mar Drugs 8;14(6).

163. Vazquez C, Botella-Carretero JI, Corella D, Fiol M, Lage M, Lurbe E, Richart C, Fernandez-Real JM, Fuentes F, Ordonez A et al (2014). White fish reduces cardiovascular risk factors in patients with metabolic

syndrome: The WISH-CARE study, a multicenter randomized clinical trial. Nutr Metab Cardiovasc Dis 24, 328–335.

164. Howard A, Udenigwe CC (2013). Mechanisms and prospects of food protein hydrolysates and peptide-induced hypolipidaemia. Food Funct 4, 40–51.

165. El Khoury D, Anderson GH (2013). Recent advances in dietary proteins and lipid metabolism. Curr Opin Lipidol 24, 207–213.

166. Kritchevsky D, Tepper SA, Czarnecki SK, Klurfeld DM (1982). Atherogenicity of animal and vegetable protein. Influence of the lysine to arginine ratio. Atherosclerosis 41, 429–431.

167. Wergedahl H, Liaset B, Gudbrandsen OA, Lied E, Espe M, Muna Z, Mork S, Berge RK (2004). Fish protein hydrolysate reduces plasma total cholesterol, increases the proportion of HDL cholesterol, and lowers acyl-CoA: Cholesterol acyltransferase activity in liver of Zucker rats. J Nutr 134, 1320–1327.

168. Carroll KK, Hamilton RMG (1975). Effects of dietary protein and carbohydrate on plasma cholesterol

levels in relation to atherosclerosis. J Food Sci 40:18–23.

169. Zhang X, Beynen AC (1993). Influence of dietary fish proteins on plasma and liver cholesterol concentrations in rats. Br J Nutr 69:767–777.

170. Shukla A, Bettzieche A, Hirche F, Brandsch C, Stangl GI, Eder K (2006). Dietary fish protein alters blood lipid concentrations and hepatic genes involved in cholesterol homeostasis in the rat model. Br J Nutr 96:674–682.

171. Hosomi R, Fukunaga K, Arai H, Kanda S, Nishiyama T, Yoshida M (2012). Fish protein hydrolysates affect cholesterol metabolism in rats fed non-cholesterol and high-cholesterol diets. J Med Food 15:299–306.

172. Vikoren LA, Nygard OK, Lied E, Rostrup E, Gudbrandsen OA (2013). A randomised study on the effects of fish protein supplement on glucose tolerance, lipids and body composition in overweight adults. Br J Nutr 109:648–657.

173. Huang WY, Davidge ST, Wu J (2013). Bioactive natural constituents from food sources-potential use

in hypertension prevention and treatment. Crit Rev Food Sci Nutr 53:615–630.

174. Fujita H, Yoshikawa M (1999). LKPNM: A prodrug-type ACE-inhibitory peptide derived from fish protein. Immunopharmacology 44:123–127.

175. Yokoyama K, Chiba H, Yoshikawa M (1992). Peptide inhibitors for angiotensin I-converting enzyme from thermolysin digest of dried bonito. Biosci Biotechnol Biochem 56:1541–1545.

176. Tanaka H, Watanabe K, Ma M., Hirayama M, Kobayashi T, Oyama H, Sakaguchi Y, Kanda M, Kodama M, Aizawa Y (2009). The Effects of gamma-Aminobutyric Acid, Vinegar, and Dried Bonito on Blood Pressure in Normotensive and Mildly or Moderately Hypertensive Volunteers. J Clin Biochem Nutr 45:93–100.

177. Enari H, Takahashi Y, Kawarasaki M, Tada M, Tatsuta K (2008). Identification of angiotensin I-converting enzymeinhibitory peptides derived from salmon muscleand their antihypertensive effect. Fish Sci 74:911–920.

178. Hartmann R, Meisel H (2007). Food-derived peptides with biological activity: From research to food applications. Curr Opin Biotechnol 18:163–169.

179. Fernandez-Hernando C, Ramirez CM, Goedeke L et al (2013). MicroRNAs in metabolic disease. Arterioscler Thromb Vasc Biol 33:178–185.

180. Ambros V (2004). The functions of animal microRNAs. Nature 431:350–355.

181. Filipowicz W, Bhattacharyya SN, Sonenberg N (2008). Mechanisms of post-transcriptional regulation by microRNAs: are the answers in sight?. Nat Rev Genet 9:102–114.

182. Winter J , Jung S, Keller S, Gregory RI & Diederichs S (2009) Many roads to maturity: microRNA biogenesis pathways and their regulation. Nat Cell Biol 11, 228 – 234.

183. Krek A, Grun D, Poy MN et al (2005). Combinatorial microRNA target predictions. Nat Genet 37:495–500.

184. Grimson A, Farh KK, Johnston WK et al (2007). MicroRNA targeting specificity in mammals: determinants beyond seed pairing. Mol Cell 27:91–105.

185. Valadi H, Ekstrom K, Bossios A et al (2007). Exosome-mediated transfer of mRNAs and microRNAs is a novel mechanism of genetic exchange between cells. Nat Cell Biol 9:654–659.

186. Zernecke A, Bidzhekov K, Noels H et al (2009). Delivery of microRNA-126 by apoptotic bodies induces CXCL12-dependent vascular protection. Sci Signal 2:ra81.

187. Vickers KC, Palmisano BT, Shoucri BM et al (2011). MicroRNAs are transported in plasma and delivered to recipient cells by high-density lipoproteins. Nat Cell Biol 13:423–433.

188. Arroyo JD, Chevillet JR, Kroh EM et al (2011). Argonaute2 complexes carry a population of circulating microRNAs independent of vesicles in human plasma. Proc Natl Acad Sci U S A 108:5003–5008.

189. Pan S, Yang X, Jia Y et al (2014). Microvesicle-shuttled miR-130b reduces fat deposition in recipient primary cultured porcine adipocytes by inhibiting PPAR-gamma expression. J Cell Physiol 229:631–639.

190. Wang YC, Li Y, Wang XY et al (2013). Circulating miR-130b mediates metabolic crosstalk between fat and muscle in overweight/obesity. Diabetologia 56:2275–2285.
191. Price NL, Ramirez CM, Fernandez-Hernando C (2014). Relevance of microRNA in metabolic diseases. Crit Rev Clin Lab Sci 51:305–320.
192. Rotllan N, Price N, Pati P, Goedeke L, Fernández-Hernando C (2016). MicroRNAs in lipoprotein metabolism and cardiometabolic disorders. Atherosclerosis 246: 352-360.
193. Rotllan N, Ramirez CM, Aryal B et al (2013). Therapeutic silencing of microRNA-33 inhibits the progression of atherosclerosis in Ldlr-/- mice–brief report. Arterioscler Thromb Vasc Biol 33:1973–1977.
194. Rayner KJ, Sheedy FJ, Esau CC et al (2011). Antagonism of miR-33 in mice promotes reverse cholesterol transport and regression of atherosclerosis. J Clin Investig 121:2921–2931.
195. Soh J, Iqbal J, Queiroz J et al (2013). MicroRNA-30c reduces hyperlipidemia and atherosclerosis in mice

by decreasing lipid synthesis and lipoprotein secretion. Nat Med 19:892–900.

196. Goedeke L, Rotllan N, Canfran-Duque A et al (2015). MicroRNA-148a regulates LDL receptor and ABCA1 expression to control circulating lipoprotein levels. Nat Med 21:1280–1289.

197. Wagschal A, Najafi-Shoushtari SH, Wang L et al (2015). Genome-wide identification of microRNAs regulating cholesterol and triglyceride homeostasis. Nat Med 21:1290–1297.

Chapter 2

L-homoarginine administration reduces neointimal hyperplasia in balloon-injured rat carotids

Federica Dellera[1*]; Giulia S. Ganzetti[1*]; Alberto Froio[2]; Stefano Manzini[1]; Marco Busnelli[1]; Andreas Meinitzer[3]; Cesare R. Sirtori[1]; Giulia Chiesa[1]; Cinzia Parolini[1]

[1] Department of Pharmacological and Biomolecular Sciences, Università degli Studi di Milano, Milano, Italy;
[2] Department of Surgery and Interdisciplinary Medicine, University of Milano-Bicocca, Milano, Italy;
[3] Medical University of Graz, Graz, Austria
[*] The authors equally contributed to the work

Published on: *Thrombosis and Haemostasis, 2016 Aug 1;116(2):400-2. doi: 10.1160/TH15-10-0831. Epub 2016 Jun 9.*

LETTER TO THE EDITOR

Identifying new players in cardiovascular health is crucial to improve risk prediction and to establish novel targets of treatment (1). Recent studies have indicated a particular relevance of L-homoarginine (homoarginine) metabolism in cardiovascular health (2–4). Homoarginine is an arginine homologue whose physiological role is unknown, that differs from arginine by an additional methylene group. Because of this structural similarity, homoarginine may be a substrate, alternative to arginine, for nitric oxide synthase (NOS) (5). Additionally, it may also indirectly increase nitric oxide (NO) production by inhibiting arginase activity, thus raising arginine availability (6). In support of these evidences, homoarginine levels have been associated with endothelial function (3, 7). Data from clinical studies have indicated that low homoarginine concentrations independently predict mortality from cardiovascular disease, including sudden cardiac death, heart failure, and fatal ischaemic stroke (4, 8–11). Two independent Genome-Wide Association Studies (GWAS) documented a strong association between serum homoarginine

concentration and the region on chromosome 15 containing the arginine: glycine amidinotransferase (AGAT) gene (12, 13). AGAT plays a central role in energy metabolism by catalysing the conversion of arginine and glycine to ornithine and guanidinoacetate, which is subsequently methylated to creatine. However, when AGAT uses lysine instead of glycine, homoarginine is formed (14). Interestingly, AGAT knockout mice are characterised by extremely low levels of homoarginine and, when experimental ischemic stroke was induced, these mice had larger infarct volumes and worse neurological deficits compared to controls. Importantly, these features were attenuated by homoarginine supplementation (12). The possible role of homoarginine on smooth muscle cell proliferation and migration that can occur after arterial balloon angioplasty has never been explored. To this aim, balloon injury was performed in the left carotid artery of Sprague-Dawley rats, followed by the insertion of a cannula into the right jugular vein for continuous i. v. drug administration (15). Thirty-six male Sprague-Dawley rats were randomly divided into three treatment groups: group 1, infused with saline (CTR); group 2, infused with L-

arginine (30 mg/kg/day in saline, ARG); group 3, infused with L-homoarginine (30 mg/kg/day in saline, HOMO). The intravenous infusion lasted 14 days, starting from the day of arterial injury, and was achieved by connecting the cannula to an osmotic infusion pump containing 2 ml of the solutions described above. Systolic blood pressure was measured by tail cuff volume-oscillometric method in conscious animals, before and 14 days after balloon injury. At the end of drug treatments, blood was collected, rats were humanly sacrificed and carotids harvested for analyses (see thrombosis-online.com). No signs of toxicity by treatments were detected. Homoarginine-treated rats showed a significant reduction of vessel intimal/medial area ratio compared to controls ($p<0.05$; Figure 1 A). This inhibition of neointimal hyperplasia was similar to that observed in the ARG group, where the intimal/medial ratio was also lower than that measured in control rats, supporting previous results (15) (Figure 1 A). No differences were observed in the medial area among the three experimental groups (data not shown). A significant decrease of neointimal cell proliferation was observed in homoarginine and arginine-treated rats compared to

controls (Figure 1 B), whereas only a trend towards increased cell apoptosis was observed (15.5 ± 5.1 %, 14.7 ± 4.5 %, 10.3 ± 5.1 % in ARG, HOMO, CTR, respectively, $p>0.05$). Homoarginine, arginine and ornithine concentrations were measured in blood collected from fasted rats at the end of the treatments. Homoarginine serum levels were dramatically high in homoarginine-treated rats compared to CTR and ARG groups (38.5 ± 8.4 µM, 1.2 ± 0.1 µM, 1.1 ± 0.3 µM in HOMO, ARG, CTR groups, respectively; $p<0.0001$). Arginine concentration was measured in plasma to avoid confounding effects caused by the release of arginine from platelets (16). In both ARG and HOMO groups, arginine plasma levels were moderately, but significantly increased compared to controls (137.3 ± 15.6 µM, 139.3 ± 25.9 µM, and 116.2 ± 12.9 µM in ARG, HOMO and CTR groups, respectively; $p<0.05$). The observed increase of arginine by homoarginine treatment is in line with previous observations suggesting that homoarginine may interfere with arginine metabolism by inhibiting arginase activity (6). No differences were detected in systolic blood pressure among the rats at baseline (data not shown), as well as at the end of treatment (156 ± 15

mmHg, 159 ± 11 mmHg, and 143 ± 14 mmHg in CTR, ARG, and HOMO groups, respectively, $p>0.05$). The lack of effect by treatments on blood pressure could be consequent to the moderate variations in arginine levels among groups. To evaluate if homoarginine and arginine treatments could result in higher NO availability, nitrite serum concentrations were measured as index of intracellular NO production and endothelial NO synthase activity (17). ARG and HOMO groups had higher levels of nitrite compared to saline-treated rats (2.4 ± 1.2 μM, 2.2 ± 0.8 μM, and 1.1 ± 0.4 μM in L-ARG, HOMO and CTR groups, respectively; $p<0.05$). Possible changes by treatment of eNOS, iNOS and Arginase I expression were evaluated. As shown in Figure 1 B-D, no significant differences were observed among groups for all these parameters. These results suggest that the higher nitrite levels in ARG and HOMO groups are not consequent to increased enzyme activity, but to higher substrate availability, as previously shown with arginine treatments in similar experimental settings (18). These results support the hypothesis that homoarginine may exert its antiproliferative effect by increasing NO release from vascular cells (19). Finally, in the HOMO group a

significant increase in serum concentration of ornithine was observed compared to CTR and ARG groups (91.0 ± 12.9 μM, 73.8 ± 11.7 μM, and 69.4 ± 9.2 μM in HOMO, ARG and CTR, respectively; $p<0.05$). The observed increase of ornithine levels may contribute to the antiproliferative effect observed in homoarginine-treated rats, since ornithine has been shown to increase NO availability, acting as arginase inhibitor (6,19). In summary, the present study shows, for the first time, that an *in vivo* administration of homoarginine is able to inhibit neointimal formation, at least in part, by inhibiting cell proliferation and by increasing both arginine availability and NO production. Taken together these results corroborate previous clinical evidences showing an association between homoarginine levels, endothelial function and cardiovascular health (3, 4, 10, 11). Moreover, our data suggest homoarginine as a therapeutic/nutraceutical option for cardiovascular protection.

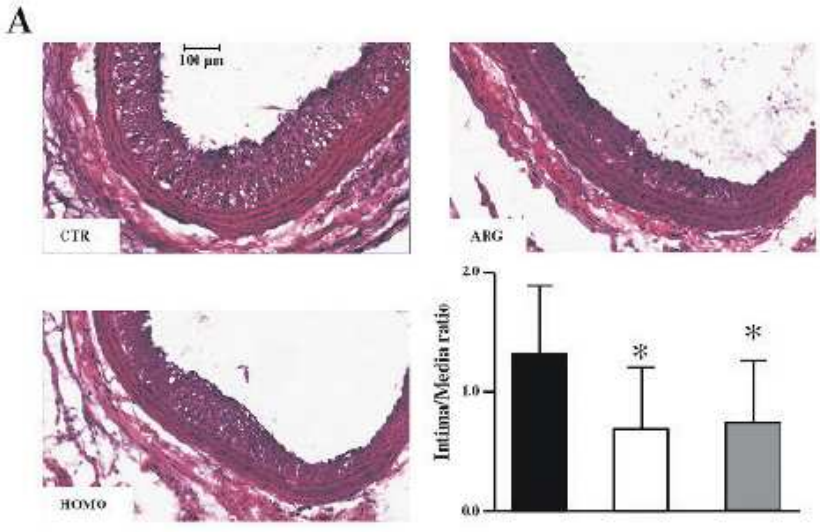
A
100 μm
CTR
ARG
HOMO
Intima/Media ratio
2.0
1.0
0.0
*
*

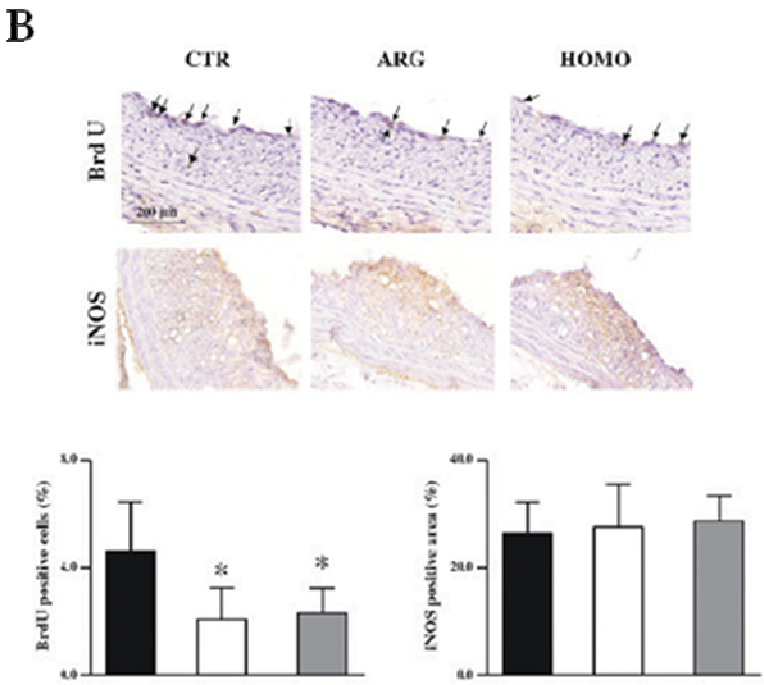
B
CTR
ARG
HOMO
Brd U
200 μm
iNOS
BrdU positive cells (%)
5.0
4.0
3.0
*
*
iNOS positive area (%)
40.0
20.0
0.0

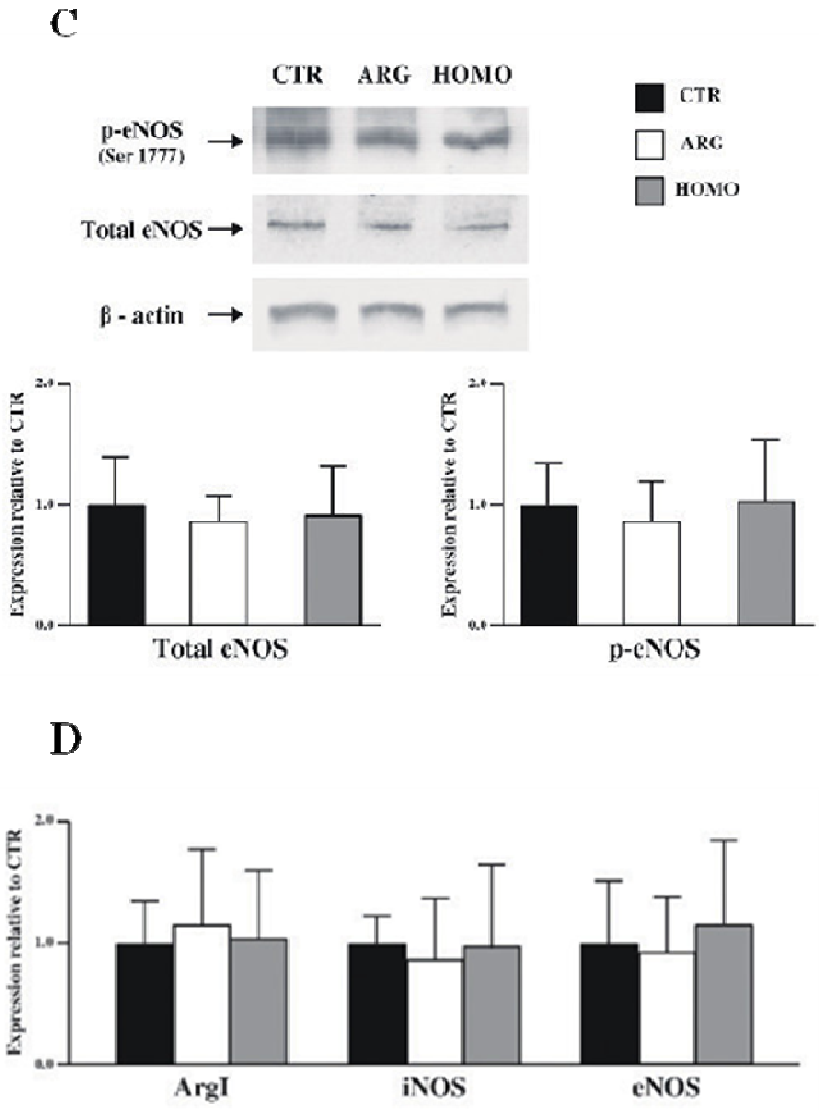

Figure 1 Homoarginine treatment inhibited neointimal hyperplasia in balloon-injured rat carotids.

A) Representative photomicrographs of cross-sections of the left carotid artery harvested from saline- (CTR), arginine- (ARG) and homoarginine- (HOMO) treated rats. Ratio of intimal to medial areas

measured in CTR, ARG and HOMO groups 14 days after balloon injury is shown, and data are expressed as: mean ± SD (n=12). **B)** Representative photomicrographs of immunostaining for bromodeoxyuridine (BrdU) and inducible NO synthase (iNOS) using specific antibodies. Histograms represent the percentage of BrdU positive cells and iNOS positive area measured in left carotids of CTR, ARG and HOMO groups. Data are expressed as: mean ± SD (n=5). **C)** Protein expression of total endothelial NOS (eNOS) and Ser 1177 phosphorilated eNOS (p-eNOS) in uninjured right carotids of saline-, ARG- and HOMO-treated rats. Representative Western blots of total eNOS and p-eNOS, and mean expression values are shown. Data are relative to the levels in CTR animals set as 1 and expressed as mean ±SD (n=5). **D)** Relative mRNA concentrations of Arginase I (ArgI), iNOS and eNOS in right carotids harvested from saline-, ARG- and HOMO-treated rats, normalized to reference gene Ppia. Data are relative to the levels in CTR animals set as 1 and expressed as mean ± SD (n=5). *$p<0.05$ vs CTR.

Conflicts of interest

None declared.

REFERENCES

1. Hoefer IE, Steffens S, Ala-Korpela M, et al. Novel methodologies for biomarker discovery in atherosclerosis. Eur Heart J 2015; 36: 2635–2642.

2. Kakoki M, Kim HS, Edgell CJ, et al. Amino acids as modulators of endothelium-derived nitric oxide. Am J Physiol Renal Physiol 2006; 291: F297-F304.

3. Valtonen P, Laitinen T, Lyyra-Laitinen T, et al. Serum L-homoarginine concentration is elevated during normal pregnancy and is related to flowmediated vasodilatation. Circ J 2008;72: 1879–1884.

4. März W, Meinitzer A, Drechsler C, et al. Homoarginine, cardiovascular risk, and mortality. Circulation 2010; 122: 967–975.

5. Moali C, Boucher JL, Sari MA, et al. Substrate specificity of NO synthases: detailed comparison of L-arginine, homo-L-arginine, their N omega-hydroxy derivatives, and N omega-hydroxynor-L-arginine. Biochemistry 1998; 37: 10453–10460.

6. Hrabák A, Bajor T, Temesi A. Comparison of substrate and inhibitor specificity of arginase and nitric oxide (NO) synthase for arginine analogues and related compounds in

murine and rat macrophages. Biochem Biophys Res Commun 1994; 198: 206-212.

7. Kakoki M, Kim HS, Arendshorst WJ, et al. L-Arginine uptake affects nitric oxide production and blood flow in the renal medulla. Am J Physiol Regul Integr Comp Physiol 2004; 287: R1478-R1485.

8. Pilz S, Meinitzer A, Tomaschitz A, et al. Low homoarginine concentration is a novel risk factor for heart disease. Heart 2011; 97: 1222–1227.

9. Drechsler C, Meinitzer A, Pilz S, et al. Homoarginine, heart failure, and sudden cardiac death in haemodialysis patients. Eur J Heart Fail 2011; 13: 852–859.

10. Pilz S, Meinitzer A, Gaksch M, et al. Homoarginine in the renal and cardiovascular systems. Amino Acids 2015; 47: 1703–1713.

11. Atzler D, Schwedhelm E, Choe CU. L-homoarginine and cardiovascular disease. Curr Opin Clin Nutr Metab Care 2015; 18: 83–88.

12. Choe CU, Atzler D, Wild PS, et al. Homoarginine levels are regulated by L-arginine:glycine amidinotransferase and affect stroke outcome: results from human and murine studies. Circulation 2013; 128: 1451–1461.

13. Kleber ME, Seppälä I, Pilz S, et al. Genome-wide association study identifies 3 genomic loci significantly associated with serum levels of homoarginine: the AtheroRemo Consortium. Circ Cardiovasc Genet 2013; 6: 505–513.

14. Davids M, Ndika JD, Salomons GS, et al. Promiscuous activity of arginine:glycine amidinotransferase is responsible for the synthesis of the novel cardiovascular risk factor homoarginine. FEBS Lett 2012; 586: 3653–3657.

15. Ohwada T, Ishibashi T, Yaoita H, et al. Different contribution of apoptosis to the antiproliferative effects of L-arginine, enalapril and losartan on neointimal growth inhibition after balloon arterial injury. Circ J 2002; 66: 965–971.

16. Teerlink T, Nijveldt RJ, de Jong S, et al. Determination of arginine, asymmetric dimethylarginine, and symmetric dimethylarginine in human plasma and other biological samples by high-performance liquid chromatography. Anal Biochem 2002;

303: 131–137.

17. Wang BS, Huang GJ, Lu YH, et al. Anti-inflammatory effects of an aqueous extract of Welsh onion green leaves in mice. Food Chem 2013; 138: 751–756.
18. Forbes SP, Alferiev IS, Chorny M, et al. Modulation of NO and ROS production by AdiNOS transduced vascular cells through supplementation with L-Arg and BH4: implications for gene therapy of restenosis. Atherosclerosis 2013; 2301: 23–32.
19. Durante W. Role of arginase in vessel wall remodeling. Front Immunol 2013; 4: 111.

SUPPLEMENTARY METHODS

Animals and experimental protocol

Procedures involving animals and their care, as well as animal monitoring during treatment, were conducted in accordance with institutional guidelines that are in compliance with national (D.L. No. 26, March 4, 2014, G.U. No. 61 March 14, 2014) and international laws and policies (EEC Council Directive 2010/63, September 22, 2010: Guide for the Care and Use of Laboratory Animals, United States National Research Council, 2011).

Blood pressure measurement

Systolic blood pressure was measured by tail cuff volume-oscillometric method in conscious animals, before and 14 days after balloon injury, using a BP-2000 Blood Pressure Analysis System™ (2Biological Instruments, Besozzo, Varese, Italy).

Morphometric analysis

Harvested left carotids were fixed for 30 min in 10% formalin, placed overnight at 4°C in 20% sucrose, and then embedded in OCT compound (Sakura Finetek Europe B.V.,

Alphen aan den Rijn, The Netherlands). Serial cryosections (7 µm thick) were cut and stained with hematoxylin and eosin (Bio-Optica, Milano, Italy). The Aperio ScanScope GL Slide Scanner (Aperio Technologies, Vista, CA, USA) equipped with a Nikon 20x/0.75 Plan Apochromat objective producing a 0.25 µm/pixel scanning resolution with a 40x magnification was used to acquire images (1). The Aperio ImageScope software (version 8.2.5.1263) was used to measure intimal and medial area of the cross-sections and the ratio of the neointimal area to that of the media was calculated.

Immunohistochemical analysis

To evaluate DNA synthesis in vascular cells, five rats from each experimental group were injected with bromodeoxyuridine (BrdU, 100 mg/kg, intraperitoneally) 24 hours and 1 hour before sacrifice (2). Harvested left carotids were processed as described above. Cryosections were incubated overnight at 4°C with a murine monoclonal antiBrdU antibody (Bu20a clone, Dako Italia, Cernusco sul Naviglio, Italy). After washing with PBS, sections were incubated with the secondary antibody (ImmPRESS

Reagent Kit, Anti-mouse Ig, Vector Laboratories, Burlingame, USA) and then visualized with 3,3'-diaminobenzidine tetrahydrochloride (DAB; Sigma-Aldrich, Milano, Italy). The sections were counterstained with Gill's hematoxylin (Bio-Optica, Milano, Italy). To assess the expression of iNOS in the neointima and the presence of vascular cell apoptosis, cryosections were incubated overnight at 4°C with a rabbit polyclonal antiiNOS primary antibody (LifeSpan BioSciences, Seattle, USA) and with a rabbit polyclonal anti-cleaved caspase-3 (Asp175) antibody (Cell Signaling, Danvers, USA), respectively. After washing, slides were incubated for 30 min with the secondary antibody (ImmPRESS Reagent Kit, Anti-rabbit Ig, Vector Laboratories, Burlingame, USA) and immunostaining was visualized by using DAB. Sections were counterstained with Gill's hematoxylin solution. All cryosections were acquired with the Aperio ScanScope GL Slide Scanner, as described above. BrdU-positive rate was defined as the percentage of BrdU-positive cells in 200 cells of neointima in random fields under high magnification. The percentage of DAB-positive area was evaluated using ImageScope software, Aperio (Aperio Technologies, Vista, USA).

Biochemical measurements

Plasma arginine and serum homoarginine and ornithine concentrations were measured in samples stored at -80°C by a high-performance liquid chromatography method, as previously described (3-5). Intra-assay and interassay CVs were below 10%. Serum levels of nitrite were measured using the assay based on the Griess reaction, as described by Wang et al (6). Briefly, serum samples were diluted four times and 3 deproteinized. Supernatants were mixed with the Griess reagent (0.1% naphthylethylenediamide dihydrochloride, 1% sulphanilamide in 5% phosphoric acid) and incubated for 10 min at room temperature. The absorbance was then measured and compared to a sodium nitrite calibration curve. The nitrite serum levels were expressed in μM.

RNA extraction and quantitative PCR

Total RNA was isolated from right (uninjured) carotid arteries using the NucleoSpin RNA extraction kit (Macherey-Nagel, Duren, Germany) according to the manufacturer's instructions. RNA concentration and purity

were estimated evaluating the ratio of optical density at 260 and 280 nm (Nanodrop 1000, ThermoScientific, Wilgminton, DE). Total RNA was reverse transcribed with random hexamer primers and MultiScribe reverse transcriptase (Life Technologies, Carlsbad, CA) following the manufacturer's instructions. Gene expression was evaluated by quantitative PCR on a CFX Connect 96 thermal cycler by using an iTaq Universal SYBR® Green Supermix (Biorad, Segrate, Italy). The following specific primer pairs (all in 5'→3' order) were used: Arginase 1 (Arg1, TGGACCCAGTATTCACCCCG, AGTCCTGAAAGTAGCCCTGTCTT), Inducible Nitric Oxide Synthase (iNOS, AGGGAGTGTTGTTCCAGGTG, TCTGCAGGATGTCTTGAACG) and Endothelial Nitric Oxide Synthase (eNOS, CTGCAGGACAGCACAGGAAA, ACCGTGATGGCTGAACGAAG). Expression levels were normalized to housekeeping gene Peptidylprolyl Isomerase A (Ppia, AGCACTGGGGAGAAAGGATT, AGCCACTCAGTCTTGGCAGT), used as reference. Efficiency and melting curve were calculated for each primer pair. Fold changes were calculated with the ΔΔCt method.

Western blotting analysis

Right (uninjured) carotid arteries were lysed using an Ultra-Turrax T25 in ice-cold RIPA buffer (50 mM Tris–Cl pH 8.0, 150 mM NaCl, 1% NP-40, 0.5% sodium deoxycholate, 0.1% sodium dodecyl sulfate) supplemented with 2x Protease Inhibitor Cocktail (Sigma-Aldrich, Seelze, Germany) and 2x HaltTM Phosphatase Inhibitor Cocktail (Thermo Scientific, Waltham, MA). Lysates were sonicated and the protein 4 concentration was determined as previously described (7). 4 fractionated by SDS–PAGE in 12% acrylamide gels and then transferred onto Hybond-C extra nitrocellulose membranes (Amersham, Buckinghamshire, UK). The following antibodies (Cell Signaling, Danvers, MA) were used at 1:1000 dilution for overnight hybridization at 4°C: eNOS (#9570) and Phospho-eNOS Ser1177 (p-eNOS, #9570). Membranes were then washed and further incubated with 1:5000 horseradish peroxidase-conjugated anti-rabbit IgG (#7074). The signal was detected with the Pierce ECL Western Blotting Substrate (Thermo Scientific). Bands were quantified with Image Studio (LI-COR, Lincoln, NE).

Statistical Analysis

Results are expressed as mean ± SD. Statistical analysis was performed using Systat 13 Software (Systat Software Inc., San Jose, USA). Differences among the experimental groups were determined with analysis of variance (ANOVA) and when significant differences were found, a Tukey test was performed. A value of $P<0.05$ was considered statistically significant.

Suppl. References

1. Parolini C, Busnelli M, Ganzetti GS, Dellera F, Manzini S, Scanziani E, Johnson JL, Sirtori CR, Chiesa G. Magnetic resonance imaging visualization of vulnerable atherosclerotic plaques at the brachiocephalic artery of apolipoprotein E knockout mice by the blood-pool contrast agent B22956/1. Mol Imaging. 2014;13: 1-9.

2. Tsihlis ND, Vavra AK, Martinez J, Lee VR, Kibbe MR. Nitric oxide is less effective at inhibiting neointimal hyperplasia in spontaneously hypertensive rats. Nitric Oxide. 2013;35:165-174.

3. Teerlink T, Nijveldt RJ, de Jong S, van Leeuwen PA. Determination of arginine, asymmetric dimethylarginine,

and symmetric dimethylarginine in human plasma and other biological samples by high-performance liquid chromatography. Anal Biochem. 2002;303: 131-137. 5

4. Schwarz EL, Roberts WL, Pasquali M. Analysis of plasma amino acids by HPLC with photodiode array and fluorescence detection. Clin Chim Acta. 2005;354: 83- 90.

5. Meinitzer A, Puchinger M, Winklhofer-Roob BM, Rock E, Ribalta J, Roob JM, Sundl I, Halwachs-Baumann G, März W. Reference values for plasma concentrations of asymmetrical dimethylarginine (ADMA) and other arginine metabolites in men after validation of a chromatographic method. Clin Chim Acta. 2007;384: 141-148.

6. Wang BS, Huang GJ, Lu YH, Chang LW. Anti-inflammatory effects of an aqueous extract of Welsh onion green leaves in mice. Food Chem. 2013;138: 751-756.

7. Manzini S, Pinna C, Busnelli M, Cinquanta P, Rigamonti E, Ganzetti GS, Dellera F, Sala A, Calabresi L, Franceschini G, Parolini C, Chiesa G. Beta2-adrenergic activity modulates vascular tone regulation in lecithin:cholesterol acyltransferase knockout mice. Vascul Pharmacol. 2015;74:114-121.

Chapter 3

A Salmon Protein Hydrolysate Exerts Lipid-Independent Anti-Atherosclerotic Activity in ApoE-Deficient Mice

Cinzia Parolini[1*], Rita Vik[2*], Marco Busnelli[1], Bodil Bjørndal[2], Sverre Holm[3], Trond Brattelid[4], Stefano Manzini[1], Giulia S. Ganzetti[1], Federica Dellera[1], Bente Halvorsen[3], Pål Aukrust[3], Cesare R. Sirtori[1], Jan E. Nordrehaug[5], Jon Skorve[2], Rolf K. Berge[2,5], Giulia Chiesa[1]

[1] Department of Pharmacological and Biomolecular Sciences, Universita` degli Studi di Milano, Milan, Italy
[2] Department of Clinical Science, University of Bergen, Bergen, Norway
[3] Research Institute of Internal Medicine, Rikshospitalet University Hospital, Oslo, Norway
[4] National Institute of Nutrition and Seafood Research, NIFES, Bergen, Norway
[5] Department of Heart Disease, Haukeland University Hospital, Bergen, Norway
[*] The authors equally contributed to the work

Published on: *PlosOne 2014 May 19;9(5):e97598.*

ABSTRACT

Fish consumption is considered health beneficial as it decreases cardiovascular disease (CVD)-risk through effects on plasma lipids and inflammation. We investigated a salmon protein hydrolysate (SPH) that is hypothesized to influence lipid metabolism and to have anti-atherosclerotic and anti-inflammatory properties. 24 female apolipoprotein apo E $^{-/-}$ mice were divided into two groups and fed a high-fat diet with or without 5% (w/w) SPH for 12 weeks. The atherosclerotic plaque area in aortic sinus and arch, plasma lipid profile, fatty acid composition, hepatic enzyme activities and gene expression were determined. A significantly reduced atherosclerotic plaque area in the aortic arch and aortic sinus was found in the 12 apo E $^{-/-}$ mice fed 5% SPH for 12 weeks compared to the 12 casein-fed control mice. Immunohistochemical characterization of atherosclerotic lesions in aortic sinus displayed no differences in plaque composition between mice fed SPH compared to controls. However, reduced mRNA level of Icam1 in the aortic arch was found. The plasma content of arachidonic acid (C20:4n-6) and oleic acid (C18:1n-9) were increased and decreased, respectively. SPH-feeding

decreased the plasma concentration of IL-1β, IL-6, TNF-α and GM-CSF, whereas plasma cholesterol and triacylglycerols (TAG) were unchanged, accompanied by unchanged mitochondrial fatty acid oxidation and acyl-CoA:cholesterol acyltransferase (ACAT)-activity. These data show that a 5% (w/w) SPH diet reduces atherosclerosis in apo E $^{-/-}$ mice and attenuate risk factors related to atherosclerotic disorders by acting both at vascular and systemic levels, and not directly related to changes in plasma lipids or fatty acids.

INTRODUCTION

Cardiovascular disease (CVD) is responsible for approximately 16–17 million deaths annually, making it the leading cause of mortality in Western countries (1), (2). The disease encompasses conditions such as coronary artery disease, carotid and cerebral atherosclerotic disease and peripheral artery atherosclerosis resulting in chronic and acute ischemia in affected organs. The underlying pathological process is lipid accumulation leading to atherosclerosis, a slowly progressing chronic disorder of large and medium-sized arteries that can lead to intravascular thrombosis with subsequent development of complications like myocardial infarction (MI), stroke and acute ischemia of the limb (3). In the last years, inflammation has emerged as an additional key factor in the development of atherosclerosis and seems to be involved in all stages, from the small inflammatory infiltrate in the early lesions, to the inflammatory phenotype characterizing an unstable and rupture-prone atherosclerotic lesion (4). In fact, today atherosclerosis is regarded as a disorder characterized by a status of non-resolved inflammation, with bidirectional interaction

between lipids and inflammation as a major phenotype. Inflammation in atherosclerosis leads to activation of endothelial cells, enhanced expression of adhesion molecules, inflammatory cytokines and macrophage accumulation.

Liver is the main organ regulating lipid metabolism, affecting blood lipids, especially plasma triacylglycerols (TAG) (5). Recently, investigators have suggested that the liver plays a key role in the inflammatory state of an individual (6, 7) and that dietary cholesterol absorbed by the liver contributes to inflammation (8). Research into atherosclerosis has led to many compelling discoveries about the mechanisms of the disease and together with lipid abnormalities and chronic inflammation, oxidative stress has a crucial involvement in the initiation and progression of atherosclerosis (9).

Improvement of life style and dietary habits can reduce some risk factors such as high levels of low density lipoprotein (LDL)-cholesterol, TAG and inflammatory molecules (10). Fish consumption is consider health beneficial as it lowers plasma lipids and attenuates inflammation (11). This is linked to the long-chained n-3

polyunsaturated fatty acids (PUFA) content, in particular eicosapentaenoic acid (EPA) and docosahexaenoic acid (DHA). However, fish protein is a rich source of bioactive peptides with valuable nutraceutical and pharmaceutical potentials beyond that of n-3 PUFAs (11). Fish protein hydrolysates are generated by enzymatic conversion of fish proteins into smaller peptides, which normally contain 2–20 amino acids. In recent years, fish protein hydrolysates have attracted much attention from food scientists due to a highly balanced amino acid composition, as well as the presence of bioactive peptides (12). The organic acid taurine is mainly found in marine proteins, and is suggested to induce cholesterol-lowering effect by increasing excretion through bile, thus potentially exerting an anti-atherosclerotic effect (13). Recent studies show TAG-lowering effects (14, 15), antioxidant capacity (12), antihypertensive (11) and cholesterol-lowering effects (16, 17) and potential to reduce markers of reactive oxygen species (18) from fish protein. Therefore, fish protein hydrolysates have been implicated in several processes with potential anti-atherogenic effects. In this study, we examined the anti-atherosclerotic potential of a salmon

protein hydrolysate (SPH) on atherosclerotic development in apolipoprotein E-knockout (apo $E^{-/-}$) mice.

MATERIALS AND METHODS

Experimental Design

The study was conducted according to national (D.L. 116, G.U. Suppl. 40, February 18, 1992, Circolare No. 8, G.U July 1994) and international laws and policies (EEC Council Directive 2010/63, September 22, 2010: Guide for the Care and Use of Laboratory Animals, United States National Research Council, 2011). The Italian Ministry of Health approved the protocol (n° 04/2012).

24 female apo $E^{-/-}$ mice from the breeding strain C57BL/6, 8 weeks old, were purchased from Charles River Laboratories (Calco, Italy), and kept under standard laboratory conditions (12 hours light cycle, temperature 22±1°C, humidity 55±5%), with free access to standard chow and tap water. After 1 week of acclimatization under these conditions, mice were randomly divided into two groups of 12 mice. Although apo $E^{-/-}$ mice spontaneously develop atherosclerosis, both groups were fed a high-fat diet (23.7% w/w) consisting of 21,3% lard (Ten Kate Vetten

BV, Musselkanaal, Netherlands) and 2.4% soy oil (Dyets. Inc., Betlehem, PA, USA) to accelerate the atherosclerotic formation. The control diet contained 21% w/w casein as protein source, whereas 5% casein was replaced with an equal amount of salmon protein hydrolysate (SPH) (Marine Bioproducts, Storebø, Norway) in the intervention diet. The SPH was produced by enzymatic hydrolysis from salmon by-products (spine) using controlled autolysis with an alkaline protease and a neutral protease, and the resulting protein hydrolysate was then subjected to a second enzymatic treatment with an acid protease A. The final hydrolysate was fractionated using micro- and ultra-filtration and the size distribution of the peptides was analysed. The final preparation consisted of peptides <1200 Da and 25% of the peptides were below 200 Da. The diets were isocaloric containing 21% protein, 24% fat, 42% carbohydrates and 6% micronutrients, and administered for 12 weeks. Other diet ingredients were from Dyets. Inc., and the full composition of the diets, as well as amino acid composition, is given in **Table S1**.

Harvesting of Tissue

During the treatment period, blood samples were collected at day 1 and after 77 days from the retro-orbital plexus into tubes containing 0.1% (w/v) EDTA after an overnight fast. Blood samples were chilled on ice for at least 15 minutes and stored at −80°C until analyses.

After 12 weeks of treatment, mice were sacrificed under general anaesthesia with 2% isoflurane (Forane, from Abbot Laboratories Ltd, Illinois, USA) and blood was removed by perfusion with phosphate-buffered saline (PBS). Aorta was rapidly dissected from the aortic root to the iliac bifurcation, periadventitial fat and connective tissue was removed as much as possible. Aorta was longitudinally opened pinned flat on a black wax surface in ice-cold PBS, photographed unstained (19) for subsequent plaque quantification (see *En face analysis*), and then immediately put in a tissue-freezing medium, snap-frozen in liquid nitrogen and stored at −80°C. For histological/immunohistochemical analysis, six hearts from each group were removed, fixed in 10% formalin for 30 min and transferred into PBS containing 20% sucrose (w/v) overnight at 4°C before being embedded in OCT compound

(Sakura Finetek Euope B.V., Alphen aan den Rijn, The Netherlands) and stored at −80°C. An equal subset of hearts and all livers were immediately snap-frozen in liquid nitrogen for subsequent analyses.

En Face Analysis

Aorta images were recorded with a stereomicroscope-dedicated camera (IC80 HD camera, MZ6 microscope, Leica Microsystems, Germany) and analysed using ImageJ image processing program (http://rsb.info.nih.gov/ij/). An operator blinded to dietary treatment quantified the atherosclerotic plaques.

Aortic Sinus Histology/immunohistochemistry

Serial cryosections (7 µm thick) of the aortic sinus were cut. Approximately 25 slides with 3 cryosections/slide were obtained, spanning the three cusps of the aortic valves. Every fifth slide was fixed and stained with hematoxylin and eosin (Bio-Optica, Milano, Italy) to detect plaque area. Plaque area was calculated as the mean area of those sections showing the three cusps of the aortic valves. Adjacent slides were stained to characterize plaque

composition. Specifically, Masson's Trichrome (04-010802, Bio-Optica, Milano, Italy) was used to detect extracellular matrix deposition and Oil red O staining (Sigma-Aldrich, St. Louis, MO, USA) was used to detect intraplaque neutral lipids.

Macrophages and T-lymphocytes were detected using an anti-F4/80 antibody (ab6640, Abcam, Cambridge, UK), and an anti-CD3 antibody (ab16669, Abcam, Cambridge, UK), respectively. A biotinylated secondary antibody was used for streptavidine-biotin-complex peroxidase staining (Vectastain Abc Kit, Vector Laboratories, Peterborough, UK). 3,3'-Diaminobenzidine was used as chromogen (Sigma-Aldrich, St. Louis, MO, USA), and sections were counterstained with hematoxylin (Gill's Hematoxylin, Bio-Optica, Milano, Italy). To acquire and process digital images an Aperio ScanScope GL Slide Scanner (Aperio Technologies, Vista, CA, USA), equipped with a Nikon 20×/0.75 Plan Apochromat objective producing a 0.25 µm/pixel scanning resolution with a 40× magnification and the Aperio ImageScope software (version 8.2.5.1263) was used. A blinded operator to the study quantified plaque area, extracellular matrix and lipid deposition, as well as

inflammatory cell infiltrate. The amount of extracellular matrix, lipids, macrophages and T-lymphocytes was expressed as percent of the stained area over the total plaque area.

Plasma Lipid and Fatty Acid Composition Measurements

Enzymatically measurements of plasma lipids were performed with an automated method for direct measurement of lipids on a Hitachi 917 system (Roche Diagnostics GmbH, Mannheim, Germany) using triacylglycerol (GPO-PAP), total- and free cholesterol kits (CHOD-PAP) from Roche Diagnostics, and phospholipids FS kit and a non-esterified fatty acids (NEFA) kit from DiaSys (Diagnostic Systems GmbH, Holzheim, Germany). Total plasma fatty acid composition was analyzed as previously described (20).

Gene Expression in Liver, Heart and Aorta

Total cellular RNA was purified from 20 mg liver, total homogenized heart and pooled aorta samples from six mice using the RNeasy kit and the protocol for purification of total RNA from animal cells and fibrous tissue (Qiagen

GmbH, Hilden, Germany), as described by Vigerust *et al*. and Strand *et al*., respectively (21, 22). cDNA was obtained as described by Strand *et al.* (22). Real-time PCR was performed on an ABI prism 7900 H sequence detection system (Applied Biosystems, Foster City, CA, USA) using 384-well multiply PCR plates (Sarstedt Inc., Newton, NC, USA) and probes and primers from Applied Biosystems, Foster City, CA, USA as described by Strand *et al*. (22). The primers used are listed in **Table S2**. Six different reference genes were included for liver: 18*s* (Kit-FAM-TAMRA (Reference RT-CKFT-18s)) from Eurogentec (Seraing, Belgium), ribosomal protein, large, P0 (*Rplp0*, AX-061958-00-0100), hypoxanthine guanine phosphoribosyltransferase 1 (*Hprt1*, AX-045271-00), ribosomal protein, large, 32 (*Rpl32*, AX-055111-00), polymerase (RNA)II(DNA directed) polypeptide A, (*Polr2a,* AX-046005-00) and TATA-box binding protein (*Tbp*, AX-041188-00) all five from Thermo Fisher Scientific Inc. (Waltham, MA, USA). For the heart *18s*, *Rplp0* and *Hprt1* were used, and for aorta *18s*, *Rplp0*, *Rpl32* and *Hprt1*. The software GeNorm (http://www.gene-quantification.de/hkg.html) was used to evaluate the reference genes, and data normalized to

Rplp0 and *Rpl32* for liver, *Hprt1* for heart and *Rplp0* and *Hprt1* for aorta, are presented.

Hepatic Enzyme Activities

Livers were homogenized and the post-nuclear fraction isolated as described earlier (23). The assay for carnitine palmitoyltransferase (CPT)-2 was performed according to Bremer (24) and Skorve *et al* (25), but with some modifications: the reaction mix contained 17.5 mM HEPES pH 7.5, 52.5 mM KCl, 5 mM KCN, 100 mM palmitoyl-CoA and 0.01% Triton X-100. The reaction was initiated with 100 µM [methyl-14C]-L-carnitine (1100 cpm/ηmol), and 35 µg total protein was used. Palmitoyl-CoA oxidation was measured in the post-nuclear fraction from liver as acid-soluble products (26). The activity of fatty acyl-CoA oxidase (ACOX)-1 and acyl-CoA: cholesterol transferase (ACAT) were measured in post-nuclear fractions as described by Madsen *et al.* (26) and Field *et al*. (27), respectively.

Measurements of Plasma Inflammatory Markers

Levels of interleukin (IL)-1β, IL-6, IL-10, tumor necrosis factor (TNF)-α and granulocyte-macrophage colony-stimulating factor (GM-CSF) were analyzed on plasma samples collected at day 77 of treatment by Multiplex suspension technology using a customized Bio-Plex Pro Mouse assay (Bio-Rad Laboratories, Hercules, CA).

Statistical Analysis

The results are presented as mean with standard deviation (SD) for 4–12 mice per group. Normal distribution was assessed by the Kolmogorov-Smirnov test. Unpaired Student's *t*-test was used to evaluate statistical differences between groups; Mann-Whitney test was applied when data were not normally distributed. A value of $P<0.05$ was considered statistically significant. Statistical analyses were performed using Prism Software (GraphPad Prism version 5.0; GraphPad Prism, San Diego, CA, USA).

RESULTS

The SPH-diet Decreased Atherosclerotic Plaque Development

After 12 weeks on a high-fat diet, 5% SPH-fed mice displayed a weight gain similar to the control group. At sacrifice, the average weight gain was 5.98±1.78 g (mean ± SD) in controls and 5.04±0.88 g in SPH mice ($P>0.05$). A significantly lower plaque development was observed in the aortic arch in SPH-fed mice compared to control mice (0.55±0.33 vs. 1.63±0.99×10^6 μm^2; **Fig. 1**, corresponding to 0.91±0.55 vs. 2.72±1.72% of the aortic surface covered by plaque). There were no differences in thoracic (1.08±0.47 vs. 0.85±0.41×10^6 μm^2; **Fig. 1**, corresponding to 1.71±0.84 vs. 1.41±0.68% of the aortic surface covered by plaque) or abdominal aorta sections (0.81±0.53 vs. 0.78±0.53×10^6 μm^2; **Fig. 1**, corresponding to 1.36±0.89 vs. 1.29±0.88% of the aortic surface covered by plaque).

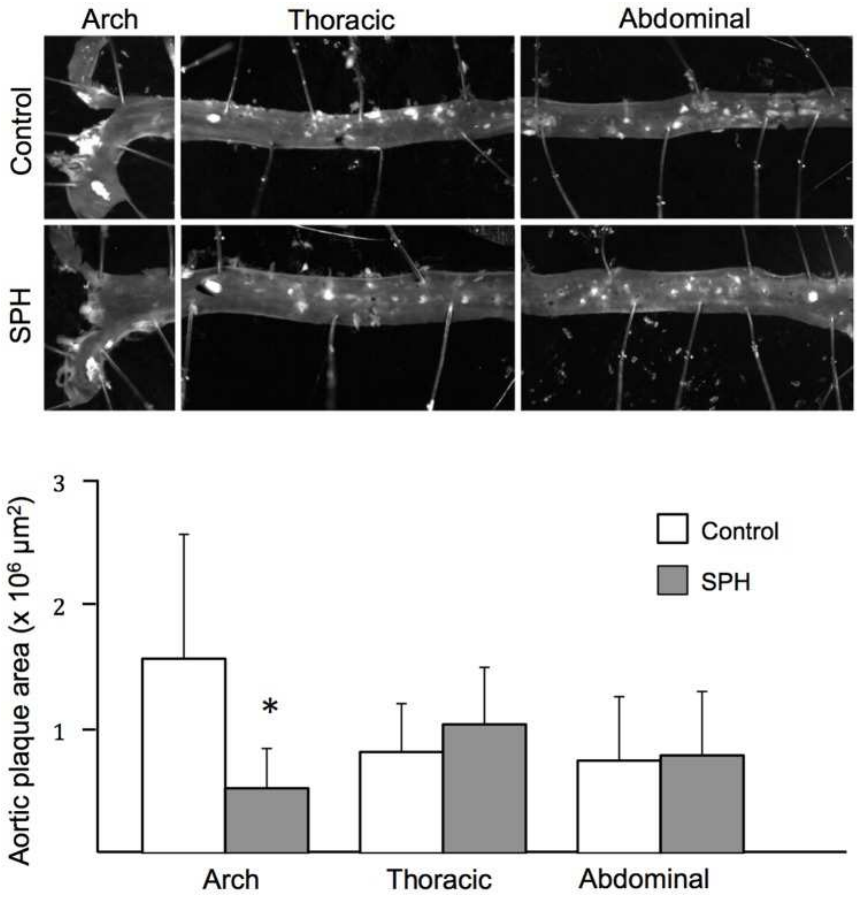

Fig. 1 Atherosclerotic plaque level in apo $E^{-/-}$ mice fed a high-fat diet (control) or a diet with 5% SPH.

After 12 weeks of dietary treatment, whole aorta was collected and *en-face* analysis was performed to quantify aortic surface covered by atherosclerotic plaques. Bars represent means ± SD of 12 mice for each diet. Unpaired *t*-test was used to detect statistical significance (*P<0.05).

A significant reduction in lesion area was observed at the aortic sinus of mice fed SPH compared to controls ($1.27\pm0.41\times10^5$ μm^2 vs. $2.02\pm0.31\times10^5$ μm^2; **Fig. 2A–C**). Plaque stability is an important factor concerning the severity of atherosclerosis. However, histological/immunohistochemical characterization of atherosclerotic lesions displayed no significant difference in plaque composition between mice fed SPH and controls, showing a comparable percentage of area occupied by extracellular matrix (34.56±0.56% vs. 30.31±18.25%; **Fig. 2D–F**), lipids (74.06±7.48% vs. 79.68±6.45%; **Fig. 2G–I**), macrophages (64.47±4.47% vs. 60.57±3.71%; **Fig. 2J–L**), and lymphocytes (27.36±11.73% vs. 22.62±7.24%; **Fig. 2M–O**).

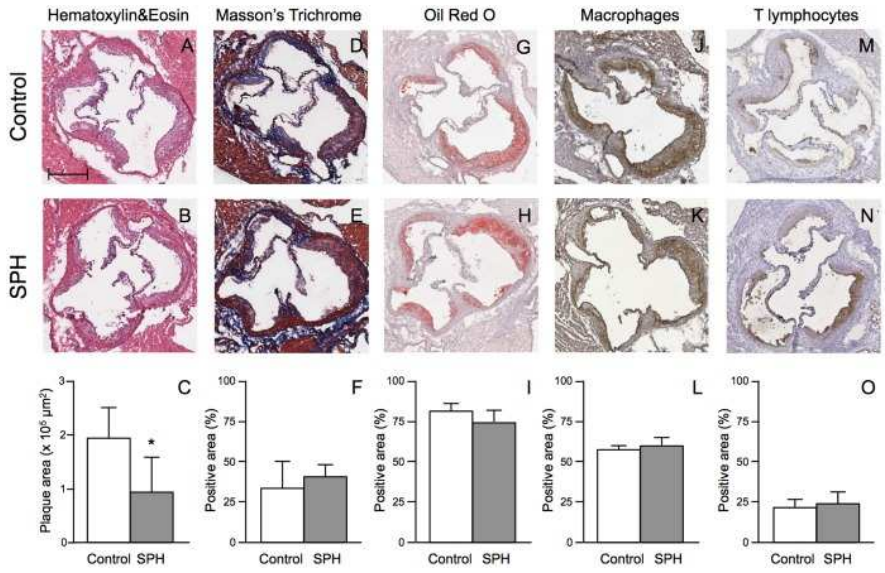

Fig. 2 Histological and immunohistochemical characterization of plaques in the aortic sinus in apo $E^{-/-}$ mice fed a high-fat diet (control) or a diet with 5% SPH for 12 weeks.

Representative photomicrographs and quantification of maximum plaque area (panels A–C). Representative photomicrographs and quantification of extracellular matrix deposition (panels D–F), Lipid deposition (panels G–I), Macrophages (panels J–L) and T lymphocytes (panels M–O). The amount of extracellular matrix, lipids, macrophages and T-lymphocytes is expressed as percentage of the stained area over the total plaque area. Bar in panel A = 100 µm. Positive area (%) refers to the percentage of the plaque area occupied by connective tissue, lipids, macrophages and T lymphocytes, respectively. Data are shown as means ± SD for 6 mice

for each diet and unpaired *t*-test was used to detect significance (*P<0.05).

Inflammation and oxidative stress are strong contributing factors in atherosclerosis, thus gene expression of inflammatory markers and redox regulators in aorta and heart were measured. Accompanied by decreased plaque area in sinus and aortic arch, mRNA level of intracellular adhesion molecule (*Icam1*) was decreased with 59.54%, in addition to a small decrease in expression of vascular cell adhesion molecule (*Vcam1*) and monocyte chemoattractant protein 1 (*Mcp1*) in pooled aortic arch from six mice, whereas mRNA level of inducible nitric oxidase 2 (*Nos2*) was not modified by the dietary treatment with SPH (**Fig. 3A**). In contrast, no changes were found in gene expression in the heart of *Icam1*, *Vcam1*, *Mcp1*, *Nos2* or *Tnfa*, nor of the antioxidant markers superoxide dismutase 1, soluble (*Sod1*), superoxide dismutase 2, mitochondrial (*Sod2*) or catalase (*Cat*) (data not shown).

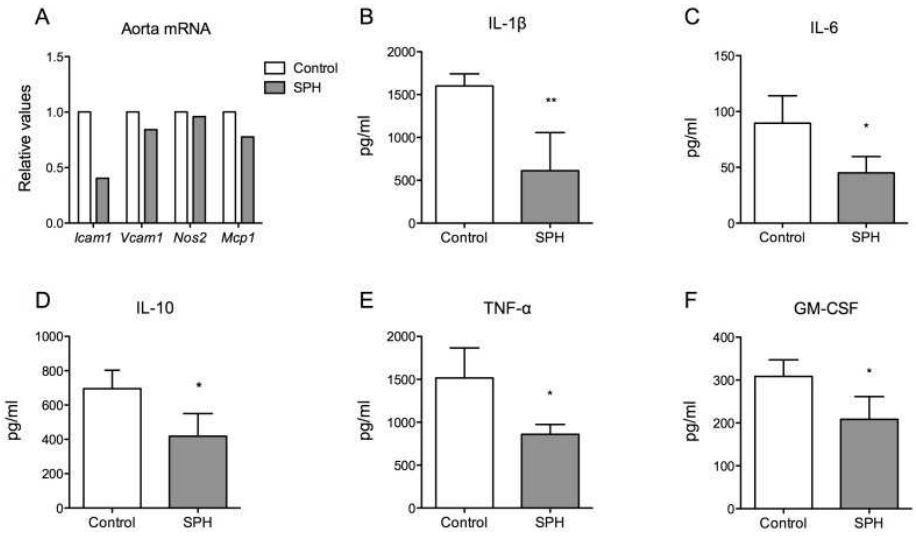

Fig. 3 Levels of mRNA expression in aorta and inflammatory mediators in plasma in apoE$^{-/-}$ mice fed a high-fat diet (control) or a diet with 5% SPH for 12 weeks.

(A) The gene expressions of the inflammatory markers *Icam1*, *Vcam1*, *Nos2* and *Mcp1* were measured in pooled aortic arch from six mice. Inflammatory markers in blood samples collected at day 77 of treatment were analysed (B) IL-1β, (C) IL-6, (D) IL-10, (E) TNF-α, (F) GM-CSF and bars represent means ± SD of 4 pooled samples of 3 mice for each diet. Unpaired *t*-test was used to assess statistical significance and results significantly different from control are indicated (*P<0.05, **P<0.01).

Decreased Plasma Levels of Inflammatory Markers

To further elucidate the potential anti-inflammatory effects of SPH in this experimental model of atherosclerosis, we examined plasma levels of inflammatory mediators. As shown in **Fig. 3B–F**, levels of IL-1β, IL-6, IL-10, TNF-α and GM-CSF were significantly lower in SPH-treated mice compared to controls.

SPH-intervention Affected Hepatic mRNA Expression Involved in Lipogenesis

Hyperlipidemia is closely linked to atherosclerotic development. Liver is the main tissue regulating lipid metabolism, and mitochondrial β-oxidation is important in regulating plasma TAG. Hepatic gene expression showed a significant downregulation in mRNA level of *Acaca* in SPH-fed mice (**Fig. 4A**). Moreover, the mRNA level of *Scd1* was significantly downregulated as well (**Fig. 4B**).

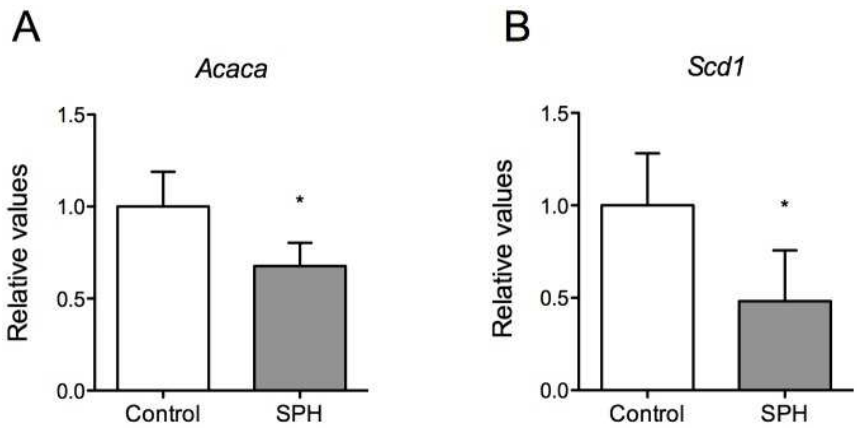

Fig. 4 Hepatic gene expression in apoE$^{-/-}$ mice fed a high-fat diet (control) or a diet with 5% SPH for 12 weeks.

Hepatic mRNA levels of (**A**) *Acaca* and (**B**) *Scd1*. Data for gene expressions are shown as mean values relative to control ± SD for 4 mice for each diet. Mann-Whitney test was used to assess statistical significance (*P<0.05).

Noteworthy, SPH administration had no effect on palmitoyl-CoA oxidation in the presence and absence of malonyl-CoA (**Fig. A** in **Table S1)**, nor on mitochondrial and peroxisomal fatty acid oxidation as the enzyme activities of CPT2 and ACOX1, respectively, were unchanged (**Fig. B** and **C** in **Figure S1**). ACAT activity, involved in cholesteryl ester synthesis, was also unaltered (**Fig. D** in **Figure S1**).

Effects of SPH on Lipid Concentration and Fatty Acid Composition in Plasma

In order to evaluate the effect of SPH treatment on plasma lipid concentration, blood was collected for enzymatic measurement of lipid profile after 77 days of dietary treatment. As shown in **Table 1**, plasma total- and free-cholesterol, as well as TAG, cholesteryl esters and phospholipids concentrations displayed comparable levels between SPH-group and control group at the end of treatment period, whereas NEFAs increased in SPH-fed mice vs. controls (**Table 1**). Moreover, no difference was observed between the two groups in the relative amount of saturated fatty acids (SFA) (**Table 2**). The relative amount of monounsaturated fatty acids (MUFA) in SPH-fed mice was slightly lower than controls at day 77, mainly due to a small decrease in 18:1n-9 (oleic acid) and 18:1n-7 (vaccenic acid) (**Table 2**). Total n-6 PUFAs displayed a higher amount after 77 days of treatment in the SPH-group, probably due to the increase of C18:2n-6 (linoleic acid) and C20:4n-6 (arachidonic acid) compared to controls. In contrast, no differences were detected in the weight % of n-3 PUFAs between the two groups. As a consequence, a small

reduction in n-3/n-6 ratio was observed after 77 days. Overall, the effect of the SPH-diet on plasma lipids and fatty acids was modest.

[1]Lipid class	Day 77	
	Control	SPH
Cholesterol	12±0.9	11±1.0
TAGs	1.4±0.1	1.3±0.1
Phospholipids	3.0±0.1	3.0±0.1
NEFAs	0.8±0.2	1.1±0.1*
Cholesteryl esters	8.1±0.8	7.9±0.8
Free Cholesterol	3.7±0.1	3.4±0.2

[1]mmol/L.
Data are shown as mean ± SD ($n=4$).
Abbreviations: NEFA, non-esterified fatty acid; SPH, salmon protein hydrolysate; TAG, triacylglycerol.
*P<0.05 vs. control.
doi:10.1371/journal.pone.0097598.t001

Tab. 1 Plasma lipids in apoE-/- mice fed a high-fat casein diet (control) or a high-fat diet with 5% SPH after 77 days of dietary treatment.

[1]Fatty acids	Control	SPH
∑SFAs	32±0.5	34±0.5
∑MUFAs	31±0.4	30±0.4*
C18:1n-9 (oleic acid)	25±0.4	24±0.5
C18:1n-7 (vaccenic acid)	1.3±0.0	1.2±0.0*
n-6 PUFAs	28±0.4	30±0.4**
C18:2n-6 (linoleic acid)	15±0.1	16±0.2***
C20:4n-6 (arachidonic acid)	12±0.4	13±0.2*
n-3 PUFAs	6.4±0.3	6.3±0.3
C20:5n-3 (eicosapentaenoic acid)	0.53±0.0	0.4±0.0
C22:6n-3 (docosahexaenoic acid)	5.0±0.3	5.0±0.2
n-3/n-6	0.2±0.0	0.2±0.0*

[1]Fatty acids (% w/w).
Data are shown as mean ± SD ($n=4$).
Abbreviations: MUFAs, monounsaturated fatty acids; PUFAs, polyunsaturated fatty acids; SFAs, saturated fatty acids; SPH, salmon protein hydrolysate.
*P<0.05 vs. control.
**P<0.01 vs. control.
***P<0.001 vs. control.
doi:10.1371/journal.pone.0097598.t002

Tab. 2 Plasma fatty acid composition in apoE2/2 mice fed a high-fat casein diet (control) or a high-fat diet with 5% SPH after 77 days of dietary treatment.

DISCUSSION

Fish intake is inversely correlated to CVD-risk factors in both observational and clinical interventional trials (28). Particular attention has been drawn to the cardio-protective effects of fatty fish species with high levels of omega-3 PUFAs through their lipid-lowering, anti-inflammatory, antiplatelet and antiarrhythmic mechanisms (29, 30). Marine organisms are also a rich source of bioactive proteins and peptides that may induce health benefits through antihypertensive and antioxidative (28), immunomodulating (31) and lipid-lowering effects (14, 17). Thus, marine proteins and peptides have been shown to influence the two major risks for atherosclerotic development, namely hyperlipidemia and inflammation. Therefore, it was of interest to investigate a potential anti-atherosclerotic effect of SPH-diet in apo $E^{-/-}$ mice fed a high-fat diet. Although these mice spontaneously develop atherosclerosis on a standard rodent diet, a high-fat diet regimen, combined with female mice, was preferred to accelerate the progression. We

showed that apo $E^{-/-}$ mice fed a high-fat diet containing 5% (w/w) SPH for 12 weeks developed less atherosclerotic plaques compared to controls. In particular, we observed a significant reduction of plaque area in the aortic arch as well as in the aortic sinus. The pathophysiological complication of atherosclerosis is plaque rupture causing heart attack and stroke in humans. Vulnerability of plaque rupture is an important element in the fatal outcomes of atherosclerosis, and content and stability of the plaque is therefore of interest. However, there was no change in aortic sinus plaque composition of connective tissue, macrophages or lymphocytes, indicating that SPH had no effect on plaque stability. Unfortunately, apo $E^{-/-}$ mice are not susceptible to the progress of plaque rupture unless treated with a high-fat diet for over a year, thus studying plaque stability in this model is limited.

During plaque development, accumulation of adhesion molecules contributes to foam cell formation. In addition to decreased plaque area in aortic arch, a decrease in expression of the adhesion molecule *Icam1*, as well as a small reduction in *Vcam1* and the chemokine *Mcp1*, was detected in pooled aortic arch of SPH-treated mice,

suggesting a local anti-atherosclerotic effect of the SPH-diet. The plaque area decreased, but no reduction in number of macrophages was observed with immunostaining in the aortic sinus. This could be due to a simultaneous decrease in number of macrophages and plaque area, which would not be reflected in a percentage measurement. The mRNA level of inflammatory markers in heart was unaltered, and could explain the unchanged levels of macrophages. However, mRNA levels were measured in total heart that may weaken a potential reduction of these inflammatory markers. The decrease in sinus plaque area, without a change of macrophages could also be explained by shrinkage of the lipid-rich core due to fewer lipids, thus the macrophages decrease in size.

Liver is the main organ regulating lipoprotein metabolism, including plasma TAG and cholesterol levels, and a high dietary cholesterol intake has been reported to elevate liver inflammation (8). Noteworthy, the plasma concentrations of cholesterol and TAG were not affected by SPH-treatment. This was accompanied by unchanged fatty acid oxidation and ACAT activity. These results are in contrast with previous reports showing cholesterol-

lowering effects of fish protein hydrolysates in both rats and mice (14, 16). Although gene expressions of *Acaca* and the Δ9-desaturase *Scd1* were decreased, it did not affect plasma TAG in apo $E^{-/-}$mice. This lack of effect could be explained, at least partially, by the lower amount of fish protein used in the present study (5%) compared to previous studies, where 10–25% fish protein hydrolysate were applied (14, 16, 17). In C57BL/6 mice fed 5% SPH for 6 weeks, a 32% decrease in plasma TAG has been found, but no change in plasma cholesterol (data to be published). Thus, in the present study, the disturbed plasma lipid transport in the apo $E^{-/-}$ mouse model might have interfered with the potential TAG-lowering mechanism of SPH, while cholesterol-lowering effect might not be expected at this dose. A lower cholesterol level has been observed in animal studies when taurine was added in the diets (32, 33). However, in our study, the cholesterol level was not affected after intervention despite the presence of taurine in the SPH-diet.

The plasma level of NEFAs was unchanged by SPH administration and only minor alterations were observed in plasma fatty acid composition. During the 12 weeks of

feeding the plasma level of MUFAs was slightly lower in the SPH-fed group, but this was probably not of biological significance. Total n-6 PUFAs in plasma was higher in SPH-fed mice at the end-point measurement. Arachidonic acid and oleic acid was increased and decreased in the SPH group and controls, respectively, after the feeding period. The increase in arachidonic acid and linoleic acid with a simultaneously decrease in oleic acid might be due to increased synthesis of arachidonic acid and linoleic acid from their precursor oleic acid. Although arachidonic acid is considered pro-inflammatory (34), we detected reduction in plaque area in aortic arch and sinus, suggesting that SPH reduced atherosclerotic activity independent of the plasma arachidonic acid level. n-3 PUFAs, the n3/n6 ratio and anti-inflammatory index were not affected by SPH feeding, which is in contrast to previous findings (35). However, as stated previously, in the current study we used a smaller amount of fish protein (5% vs. 15%) and the mouse model could also influence the effect on fatty acid composition. Knockout of the apo E gene causes an abnormal plasma lipid composition and metabolism, which apparently this SPH-diet cannot counteract.

Cytokines play a key role in the progression of atherosclerosis and it was of interest to note that the reduction in plaque area in the aortic arch was accompanied by a lowering of inflammatory markers in plasma, as reported in another study using salmon protein on inflammatory bowel disease in rats (18). Peroxisome proliferator-activated receptors (PPAR), which are ligand-dependent transcriptional factors regulating both fatty acid (36) and amino acid metabolism (37), are shown to exert anti-inflammatory potential by inhibiting expression of cytokines and other pro-inflammatory factors (38). The mechanism is unclear, but Zhu *et al.* has recently shown that marine peptides may act as PPAR-agonists and exert an anti-inflammatory effect (39). Altogether, these results suggest that SPH administration might prevent atherosclerotic development by inhibiting activation of systemic inflammation.

A small dose of SPH 3.5% in rats has been shown to potentially exert antioxidant activities by reducing markers for oxidative stress in colon (18). In the current study, gene expressions of the antioxidants *Sod1*, *Catalase* and *Nos2* in the heart were unchanged by SPH administration,

suggesting that SPH did not affect the antioxidant defence system in the heart of apo $E^{-/-}$ mice.

Although the present study has some limitations, such as absent protein data on inflammatory mediators within the aortic lesions, it gives indication that a salmon protein source may have a protective role in atherosclerotic development through mechanisms linked to inhibition of inflammation, and not directly related to plasma lipid changes. Although the apo $E^{-/-}$ mice model has been used extensively in experiments studying atherosclerosis as it gives the opportunity to study genetic influence on atherosclerosis without using a high-fat diet rich in cholesterol, it is also a challenging model to use. These mice develop severe atherosclerosis due to accumulation of VLDL in plasma carrying most of the cholesterol. VLDL, containing apoB-48, is considered more atherogenic than the apoB-100-containing LDL. High plasma levels of LDL are also most present in humans with atherosclerosis, therefore in future studies it would be of interest to test this SPH in $LDLR^{-/-}$ mice.

SUPPORTING INFORMATION

Figure S1 Hepatic enzyme activities of enzymes involved in peroxisomal and mitochondrial b-oxidation; **(Fig. A)** Palmitoyl-CoA-b-oxidation with and without inhibition with malonyl-CoA, **(Fig. B)** CPT2 activity, **(Fig. C)** ACOX1 activity and **(Fig. D)** ACAT activity.

Figure S1

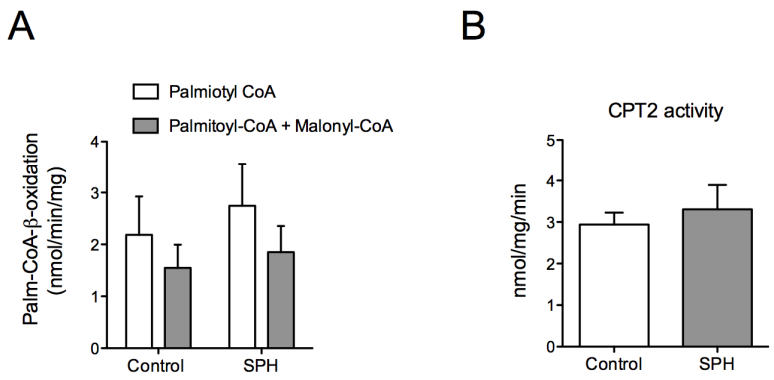

C

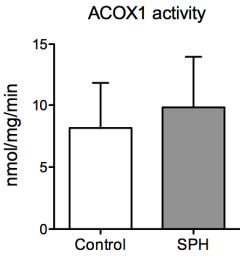
ACOX1 activity
nmol/mg/min
15
10
5
0
Control
SPH

D

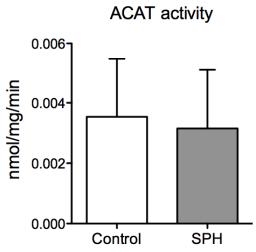
ACAT activity
nmol/mg/min
0.006
0.004
0.002
0.000
Control
SPH

Table S1

[1]Composition of the diets

[2]**Ingredients**	[3]**Control**	[4]**SPH**
Protein source		
Casein	250	200
Salmon protein hydrolysate	0	50
Fat source		
Soy oil	24	24
Lard	213	213
[5]**Amino acid composition**		
Hydroxyproline	0	0.4
Histidine	6.4	5.4
Taurine	0	0.8
Serine	13	11
Arginine	7.5	7.1
Glycine	4.2	5.4
Aspartic acid	17	15
Glutamic acid	51	44
Threonine	9.4	8.3
Alanine	6.8	7.3
Proline	24	20
Lysine	18	17
Tyrosine	9.8	7.4
Methionine	6.0	5.3
Valine	14	13
Isoleucine	11	9.7
Leucine	21	19

Phenylalanine	12	9.0

SPH, salmon protein hydrolysate

[1]The diets were isonitrogenous, and contained 21 g protein per 100 g diet

[2]Ingredients (g/kg diet)

[3]Amino acid composition (mg/g protein)

[4]Casein consisted of 84% protein and 0.2% fat

[5]SPH consisted of 91% protein

Other ingredients (g/kg diet): Cornstarch (105); Dyetrose (154); Sucrose (117); Fiber (58); Dextrin/Cellulose (20); AIN-93G-MX mineral mix (41); AIN-93G-VX vitamin mix (12); L-Cysteine (3.5); Choline bitartrate (17); *tert*-Butyl-hydroquinone (0.016)

Table S1 Composition and amino acid contents of the diets.

Table S2 Overview of analysed genes.

Table S2

Gene names of analysed genes, primer/probe sets and analysed tissues

Gene	Full name	[1]AoD no.	Liver	Heart	Aorta
Acaca	Acetyl-Coenzyme A carboxylase alpha	Mm01304277_m1	x		
Scd1	Stearoyl-Coenzyme A desaturase 1	Mm00772290_m1	x		
Cat	Catalase	Mm00437992_m1		x	
Mcp1	Monocyte chemoattractant protein	Mm00441242		x	x
Icam1	Intracellular adhesion molecule	Mm00516023_m1		x	x
Nos2	Nitric oxide synthase 2	Mm00440502_m1		x	x
Sod1	Superoxide dismutase 1, soluble	Mm01344233_g1		x	
Sod2	Superoxide dismutase 2, mitochondrial	Mm01313000_m1		x	
Tnfa	Tumor necrosis factor alpha	Mm00443260_g1		x	
Vcam1	Vascular cell adhesion molecule 1	Mm00443281		x	x

[1] Catalog number of custom TaqMan gene expression primer/probe sets from Applied Biosystems.

ACKNOWLEDGMENTS

We thank Kari Williams, Liv Kristine Øysæd, Randi Sandvik and Svein Krüger for excellent technical assistance, and Eline Milde Nevdal for assisting with the animal experiment.

AUTHOR CONTRIBUTION

Conceived and designed the experiments: CP BB TB JS RKB GC. Performed the experiments: RV MB SH TB SM GSG BH. Analyzed the data: RV BB FD. Contributed reagents/materials/analysis tools: CRS JEN. Wrote the paper: CP RV BB PA RKB.

REFERENCES

1. Lloyd-Jones DM (2010) Cardiovascular risk prediction: basic concepts, current status, and future directions. Circulation 121: 1768–1777

2. Woollard KJ (2013) Immunological aspects of atherosclerosis. Clinical Science 125: 221–235

3. Hansson GK, Robertson A-KL, Söderberg-Nauclér C (2006) Inflammation and atherosclerosis annual review of

pathology: Mechanisms of disease. Annual Reviews 1 297–329

4. van der Wal AC, Becker AE, van der Loos CM, Das PK (1994) Site of intimal rupture or erosion of thrombosed coronary atherosclerotic plaques is characterized by an inflammatory process irrespective of the dominant plaque morphology. Circulation 89: 36–44

5. Sabesin SM (1981) Lipid and lipoprotein abnormalities in alcoholic liver disease. Circulation 64: III 72–84

6. Kleemann R, Kooistra T (2005) HMG-CoA reductase inhibitors: effects on chronic subacute inflammation and onset of atherosclerosis induced by dietary cholesterol. Curr Drug Targets Cardiovasc Haematol Disord5: 441–453

7. Rein D, Schijlen E, Kooistra T, Herbers K, Verschuren L, et al. (2006) Transgenic flavonoid tomato intake reduces C-reactive protein in human C-reactive protein transgenic mice more than wild-type tomato. J Nutr136: 2331–2337

8. Kleemann R, Verschuren L, van Erk MJ, Nikolsky Y, Cnubben NH, et al. . (2007) Atherosclerosis and liver inflammation induced by increased dietary cholesterol

intake: a combined transcriptomics and metabolomics analysis. Genome Biol 8 R200.

9. Singh U, Jialal I (2006) Oxidative stress and atherosclerosis. Pathophysiology 13: 129–142

10. Ridker PM, Rifai N, Cook NR, Bradwin G, Buring JE (2005) Non-HDL cholesterol, apolipoproteins A-I and B100, standard lipid measures, lipid ratios, and CRP as risk factors for cardiovascular disease in women. JAMA 294: 326–333

11. Harnedy PA, FitzGerald RJ (2012) Bioactive peptides from marine processing waste and shellfish: A review. Journal of Functional Foods 4: 6–24

12. Chalamaiah M, Dinesh Kumar B, Hemalatha R, Jyothirmayi T (2012) Fish protein hydrolysates: proximate composition, amino acid composition, antioxidant activities and applications: a review. Food Chem 135: 3020–3038

13. Elvevoll EO, Eilertsen KE, Brox J, Dragnes BT, Falkenberg P, et al. (2008) Seafood diets: hypolipidemic and antiatherogenic effects of taurine and n-3 fatty acids. Atherosclerosis 200: 396–402

14. Liaset B, Madsen L, Hao Q, Criaeles G, Mellgren G (2009) Fish protein hydrolysate elevates plasma bile acids

and reduces visceral adipose tissue mass in rats. Biochim Biophys Acta 1791: 254–262

15. Jacques H, Gascon A, Bergeron N, Lavigne C, Hurley C, et al. . (1995) Role of dietary fish protein in the regulation of plasma lipids. Can J Cardiol 11: Suppl G 63G–71G.

16. Zhang X, Beynen AC (1993) Influence of dietary fish proteins on plasma and liver cholesterol concentrations in rats. Br J Nutr 69: 767–777

17. Wergedahl H, Liaset B, Gudbrandsen OA, Lied E, Espe M, et al. (2004) Fish protein hydrolysate reduces plasma total cholesterol, increases the proportion of HDL cholesterol, and lowers acyl- CoA:cholesterol acyltransferase activity in liver of Zucker rats. Journal of Nutrition 134: 1320–1327

18. Grimstad T, Bjorndal B, Cacabelos D, Aasprong OG, Omdal R, et al. (2012) A salmon peptide diet alleviates experimental colitis as compared with fish oil. Journal of Nutritional Science 1: 1–8

19. Palinski W, Ord VA, Plump AS, Breslow JL, Steinberg D, et al. (1994) ApoE-deficient mice are a model of lipoprotein oxidation in atherogenesis. Demonstration of oxidation-specific epitopes in lesions and high titers of autoantibodies

to malondialdehyde-lysine in serum. Arterioscler Thromb 14: 605–616

20. Bjorndal B, Vik R, Brattelid T, Vigerust NF, Burri L, et al. (2012) Krill powder increases liver lipid catabolism and reduces glucose mobilization in tumor necrosis factor-alpha transgenic mice fed a high-fat diet. Metabolism 61: 1461–1472

21. Vigerust NF, Bjorndal B, Bohov P, Brattelid T, Svardal A, et al. (2012) Krill oil versus fish oil in modulation of inflammation and lipid metabolism in mice transgenic for TNF-alpha. Eur J Nutr 52: 1315–1325

22. Strand E, Bjorndal B, Nygard O, Burrin L, Berge C, et al. (2012) Long-term treatment with the pan-PPAR agonist tetradecylthioacetic acid or fish oil is associated with increased cardiac content of n-3 fatty acids in rat. Lipids in Health and Disease 11: 82.

23. Berge RK, Flatmark T, Osmundsen H (1984) Enhancement of long-chain acyl-CoA hydrolase activity in peroxisomes and mitochondria of rat liver by peroxisomal proliferators. Eur J Biochem 141: 637–644

24. Bremer J (1981) The effect of fasting on the activity of liver carnitine palmitoyltransferase and its inhibition by malonyl-CoA. Biochim Biophys Acta 665: 628–631

25. Skorve J, al-Shurbaji A, Asiedu D, Bjorkhem I, Berglund L, et al. (1993) On the mechanism of the hypolipidemic effect of sulfur-substituted hexadecanedioic acid (3-thiadicarboxylic acid) in normolipidemic rats. J Lipid Res 34: 1177–1185

26. Madsen L, Rustan AC, Vaagenes H, Berge K, Dyroy E, et al. (1999) Eicosapentaenoic and docosahexaenoic acid affect mitochondrial and peroxisomal fatty acid oxidation in relation to substrate preference. Lipids 34: 951–963

27. Field FJ, Albright E, Mathur S (1991) Inhibition of acylcoenzyme A: cholesterol acyltransferase activity by PD128O42: effect on cholesterol metabolism and secretion in CaCo-2 cells. Lipids 26: 1–8

28. Cinq-Mars DC, Hu C, Kitts DD, Li-Chan EC (2008) Investigations into inhibitor type and mode, simulated gastrointestinal digestion, and cell transport of the angiotensin i-converting enzyme-inhibitory peptides in pacific hake (merluccius productus) fillet hydrolysate. J Agric Food Chem 56: 410–419

29. Raatz SK, Silverstein JT, Jahns L, Picklo MJ (2013) Issues of fish consumption for cardiovascular disease risk reduction,. Nutrients 5: 1081–1097

30. Jung UJ, Torrejon C, Tighe AP, Deckelbaum RJ (2008) n-3 Fatty acids and cardiovascular disease: mechanisms underlying beneficial effects. Am J Clin Nutr 87: 2003S–2009S

31. Duarte J, Vinderola G, Ritz B, Perdigon G, Matar C (2006) Immunomodulating capacity of commercial fish protein hydrolysate for diet supplementation. Immunobiology 211: 341–350

32. Murakami S, Kondo-Otha Y (1998) Tomisawa (1998) Improvement in cholesterol metabolism in mice given chronic treatment of taurine and fed a high-fat diet. Life Sciences 64: 83–91

33. Chen W, Matuda K, Nishimura N, Yokogoshi H (2004) The effect of taurine on cholesterol degradation in mice fed a high-cholesterol diet. Life Sciences. 74: 1889–1898

34. Dembinska-Kiec A, Gryglewski RJ (1986) Contribution of arachidonic acid metabolites to atherosclerosis. Wien Klin Wochenschr 98: 198–206

35. Bjorndal B, Berge C, Ramsvik MS, Svardal A, Bohov P, et al. (2013) A fish protein hydrolysate alters fatty acid composition in liver and adipose tissue and increases plasma carnitine levels in a mouse model of chronic inflammation. Lipids Health Dis 12: 143.

36. Muoio DM, Way JM, Tanner CJ, Winegar DA, Kliewer SA, et al. (2002) Peroxisome proliferator-activated receptor-alpha regulates fatty acid utilization in primary human skeletal muscle cells. Diabetes 51: 901–909

37. Kersten S, Mandard S, Escher P, Gonzalez FJ, Tafuri S, et al. (2001) The peroxisome proliferator-activated receptor alpha regulates amino acid metabolism. FASEB J 15: 1971–1978

38. Delerive P, Fruchart JC, Staels B (2001) Peroxisome proliferator-activated receptors in inflammation control. J Endocrinol 169: 453–459

39. Zhu CF, Li GZ, Peng HB, Zhang F, Chen Y, et al. (2010) Treatment with marine collagen peptides modulates glucose and lipid metabolism in Chinese patients with type 2 diabetes mellitus. Appl Physiol Nutr Metab. 36: 797–804

Chapter 4

MicroRNA expression profiles of tissues involved in cholesterol metabolism and atherosclerosis from athero-prone and athero-resistant mouse models

Presented at meetings:

(1) *Manzini S., Busnelli M., Chiara M., Parolini C., Dellera F., Ganzetti GS, Horner DS and Chiesa G. MiRNA expression profiling in normolipidemic wild-type, hyperlipidemic LDLR knockout and hypolipidemic PCSK9 knockout mice. 84th EAS Congress, May 29 - June 1, 2016; Innsbruck (Austria).*

(2) *Dellera F., Manzini S., Busnelli M., Chiara M., Parolini C., Ganzetti GS, Horner DS, Chiesa G. MicroRNA expression profiles of tissues involved in cholesterol metabolism from athero-prone and athero-resistant mouse models. ABCD National Ph.D. Meeting, April 7 – 9, 2016; Salerno (Italy).*

(3) *Manzini S., Busnelli M., Chiara M., Parolini C., Dellera F., Ganzetti GS, Horner DS, Chiesa G. Genome-wide identification of microRNAs involved in the regulation of cholesterol metabolism and atherosclerosis development. 17th ISA Congress, May 23 - 26, 2015; Amsterdam (Netherlands).*

INTRODUCTION AND AIM

MiRNAs are small non-coding RNAs which act as potent post-transcriptional regulators of gene expression. MiRNAs typically control the expression of their target genes by imperfect base-pairing to 3' UTR regions of mRNAs, thereby inducing repression of the target mRNA (1, 2). In recent years, several miRNAs have been directly linked to the regulation of key genes involved in cholesterol metabolism and atherosclerosis development, as extensively discussed in the introduction of this thesis.

Despite these recent advances, what is lacking is a global approach to the comprehension of the interplay between genes, miRNA-dependent regulation of those genes and the phenotypic effects.

The current study was aimed to identify miRNA expression profiles of tissues involved in cholesterol intake, processing, production, metabolism and in atherosclerosis development harvested from LDLR $^{-/-}$ (LDLR KO), PCSK9 $^{-/-}$ (PCSK9 KO) and wild-type C57BL/6 mice after chow (standard) or a high fat feeding (3, 4). MiRNAs showing differential expression between genotypes/dietary

regimens/tissues have been subjected to detailed *in silico* target prediction analysis, with particular attention being paid to identify members of transcriptional regulatory circuits potentially involved in cholesterol metabolism and regulated by miRNAs.

This project is ongoing and we are mainly validating the results of target prediction analysis by performing *in vitro* experiments of cell co-transfection with appropriate reporter vectors and synthetic microRNA mimics. The identification of targets for dysregulated microRNAs is expected to provide insights into transcriptional circuits subject to changes in perturbations of cholesterol metabolism and could represent a crucial step towards the identification of candidate targets for personalized therapeutic strategies.

MATERIALS AND METHODS

Experimental design: animals and diet

The study was conducted according to national (D.L. 116, G.U. Suppl. 40, February 18, 1992, Circolare N^{o}. 8, G.U July 1994) and international laws and policies (EEC Council Directive 2010/63, September 22, 2010: Guide for the Care and Use of Laboratory Animals, United States National Research Council, 2011). The Italian Ministry of Health approved the protocol.

Wild-type C57BL/6, LDLR $^{-/-}$ (prone to atherosclerosis development) and PCSK9 $^{-/-}$ mice (resistant to atherosclerosis development) (3, 4) were purchased from Charles River (Calco, Italy) and housed in the animal facility for the whole duration of the treatment (16 weeks). Starting from the sixth week from birth, animals have been fed with either standard (Chow) or Western-type diet (21% fat, 0.2% cholesterol). The latter has a high fat and cholesterol content and is commonly used to induce the development of dyslipidemia and/or plaque development in susceptible genotypes. Each experimental group was made up of 10 animals. **(Fig. 1).**

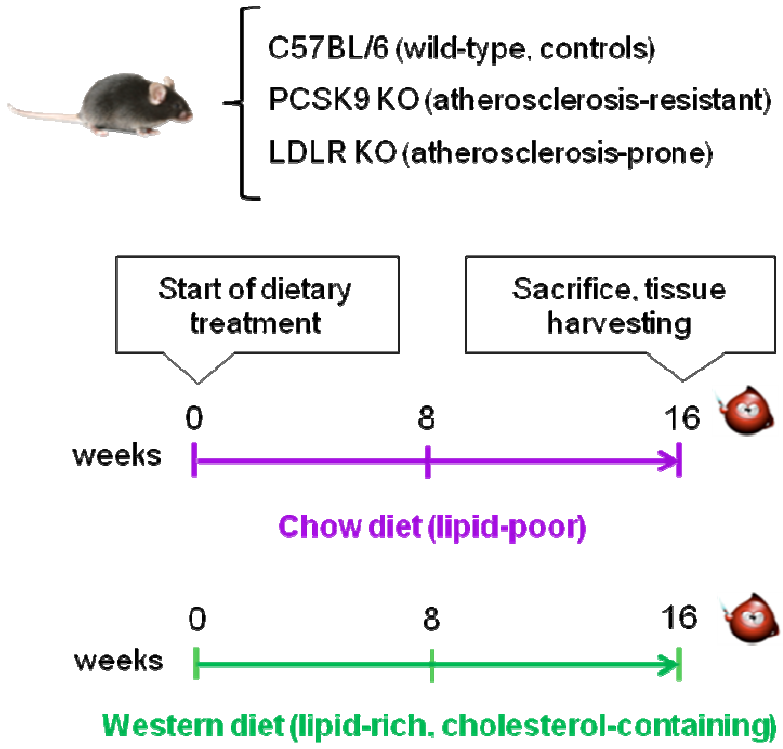

Fig. 1 Experimental design of the study

Blood and tissue harvesting

Blood samples have been collected before the start of dietary regimens and at sacrifice (16 weeks) from the mouse retro-orbital plexus into tubes containing 0.1% (w/v) EDTA after an overnight fast **(Fig. 1)** Blood samples were

chilled on ice for at least 15 minutes and stored at -80°C until analyses.

At sacrifice, heart, aorta, liver, small intestine (duodenum, jejunum, ileum), white adipose tissue and brain have been harvested and properly stored for the subsequent molecular and biochemical analyses.

Plasma lipid profile

A general characterization of the lipid profile of mice has been performed on plasma collected at sacrifice by enzymatically measuring total cholesterol and triglycerides (ABX Diagnostics, France).

Atherosclerosis development

The area covered by atherosclerotic plaques has been quantified at the aortic sinus. Serial cryosections (7 mm thick) of the aortic sinus were cut. Approximately 25 slides with 3 cryosections/slide were obtained, spanning the three cusps of the aortic valves. Every fifth slide was fixed and stained with hematoxylin and eosin (Bio-Optica, Milano, Italy) to detect plaque area. Plaque area was calculated as the mean area of those sections showing the

three cusps of the aortic valves. To acquire and process digital images, an Aperio ScanScope GL Slide Scanner (Aperio Technologies, Vista, CA, USA), equipped with a Nikon 206/0.75 Plan Apochromat objective producing a 0.25 mm/pixel scanning resolution with a 406 magnification, and the Aperio ImageScope software (version 8.2.5.1263) was used.

Total RNA extraction and construction of cDNA libraries for high throughput sequencing

Total RNA has been extracted from the tissues and organs collected (NucleoSpin® miRNA columns, Mackerey-Nagel, Germany) and libraries suitable for use with Illumina Genome Analyzer IIx (Illumina, San Diego, CA, USA) have been constructed. During the generation of cDNA libraries, techniques have been applied to enrich in low molecular weight cDNA species, maximising the miRNA component of libraries. All samples have been then sequenced with the high throughput sequencer Illumina Genome Analyzer IIx (analysis performed by IGA Technology Services S.r.l., Udine, Italy) (5).

Analysis of miRNA expression profiles and target prediction for differentially expressed miRNAs

For each experimental condition (diet/genotype/tissue) small RNA sequence reads have been mapped to known mature and precursor miRNA sequences from miRBase using the Short Oligonucleotide Analysis Package SOAP and outputs have been parsed using custom scripts prepared in the Python/PERL programming languages to obtain digital

expression values for both canonical mature miRNA and similar, incorrectly processed sequences. After exclusion of reads corresponding to RNA and rRNA degradation products, evaluation of differential expression has been performed within a statistical framework based on the negative binomial distribution and implemented in the Bioconductor packages edgeR and DEseq for the R language. Further statistical tests have been performed using the same instruments to confirm consistency of expression pattern changes between individual animals. Subsequently, all reads have been mapped to the reference murine genome using SOAP and preliminary candidate miRNA/miRNA* pairs have been identified using a simple, but effective, algorithm previously developed by Prof. David Horner (Università degli Studi di Milano, Milano, Italy). Genomic sequences corresponding to loci defined by these preliminary candidate pairs have been extracted and their predicted secondary structures modeled using RNA fold software and custom scripts to confirm the expected juxtaposition of the candidate miRNA/miRNA* sequences. Cases fulfilling these conditions have been further evaluated using a Support Vector machine trained to

recognize vertebrate miRNA precursors and simple statistical tests to demonstrate miRNA-like behaviour of small RNA mapping patterns in candidate precursor loci (strand specificity, clustering of the majority of reads in the regions of the canonical miRNA and miRNA* sequences). Candidates passing these tests have been evaluated for differential expression among experimental conditions.

Two on-line databases of established target predictions, miRDB (http://www.mirdb.org/miRDB) and TargetScan (http://www.targetscan.org), have been downloaded and used to identify all predicted targets for differentially expressed known miRNAs. Sets of predictions made by the two methods have been then used to perform KEGG pathway enrichment analyses (http://www.genome.jp/kegg/pathway) in order to identify physiological processes and pathways enriched among target predictions and thus probable physiological target according to the accepted model of multiple miRNA target associations.

Validation of candidate miRNA targets identified by high-throughput sequencing and bioinformatics analyses: *in vitro* experiments

In silico prediction of target mRNAs needed to be empirically confirmed. From the group of candidate targets of the miRNAs resulted DE, we concentrated our attention on those playing a role in cholesterol metabolism and atherosclerosis development **(Tab. 1).**

The 3' UTR of each of these genes containing the miRNA response element has been cloned into pmirGLO Dual-Luciferase miRNA Target Expression Vector (Promega Italia, Milano, Italy) **(Fig.2, upper figure).** In parallel, as a control, a vector has been constructed with the same miRNA responsive element inserted, but containing a sequence mismatch.

PmiRGLO vector is designed to quantitatively evaluate miRNA activity by the insertion of miRNA target sites downstream or 3´ of the firefly luciferase gene (*luc2*) **(Fig. 2, upper figure)**. Firefly luciferase is the primary reporter gene. Reduced firefly luciferase expression indicates the binding of endogenous or introduced miRNAs to the cloned miRNA target sequence **(Fig. 2, lower figure)**. This vector is

based on dual-luciferase technology, with *luc2* used as the primary reporter to monitor mRNA regulation and *Renilla* luciferase (*hRluc-neo*) **(Fig. 2, upper figure)** acting as a control reporter for normalization and selection.

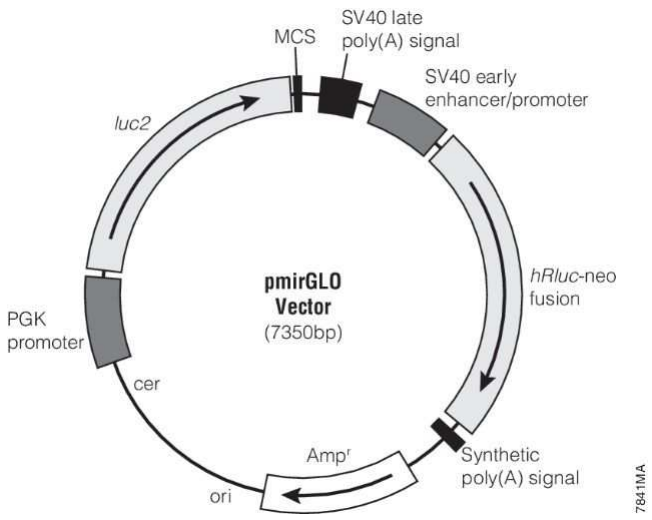

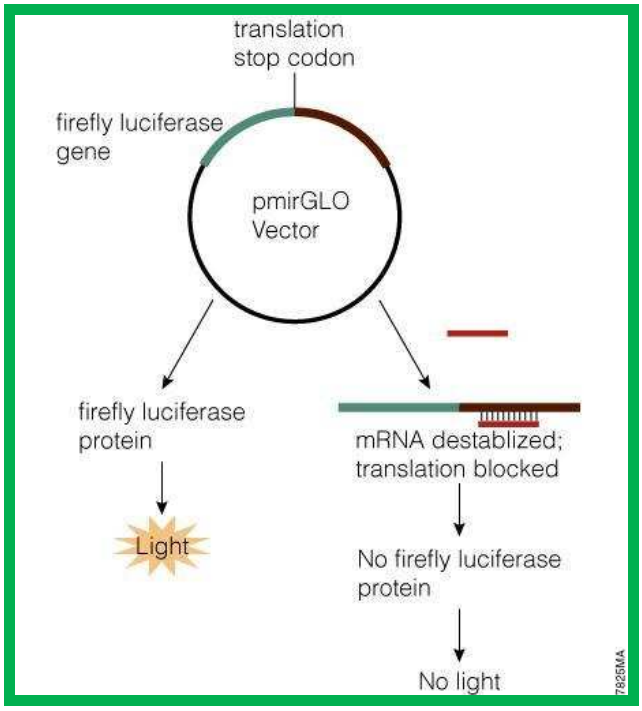

Fig. 2 PmirGLO Dual-Luciferase miRNA Target Expression Vector (upper figure) and mechanism of action for *in vitro* miRNA target validation (lower figure).

Main abbreviations: luc2, Firefly luciferase; hRluc-neo, Renilla luciferase; Amp^r, β–lactamase coding region; MCS, multiple cloning site.

For *in vitro* target validation, cell line NIH 3T3 (batch number 61062005, ATCC, USA) has been chosen. NIH 3T3 cells were cultured in DMEM high glucose with stable L-glutamine (Lonza, USA), supplemented with 10% fetal calf serum (Euroclone, Milano, Italy) and 1X penicillin/streptomycin (Euroclone, Milano, Italy). Cell cultures were incubated at 37°C in a humidified atmosphere with 5% CO_2.

The experiments needed to investigate the effect of selected DE miRNAs **(Tab. 1)** on their candidate target mRNAs are currently ongoing in our laboratory. In detail, NIH 3T3 cells will be seeded in 24-well plates. After 24 hours, at 80-90% of confluence, cells will be transiently co-transfected with the selected miRNA mimic (Exiqon, Denmark) and the vector pmiRGLO containing the candidate responsive sequence or with the same miRNA mimic and the vector containing the mismatched target sequence, used as a control. Co-transfection will be performed by using Lipofectamine 3000 diluted in Opti-MEM (both purchased from Invitrogen, Life Technologies Italia, Monza, Italy). Hsa-miR-21 and its known responsive sequence cloned into the vector will be used as a positive

control. After 4 h of incubation, the transfection medium will be replaced with fresh complete growth medium. At 48 hours after transfection, cells will be collected in order to perform Luciferase reporter assay using Dual-Luciferase® Reporter (DLR™) Assay System (Promega Italia, Milano, Italy) according to standard protocols.

RESULTS

Atherosclerosis evaluation: only LDLR$^{-/-}$ mice showed increased atherosclerotic plaque development

Plaque area has been quantified at the aortic sinus. As expected, only LDLR$^{-/-}$ mice showed atherosclerosis development. Atherosclerotic lesions were exacerbated by Western-type diet, as shown in figure 3 **(Fig. 3).**

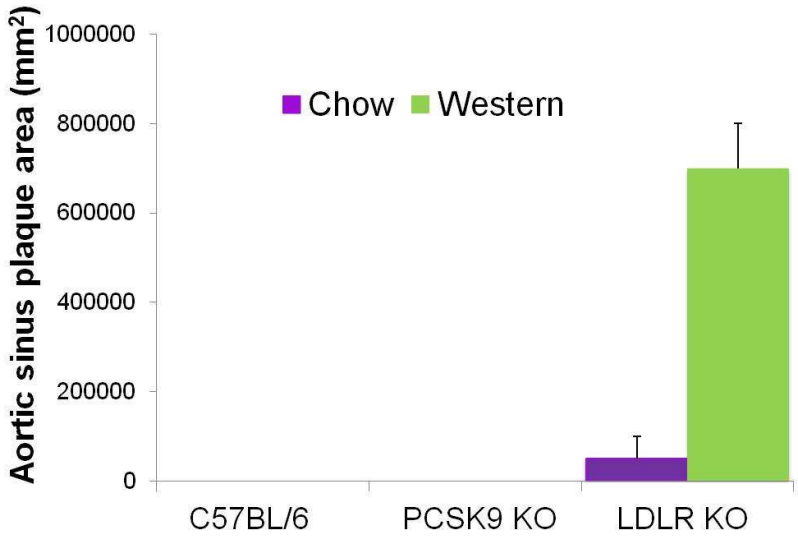

Fig. 3 Atherosclerotic plaque development in C57BL/6, PCSK9 $^{-/-}$ (PCSK9 KO) and LDLR $^{-/-}$ (LDLR KO) mice fed chow or Western diet for 16 weeks.

Plasma lipid levels

Plasma concentrations of total cholesterol (TC) and triglycerides (TG) were measured (**Fig. 4**). LDLR$^{-/-}$ mice showed significantly increased TC and TG levels when compared to C57BL/6 and PCSK9$^{-/-}$ mice (*P<0.0001 vs C57BL/6 and PCSK9; $^{\#}$P<0.005 vs C57BL/6; 1-way Anova with Tukey post-hoc).

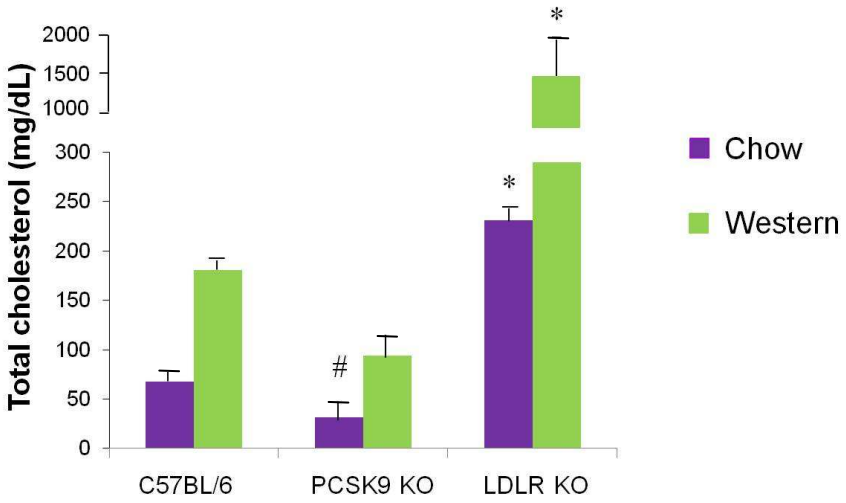

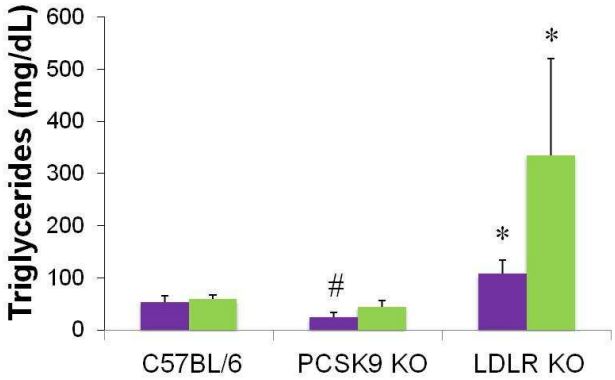

Fig. 4 Plasma total cholesterol and triglycerides in C57BL/6, PCSK9 $^{-/-}$ (PCSK9 KO) and LDLR $^{-/-}$ (LDLR KO) mice fed chow or Western diet for 16 weeks (*P<0.0001 vs C57BL/6 and PCSK9; $^{\#}$P<0.005 vs C57BL/6; 1-way Anova with Tukey post-hoc).

MiRNA expression profiles in tissues involved in cholesterol metabolism

At sacrifice, mouse tissues and organs involved in cholesterol metabolism such as aorta, liver, small intestine (duodenum, jejunum, ileum), white adipose tissue and brain have been collected and stored for the analysis of miRNA expression profiles and validation experiments.

Figure 5 **(Fig. 5)** shows miRNAs resulted as DE by the high throughput sequencing performed and the following bioinformatic analyses. A high number of DE miRNAs was observed among genotypes in several tissues with both dietary regimens, although after Western diet the overall DE number was lower than after Chow diet. The most relevant DE number has been observed at both Chow and Western diet in the comparison between C57BL/6 and $LDLR^{-/-}$ mouse aortas, which are sites of atherosclerosis development.

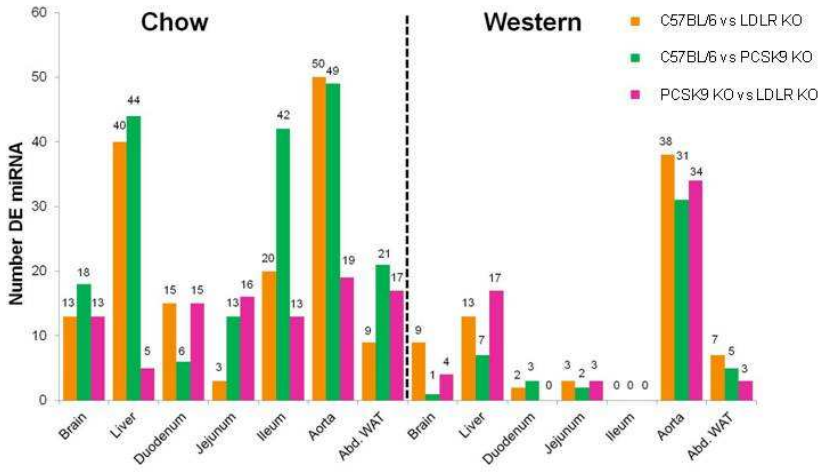

Fig. 5 Number of miRNAs resulted as DE among genotypes in the considered tissues from animals fed both Chow and Western diet

Abbreviations: Abd. WAT, abdominal white adipose tissue.

In silico target prediction analysis of DE miRNAs

MiRNAs which resulted DE in all the comparisons underwent detailed *in silico* target prediction analyses. Target mRNAs were predicted by miRDB/Targetscan softwares, then functional enrichment analysis was run for each comparison in order to provide insights into the biological interpretation of the obtained pattern of candidate genes.

In particular, focusing on the comparison between the two diets, aggregated KEGG pathways showed overlapping and

recurring enriched pathways, that are the chemokine signaling pathway, the cytokine-cytokine receptor interaction and the insulin signaling pathway, as shown in figure 6 **(Fig. 6)**.

Among the genes annotated in these pathways, we identified targets known for their role in lipid metabolism/cardiovascular disease as well as novel potential genes of interest, such as Leukemia inhibitory factor receptor (Lifr) and Braf transforming gene (Braf) **(Fig. 7)**.

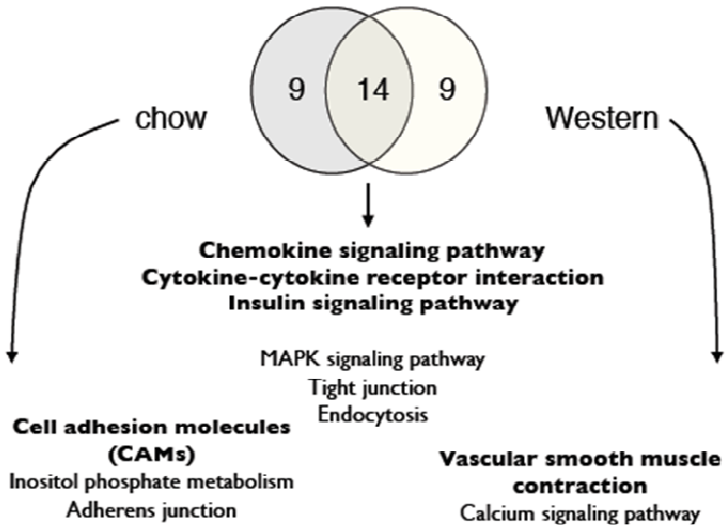

Fig. 6 Schematic summary showing the recurring pathways resulted from KEGG pathway mapping performed on our target genes in the comparison between chow - fed and Western–fed animals.

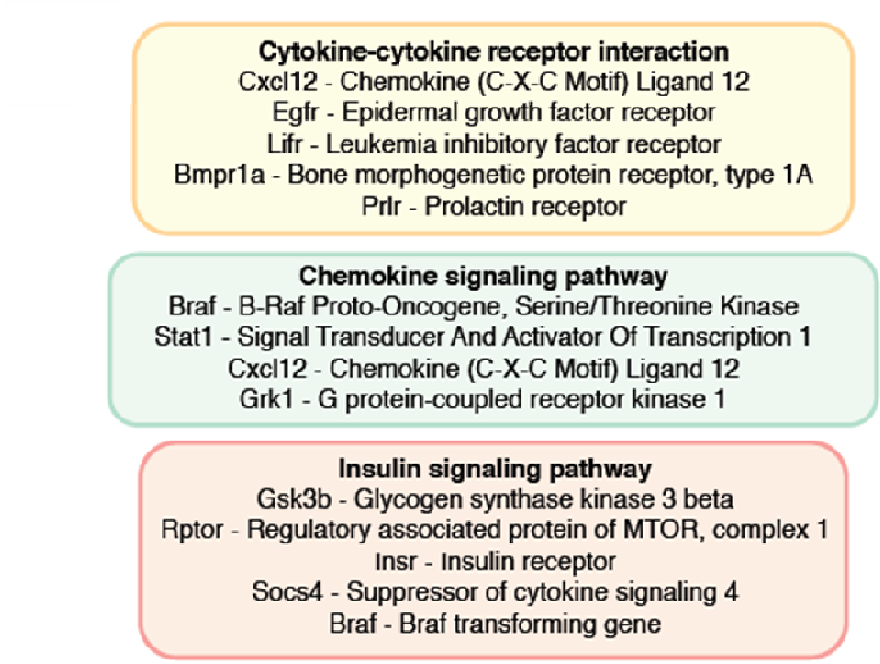

Fig. 7 Detail of target genes annotated in the shared KEGG pathways

Furthermore, as a complementary approach, we selected genes that are known to be involved in cholesterol and lipid metabolism and investigated if they were predicted as targets of DE miRNAs. Table 1 **(Tab. 1)** shows some of them and their associated DE miRNAs. The comparisons/tissues in which these miRNAs resulted DE are indicated as well.

DE miRNA	Comparison	Tissue	Diet	Target gene of interest
miR-133a-3p	C57BL/6 vs LDLRKO	brain	chow	ACAT2
miR-133a-3p	C57BL/6 vs LDLRKO	jejunum	chow	ACAT2
miR-151-3p	C57BL/6 vs PCSK9KO	aorta	chow	CYP7B1
miR-151-3p	C57BL/6 vs PCSK9KO	aorta	western	CYP7B1
miR-151-3p	LDLRKO vs PCSK9KO	aorta	western	CYP7B1
miR-151-3p	C57BL/6 vs LDLRKO	liver	chow	CYP7B1
miR-151-3p	C57BL/6 vs PCSK9KO	liver	chow	CYP7B1
miR-155-5p	C57BL/6 vs LDLRKO	aorta	western	CYP7B1
miR-155-5p	LDLRKO vs PCSK9KO	aorta	western	CYP7B1
miR-155-5p	LDLRKO vs PCSK9KO	liver	western	CYP7B1
miR-155-5p	C57BL/6 vs PCSK9KO	WAT	western	CYP7B1
miR-224-5p	C57BL/6 vs LDLRKO	aorta	chow	PCSK9
miR-224-5p	C57BL/6 vs PCSK9KO	aorta	chow	PCSK9
miR-224-5p	C57BL/6 vs PCSK9KO	aorta	western	PCSK9
miR-224-5p	LDLRKO vs PCSK9KO	aorta	western	PCSK9
miR-224-5p	LDLRKO vs PCSK9KO	brain	western	PCSK9
miR-224-5p	C57BL/6 vs LDLRKO	ileum	chow	PCSK9
miR-224-5p	C57BL/6 vs PCSK9KO	ileum	chow	PCSK9
miR-410-3p	LDLRKO vs PCSK9KO	aorta	western	PPAP2B

Tab. 1 Differentially expressed miRNAs and candidate targets involved in cholesterol metabolism and atherosclerosis development

Abbreviations: WAT, white adipose tissue

In vitro validation of candidate miRNA targets

In vitro validation of the interactions between miRNA-candidate target listed in Tab.1 are currently ongoing. To experimentally test whether selected miRNAs directly target the 3'UTR of their candidate gene *in vitro*, NIH 3T3 cells will be co-transfected with reporter constructs along with a synthetic mimic of miRNAs, as explained in detail in the section "Material and Methods". For successful predictions, the expected result is a diminished luciferase expression by cells transfected with miRNA mimics and pmirGLO vector containing the miRNA-responsive element, compared to controls.

Future steps

The future perspectives of this study include:

- the conclusion of *in vitro* validation experiments, in order to experimentally confirm the interaction between DE miRNAs and their candidate targets involved in cholesterol metabolism.

- in depth examination of pathway enrichment analyses, with a particular attention paid to signaling pathways linked to upregulated or downregulated DE miRNAs.

The aim is the identification of members of regulatory pathways subject to changes in perturbations of cholesterol metabolism. These targets could be crucial for the development of panels of biomarkers for disease development.

REFERENCES

1. Ambros V (2004). The functions of animal microRNAs. Nature 431:350–355.
2. Filipowicz W, Bhattacharyya SN, Sonenberg N (2008). Mechanisms of post-transcriptional regulation by microRNAs: are the answers in sight?. Nat Rev Genet 9:102–114.
3. Knowles JW, Maeda N (2000). Genetic modifiers of atherosclerosis in mice. Arterioscler Thromb Vasc Biol 20:2336 –2345.
4. Denis M, Marcinkiewicz J, Zaid A, et al (2012). Gene inactivation of proprotein convertase subtilisin/kexin type 9 reduces atherosclerosis in mice. Circulation 125:894–901.
5. Harismendy O, Ng PC, Strausberg RL, Wang X, Stockwell TB, Beeson KY, Schork NJ, Murray SS, Topol EJ,Levy S, Frazer KA (2009). Evaluation of next generation sequencing platforms for population targeted sequencing studies. Genome Biol 10(3):R32.

Chapter 5

Conclusions and Future perspectives

During my PhD program I have contributed to the realization of different research projects, all related to the study of atherosclerosis and cholesterol metabolism through the use of animal models.

Among these, I have focused my PhD thesis mainly on two of the studies I co-authored (Chapter 2 and 3), one as first author. Moreover, a third study, still ongoing and whose results have been presented at National and International conferences, has been presented as well, even though further investigations are needed to complete it (Chapter 4).

The first project discussed (Chapter 2) is focused on the effect of L-homoarginine, an L-arginine homologue derived from lysine, on neointimal hyperplasia, a pathological condition which can occur at sites of subclinical atherosclerosis or after angioplasty interventions. For the first time, we have demonstrated that *in vivo* administration of homoarginine in a rat model of carotid balloon injury was able to inhibit neointimal formation, at least in part, by inhibiting vascular cell proliferation and by increasing both arginine availability and nitric oxide

production, suggesting homoarginine as a potential therapeutical option for cardiovascular protection.

The second study presented (Chapter 3) is instead focused on the study of the effect of a salmon protein hydrolysate on atherosclerosis development in apo E-deficient mice, on the basis of previous evidences indicating that fish protein peptides and hydrolysates are able to exert beneficial effects on cardiovascular risk factors. Mice fed a high-fat diet with 5% salmon protein hydrolysate for 12 weeks showed a significantly reduced atherosclerotic plaque area in the aortic arch and aortic sinus versus controls. The effect of this dietary supplementation was shown to be mediated by the inhibition of systemic inflammation activation and it seemed to be independent of changes in plasma lipid levels.

Finally, the fourth chapter of this thesis presents the results obtained to date regarding the characterization of microRNA expression patterns in tissues involved in cholesterol metabolism and atherosclerosis, harvested from LDLR-deficient, PCSK9-deficient and wild-type C57BL/6 mice after chow or a high fat feeding. Briefly, we have identified the microRNAs which resulted DE in our

experimental conditions (different genotypes/tissues/diet) by high-throughput sequencing and bioinformatics analyses. A detailed *in silico* target prediction study was then performed to identify the genes regulated by DE microRNAs. We are currently validating the *in silico* analysis results by cell transfection with appropriate reporter vectors and microRNA mimics.

The identification of targets for dysregulated microRNAs is aimed at highlighting transcriptional regulatory circuits subject to changes in atherosclerosis and in conditions of perturbation of cholesterol metabolism.

The prevention and management of atherosclerosis and disturbs of cholesterol metabolism are still an open challenge.

In order to gain more insight into the disease, approaches at different levels have been taken and this thesis presented some of them.

Through the use of animal models, we demonstrated that natural compounds or treatments based on novel cardiovascular risk factors may exert a protective role in

atherosclerosis development and in its clinical complications, such as neointimal hyperplasia.

In particular, our studies suggest L-homoarginine and protein sources derived from salmon as therapeutic/nutraceutical options for cardiovascular protection, even though further investigations are needed in order to assess the possibility to translate the obtained results in humans.

Finally, miRNAs have been demonstrated to play an important, although still vaguely characterized, role on atherosclerosis formation and cholesterol metabolism regulation (1). Recent evidences and our preliminary data suggest that the identification of a miRNA profile could probably represent an approach to detect vulnerable patients and disease states (2).

Targeting miRNAs may represent a new pharmacological tool to modulate the atherosclerotic process. Clearly, further studies are encouraged to help us understand the role of miRNAs in atherosclerosis and dyslipidemias.

REFERENCES:

1. Andreou I, Sun X, Stone PH, Edelman ER, Feinberg MW (2015). MiRNAs in atherosclerotic plaque initiation, progression, and rupture. Trends Mol Med 21: 307–318.

2. Ren J, Zhang J, Xu N, Han G, Geng Q, Song J, et al (2013). Signature of circulating microRNAs as potential biomarkers in vulnerable coronary artery disease. PLoS One 8: e80738.

Publications

1. Dellera F, Ganzetti GS, Froio A, Manzini S, Busnelli M, Meinitzer A, Sirtori CR, Chiesa G, Parolini C (2016). L-homoarginine administration reduces neointimal hyperplasia in balloon-injured rat carotids. Thromb. Haemost 116(2).

2. Arnaboldi F, Busnelli M, Cornaghi L, Manzini S, Parolini C, Dellera F, Ganzetti GS, Sirtori CR, Donetti E, Chiesa G (2015). High-density lipoprotein deficiency in genetically modified mice deeply affects skin morphology: A structural and ultrastructural study. Exp Cell Res 338(1):105-12.

3. Parolini C, Busnelli M, Ganzetti GS, Dellera F, Manzini S, Scanziani E, Johnson JL, Sirtori CR, Chiesa G (2014). Magnetic resonance imaging visualization of vulnerable atherosclerotic plaques at the brachiocephalic artery of apolipoprotein E knockout mice by the blood-pool contrast agent B22956/1. Mol Imaging 13.

4. Parolini C, Vik R, Busnelli M, Bjørndal B, Holm S, Brattelid T, Manzini S, Ganzetti GS, Dellera F, Halvorsen B, Aukrust P, Sirtori CR, Nordrehaug JE, Skorve J, Berge RK, Chiesa G (2014). A salmon protein hydrolysate exerts lipid-

independent anti-atherosclerotic activity in ApoE-deficient mice. PLoS One 9(5).

5. Vik R, Busnelli M, Parolini C, Bjørndal B, Holm S, Bohov P, Halvorsen B, Brattelid T, Manzini S, Ganzetti GS, Dellera F, Nygård OK, Aukrust P, Sirtori CR, Chiesa G, Berge RK (2013). An immunomodulating fatty acid analogue targeting mitochondria exerts anti-atherosclerotic effect beyond plasma cholesterol-lowering activity in apoe(-/-) mice. PLoS One 8(12):e81963.